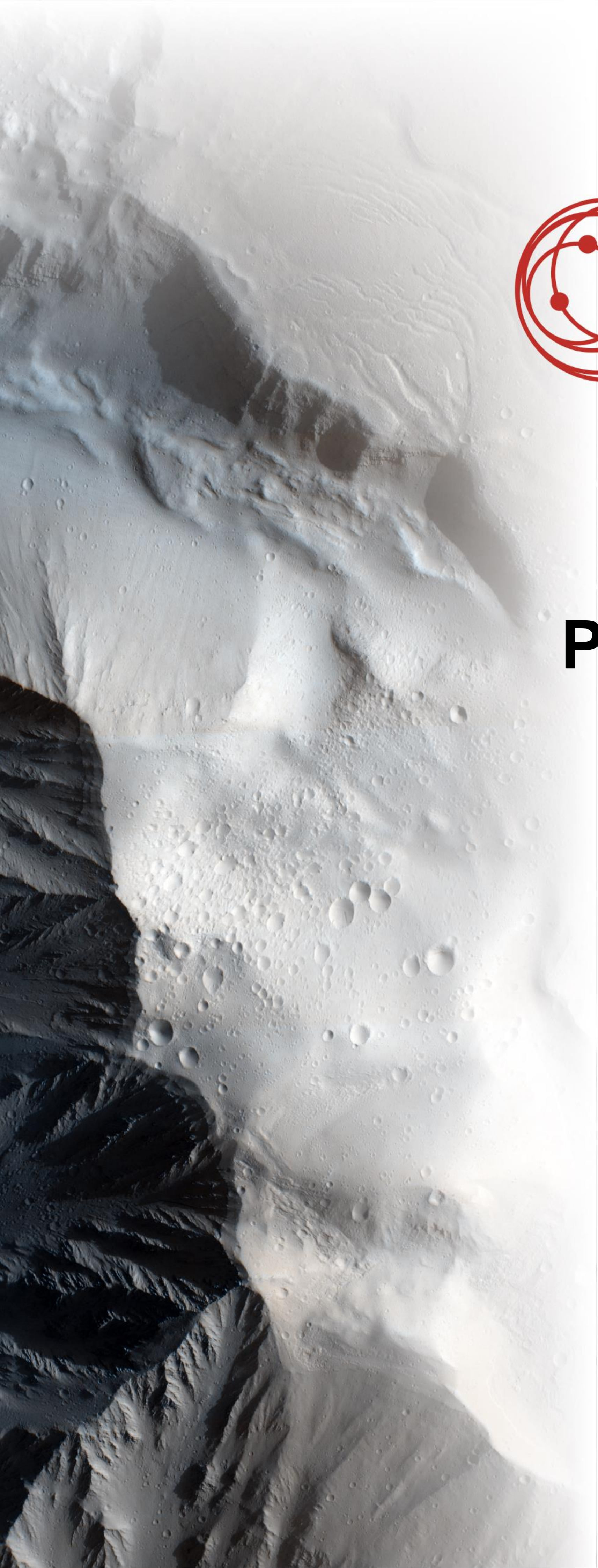

BPSC 2022

PROGRAMME

The Open University

Support and Sponsorship

This meeting would not have been possible without the support of The Open University and our sponsors.

We would like to thank the OU, STEM faculty research support and School of Physical sciences for their facilities and administrative support.

We also thank our sponsors; The UK Space Agency, Royal Astronomical Society, The Geochemistry Group, Astrobiology Society of Britain, CAMECA, ESRI, and the Open University Space Strategic Research Area. There contributions have supported registration costs, funded workshops and made it possible for us to support early career researchers with travel awards.

Foreword

Hello,

We are pleased to (finally) welcome you to The Open University for the 3rd British Planetary Science Conference.

A lot has changed since January 2020 when we first envisaged hosting this conference. Little did we know what science would fall out of the sky or that terrestrial misfortune would have kept us apart and mean that we are still anticipating ExoMars rover operations. However, we still have a vibrant interdisciplinary community collectively exploring the natural history of the solar system. For BPSC2022 we have built a program which reflects the variety of those scientific interests and represents the diversity of our community. We are very much looking forward to hearing from familiar faces and welcoming contributions from many new researchers.

We hope you all enjoy this meeting.

All the best,

BPSC organising team

Peter Fawdon, Mark Fox-Powell, Elena Favaro, Lee White, James Holmes, Rachael Hamp, Annie Lennox, Nisha Ramkissoon

BPSC 2022

Programme Overview

21st – Workshops and icebreaker

	Session	
0930	**Registration opens for morning workshops**	Medlar Suite, in The Hub Teas until 11
1000	**Analytical techniques**	The Hub theatre
1100	**GIS and Planetary Surfaces**	Library IT Suite 2
1200	**Lunch & registration for afternoon workshop**	Lunch vouchers will be provided at registration
1300	**Simulating Extra-Terrestrial Environments**	Gass seminar room
1500 1630		Tea service at workshops End of workshops
	Icebreaker events	
1700	UK Planetary Forum Early Careers Meet up	Kents Hill Park Lounge Bar Open to all ECRs
1800	Icebreaker welcome	Kents Hill Park Lounge Bar Open for everyone
1830	Icebreaker BBQ food	Booked with registration
Until late	Icebreaker continues	Kents Hill Park Lounge Bar Open for everyone

22nd – Oral presentations and Posters

		Session	
0830		Teas	Poster set up
0900		**Welcome**	
0920	**1**	**Meteorites**	Oral presentations, Q&A Berrill Lecture Theatre
	2	Lightning talk group 1a	Berrill Lecture Theatre
	3	Lightning talk group 1b	Berrill Lecture Theatre
1100		Teas and pastries	Posters in the library
1130	**4**	**Icy Satellites**	Oral presentations, Q&A Berrill Lecture Theatre Q&A
	5	Lightning talk group 2	Berrill Lecture Theatre
1300		**Lunch**	Posters and lunch in the library
1400	**6**	Lightning talk group 3a	
	7	**Exploration and Mars**	Oral presentations, Q&A Berrill Lecture Theatre
	8	Lightning talk group 3b	Berrill Lecture Theatre
	9	Lightning talk group 3c	Berrill Lecture Theatre
1600		**Posters**	Afternoon tea and refreshments
1830		End of day	Library closes

23rd – Oral presentations, the Barrie Jones Award and Conference Dinner

		Session	
0845		Teas	
0920	**10**	**Icy Bodies & Outer Solar System**	Oral presentations, Q&A Berrill Lecture Theatre
1100		Teas and pastries	Posters in the Library
1130	**11**	**Winchcombe & Carbonaceous Chondrites**	Oral presentations, Q&A Berrill Lecture Theatre
1300		**Lunch**	Posters and lunch in the Library
1400	**12**	**Habitability and Life**	Oral presentations, Q&A Berrill Lecture Theatre
1530		Teas and pastries	Library
1600	**13**	**Exploring Mars**	Oral presentations, Q&A Berrill Lecture Theatre
1730		**Barrie Jones Reception and Memorial Award Lecture**	Reception in the Berrill Café
1800			Barrie Jones Award public lecture
1900			Leave the OU for dinner
2000		**Dinner at Kents Hill Park**	Booked with registration
2130		Ceilidh at Kents Hill Park	Included with dinner Ceilidh and lounge bar open to all

24th – Oral presentations and Community forum

		Session	
0900		Morning Tea	
0920	**14**	**The Earth and the Moon**	Oral presentations, Q&A Berrill Lecture Theatre
1100		Teas and pastries	Posters in the library
1130	**15**	**Venus and Mercury**	Oral presentations, Q&A Berrill Lecture Theatre
1300		**Lunch**	Posters and lunch in the library
1400		**Community Forum**	Community reports Society reports The future of BPSC Berrill Lecture Theatre
1600		**Closing remarks**	
1600			Clearance of posters

BPSC 2022

Abstract listings

Day 1, 22nd June

1130	**Session 4**		**Icy Satellites**	
1130	***Carly Howett***	***26***	***Exploring the outer solar system with space robots***	***40***
1145	*Q+A*		*5 min.*	
1150	Oliver King	27	Compositional Mapping of Ganymede with VLT/SPHERE using Markov Chain Monte	41
1200	Georgina Miles	28	Looking for hotspots on Enceladus outside the South Polar Terrain	42
1210	Kat Dapré	29	Seismic detection of differing interior structures on Enceladus	43
1220	Rachael Hamp	30	Geochemical cycling of the subsurface environment of Enceladus	44
1230	Álvaro del Moral	31	Exploring Europa's biological potential using laboratory simulations	45
1240	*Q+A*		*10 min.*	
1250	**Session 5**	**1250**	**Lightning talk group 2**	
1	Katherine Shirley	32	Optimising Filter Bandpass Selection for the Thermal Infrared Imager on ESA's Comet Interceptor Mission	47
2	Neil Bowles	33	MIRMIS - The Modular Infrared Molecules and Ices Sensor for ESA's Comet Interceptor.	48
3	Lucy Wright	34	High Resolution Observations of Titan's Equatorial Dynamics using Cassini CIRS Spectra	49
4	Charlotte Alexander	35	Comparing atmospheric cloud models of Jupiter, can we reduce the degeneracy of this problem?	50
5	Nisha Ramkissoon	36	Constraining the composition of Europa's subsurface ocean from water-rock interactions	51
6	Michael Macey	37	Viable metabolisms in a simulated martian chemical environment	52
7	Velislava Ilieva	38	First insights into the chemistry and microbial community composition of salt plains in a potential Mars analogue site	53
9	Mark Fox-Powell	39	Entombment of microbial biomass within rapidly frozen fluid droplets relevant to the plumes of Enceladus	54
9	Anushree Srivastava	40	Two Novel Halobacillus Species were Isolated from the Laboratory Enrichments of Epsomite Crystal from Basque Lakes, BC, Canada	55
10	Anastasia Kokori	41	The ExoClock Project: an open integrated platform for maintaining the Ariel target ephemerides with contributions from the public	56
1400	**Session 6**		**Lightning talk group 3a**	
1	Victoria Levy	42	Development of a CubeSat system to supplement lunar prospecting missions	58
2	James Cole	43	Low Power Microwave Heating of Icy Lunar Simulants	58
3	Neil Bowles	44	The Lunar Trailblazer mission: Understanding the Moon's water	60
4	Nicholas Elkington	45	Radiometric Calibration for the Lunar Thermal Mapper on NASA's Lunar Trailblazer.	61
5	Donald Bowden	46	Spectroscopic Analysis of Askival, an Aqueously Altered Cumulate in Gale Crater	62
6	Donald Bowden	47	Raman Spectroscopy of Mars Analogue Samples from Þórisjökull, Iceland	63
7	Michele Rinaldi	48	Carbon speciation in Martian magma chambers	64
8	Javier Martin-Torres	49	The Department of Planetary Sciences at the University of Aberdeen	65
1415	**Session 7**		**Exploration and Mars**	
1415	***Kevin Olsen***	***50***	***Contemporary chemistry in the Martian atmosphere observed with the ExoMars Trace Gas Orbiter***	***67***
1430	*Q+A*		*5 mins.*	
1435	Jonathon Mason	51	Martian ozone and aerosol climatology from MY34 to MY36 as measured by the NOMAD-UVIS spectrometer	68
1445	Megan Brown	52	Impacts of Heterogeneous Chemistry on Vertical Profiles of Martian Ozone	69
1455	Kylash Rajendran	53	4D Transport of Hydrogen Chloride in the Martian Atmosphere	70
1505	Paul Streeter	54	Seasonal behaviour of Mars' northern polar vortex	71
1515	Roger Stabbins	55	Seeing Minerals Clearly: Learning Dimension Reductions on Spectral Reflectance Libraries for Efficient In Situ Multispectral Image Acquisition and Analysis	72
1425	*Q+A*		*10 mins.*	

BPSC 2022

1530	Session 8		Lightning talk group 3b	
1	Jack Wright	56	Combining spectral and morphostratigraphic units on Mercury: A case study of the Rachmaninoff basin area	74
2	Annie Lennox	57	Geological Mapping of Mercury's Bach-side (the south polar Bach Quadrangle, H15)	75
3	Alistair Blance	58	Mapping Mercury's Discovery Quadrangle	76
4	Benedict Hyland	59	Global Dust Storms on Mars: The Initialisation, Growth, and Categorisation of Global Dust Storms on Mars	77
5	Juan Alday	60	Searching for odd-hydrogen in the atmosphere of Mars with the ExoMars Trace Gas Orbiter	78
6	Miracle Israel Nazarious	61	Calibration of the HABIT (HabitAbility: Brine, Irradiation and Temperature) instrument	79
7	Miracle Israel Nazarious	62	DNA extraction and sequencing from liquid planetary analogues for in-situ life detection and characterization	80
8	David Slade	63	Methane production by a hydrogenotrophic methanogen in a simulated chemical martian subsurface environment	81
9	Alexander Barrett	64	Classifying Planetary Surfaces Using Deep Learning, Results From Martian Landing Sites.	82
10	Yu Tao	65	Subpixel-Scale Topography Retrieval of Mars Using Deep Learning	83
1545	**Session 9**		**Lightning talk group 3c**	
1	Graham Driver	66	Morphological Diversity of Glacier-Like Forms on Mars	85
2	Ben Cornford	67	Morphological complexity of Concentric Crater Fills on Mars: insights into glacial history	86
3	Nisha Gor	68	Geomorphological mapping and investigation of a mountain glacier in the Argyre Region, Mars.	87
4	Neil Arnold	69	Surface topographic impact of water bodies beneath Mars' south polar ice cap	88
5	Peter Fawdon	70	The geological map of the ExoMars rover landing site.	89
6	Stuart Turner	71	Carbonate formation in Gale crater, Mars: a thermochemical modelling perspective	90
7	Amy Dugdale	72	Impact-generated modification of the mineralogy at Oxia Planum	91
8	Emma Harris	73	Distribution and morphology of the dark capping unit in Oxia Planum, Mars	92
9	Savana Woodley	74	Tectonic shortening along the Chryse Planitia - Arabia Terra dichotomy.	93
10	Parks Bowen, Adam	75	Analysing fractured terrains at the Rosalind Franklin rover landing site Oxia Planum, and comparing these with those found at Gale Crater	94
11	Joel Davis	76	Ancient Alluvial Plains at Oxia Planum, Mars	95

Day 2, 23rd June

~Time	Author	No.	Title	Page
0920	**Session 10**		**Icy Bodies & Outer Solar System**	
0920	***Emma Bunce***	***77***	***The Future Exploration of Jupiter and Ganymede***	***97***
0935	*Q+A*		*5 mins.*	
0940	Leigh Fletcher	78	Flagship Mission to Uranus: Exploring our Closest Ice Giant System	98
0950	Michael Roman	79	Uranus and Neptune in the Infrared: Recent Observations and the Future with JWST	99
1000	Nicholas Teanby	80	External atmospheric water flux at Neptune and Uranus; constraints from Herschel/HIFI observations	100
1010	Conor Nixon	81	Observations of Titan with the James Webb Space Telescope (JWST)	101
1020	*Q+A*		*5 mins.*	
1025	Geraint Jones	82	The Comet Interceptor Mission	102
1035	Samuel Grant	83	Prediction and Detection of Solar Orbiter's December 2021 encounter with Comet Leonard	103
1045	Laura Buchanan	84	Probing Colour Transitions in the Primordial Kuiper Belt	104
1055	*Q+A*		*5 mins.*	
1130	**Session 11**		**Winchcombe & Carbonaceous Chondrites**	
1130	***Ashley King***	***85***	***The Fall, Recovery, and Initial Analysis of the Winchcombe CM Chondrite***	***106***
1145	*Q+A*		*5 mins.*	
1150	Luke Daly	86	Nano-scale heterogeneity in the extent of aqueous alteration within the Winchcombe CM chondrite fall	107
1200	Dan Haspel	87	Pushing the limits of SEM-based microanalysis for the characterisation of complex, heterogeneous meteorite microstructures	108
1210	Richard Greenwood	88	Cr, Cd, Te, Ti, Zn AND O-ISOTOPE COMPOSITION OF THE WINCHCOMBE (CM2) METEORITE	109
1220	John Bridges	89	Surface Melting Processes on C-class Asteroid Ryugu	110
1230	Catherine Harrison	90	Thermal History of Dehydrated CM Chondrites Reconstructed from their Fe-sulphide Grains	111
1240	*Q+A*		*10 mins.*	
1250	Monica Grady	91	Planetary Science in the UK: An update on LARES and CAFES	112
1400	**Session 12**		**Habitability and Life**	
1400	***Eva Stueeken***	***92***	***Reassessing Earth's oldest records of carbon and nitrogen cycling***	***114***
1415	*Q+A*		*5 mins.*	
1420	Craig Walton	93	The cosmic desert: exogenous sediments on Early Earth	115
1430	Toni Galloway	94	Carbon and Nitrogen Cycling within a Geothermal Mars Analogue	116
1440	Emily Bonsall	95	Reactive iron species and organic carbon interactions in planetary materials	117
1450	Matthew Davey	96	Cryophilic microorganism utilisation and analogues for space biology	118
1500	*Q+A*		*5 mins.*	
1505	Claire Guimond	97	Theoretical limits to land coverage on rocky planets	119
1515	***Andrew Rushby***	***98***	***(Some) Land and Ice Albedo Feedbacks and the Climate and Habitability of Terrestrial Planets Orbiting M-dwarf Stars***	***120***
1530	*Q+A*		*5 mins,*	
1600	**Session 13**		**Exploring Mars**	
1600	***Steven Banham***	***99***	***A primordial Scottish delta: a roadmap for assessing habitable environments on the ancient Martian surface?***	***122***
1615	*Q+A*		*5 mins*	
1620	Ondrej Kryza	100	The effect of salinity to propagation and morphology of small-scale mudflows in low pressure environment: Insights from laboratory simulations	123
1630	Peter Grindrod	101	An Updated Global Catalogue of Rayed Craters on Mars: Potential Source Locations for Martian Meteorites	124
1640	John Edgar	102	Mechanochemical generation of perchlorates on Mars.	125

1650	*Q+A*		*5 mins*	
1655	Elena Favaro	103	The Aeolian Environment of Oxia Planum	126
1705	Amelie Roberts	104	Reconstructing the palaeoenvironment of the sediment fan at Oxia Planum, Mars	127
1715	Joseph McNeil	105	The Former Extent of the Mawrth Vallis Phyllosilicates	128
1725	*Q+A*		*5 mins,*	

Day 3, 24th June

	Author	No.	Title	Page
0920	**Session 14**		**The Earth and the Moon**	
0920	***Romain Tartese***	***106***	***What have we learnt so far from the samples returned from the Moon by the Chang'e-5 mission?***	***130***
0935	*Q+A*		*5 mins,*	
0940	Samantha Bell	107	Identification of potential exogenously-derived components in Apollo 17 73002 continuous core thin sections using QEMSCAN mapping techniques	131
0950	Giulia Magnarini	108	Evidence of recent slope deformation and the lasting effect of local tectonic stress in Taurus-Littrow Valley, the Moon	132
1000	Csilla Orgel	109	Probability of accessing stable water-ice in the lunar south polar region	133
1010	Mukesh Chiman Bhatt	110	Legal Perspectives on In-Situ Resource Utilisation in Outer Space	134
1050	*Q+A*		*5 min,*	
1025	Auriol Rae	111	Dynamic Strength and Fragmentation during High-Rate Brittle Failure	135
1035	Liza Riches	112	Shock deformation in feldspar in the Chicxulub impact structure	136
1045	Safoura Tanbakouei	113	Raman mapping of shocked basalts from Lonar Crater, India: Evidence for diamond as a biosignature resulting from shocked organic carbon	137
1055	*Q+A*		*5 min,*	
1130	**Session 15**		**Venus and Mercury**	
1130	Richard Ghail	114	What Venus reveals about the nature of Earth-sized planets	139
1140	Aedan Baker	115	Composition-Induced Density Variations in the Venusian Crust and their Implications for Tesserae Formation	140
1150	Connor Hoad	116	Is Lada Terra the Site of a Venus Overturn Upwelling ZOne (OUZO)?	141
1200	Shubham Kulkarni	117	Retrieval of main cloud structure using Venera 13 and 14 descent probe data	142
1210	Martin, Cordiner	118	Searching for Phosphine in the Atmosphere of Venus using SOFIA GREAT	143
1215	*Q+A*		*5 mins,*	
1220	Benjamin Man	119	Newly discovered widespread extensional grabens on Mercury's compressional structures	144
1230	Graeme Hall	120	The Distribution of Peak-ring Basins on Mercury and their Correlation with the High-Mg/Si Terrane	145
1240	Annie Lennox & Alistair Blance	121	Ejecta flows on Mercury: Prevalence, significance, and timing of emplacement	146
1250	Dave Rothery	122	New Images from Bepi-Colombo	147
1255	*Q+A*		*5 min,*	
1400	**Session 16**		**Community session**	
1400	Robert Massey		Update from the RAS	
1415	John Bridges		STFC roadmap update	
1425	Jack Wright		ESA funding opportunities	
1435	James Endicott		SPAN update	
1445	Caroline Harper Sue Horne		UKSA space science and exploration updates	
1515	John Pernet-Fisher		UKPF update	
1525	Lee White & BPSC local organising committee		The Future of BPSC	

Session 1:

Meteorites

1. Update on Meteorites found by the Lost Meteorites of Antarctica Project

Joy, Katherine; MacArthur, Jane; Harvey, Thomas; Jones, Rhian; Evatt, Geoff; Almeida, Natasha; Malley, James; Greenwood, Richard; Findlay Ross; King, Ashely.

Presenting author institution: The University of Manchester

The Lost Meteorites of Antarctica Project [1,2] retrieved ~120 postulated meteorites from two expeditions to the Outer Recovery (OUT) Icefields and Hutchison (HUT) Icefields, named meteorite dense collection zones, in blue icefields located south of the Shackleton Mountain Range in austral summer 2019 and 2020 [1,2]. A goal of the Lost Meteorites project is to investigate the statistics for different meteorite groups in this previously unsearched part of Antarctica and to understand if there is a sampling bias for stony and iron/stony-iron meteorite types [3]. Thirty-one meteorites collected by the project have been classified to date [4]. Of the classifications so far, four are achondrites, including a eucrite, an aubrite and two mesosiderites, and 27 are chondrites. One of these chondrites is a carbonaceous CM-anomalous chondrite and 26 are ordinary chondrites (OC), including 14 H, 10 L and 2 LL chondrites. Antarctic studies show that field areas with smaller meteorite populations (<1000) have an overabun-dance of unusual meteorite types, whereas those where >1000 meteorites were collected converge at ~90% OC [5]. Our classifications so far have a similar OC abundance. Statistics of previous Antarctic collections show 0.83% are eucrites, 0.09% are aubrites and 0.13% are mesosiderites [4]. Our recovery of an aubrite and two mesosiderites from ~120 samples is higher than these values. This may be partly a result of observing a small sample population from only two different collection areas. Samples can be requested from the Meteorite Curator at the Natural History Museum (NHM), London.

References: [1] Joy K.H. et al. (2019) 50th LPSC, 2132. [2] www.ukantarcticmeteorites.com [3] Evatt G. W. et al. (2016), Nature Communications 7, 10679. [4] www.lpi.usra.edu/meteor/metbull.php [5] Corrigan C.M. et al. (2020) 51st LPSC, 2233.

Keywords: Meteorites, Antarctica, Chondrites

2. Source of Halogen Elements in Chondrules from Enstatite Chondrites

Baker Edward, Jones, Rhian; Villeneuve, Johan,

Presenting author institution: University of Manchester

Halogen elements play a critical role in controlling melting processes in planetary and planetesimal mantles. For example, by mole, Cl is twice as potent as water at reducing liquidus temperatures in silicate melts [1]. It is therefore important to understand the source and abundance of the halogen elements in the early stages of planet formation. In the early solar nebula, halogens were likely present as H-[F,Cl,Br] gas [2]. The distribution of halogen bearing solids through the inner solar system is determined by the condensation temperatures of their carrying phases, with more refractory phases found closer to the Sun. Estimates of 50 % condensation temperature (Tc) for halogens at 10^{-4} bar range from 390 °C for K-Iodide to 674 °C for F-apatite [2,3]. We seek to constrain the dominant solid carrier phases of halogens, by examining halogen abundances in the glassy mesostasis of chondrules. To infer the halogen-bearing phases in solid chondrule precursors, we must account for modifications that might have occurred during the transient heating that chondrules experienced, as well as any secondary processes that took place on chondrite parent bodies. Potential halogen-carrying phases present in chondrule precursors include alkali-halogen salts (e.g. NaCl, KI), djerfisherite $(K,Na)_6(Fe,Ni,Cu)_{25}S_{26}Cl)$, sodalite $(Na_4Al_3Si_3O_{12}Cl)$ and apatite $(Ca_{10}(PO_4)_6(OH,Cl,F)_2)$. Halogens will be concentrated into melt during crystallization, as halogens are incompatible in most silicate phases. Simultaneously, halogens will diffuse out of the chondrule, or they may condense into the melt, from the gas.

We measured halogen abundances in the glassy mesostasis of 14 chondrules from petrologic type 3 enstatite chondrites SAH 97072, LAR12156, LAR12252, EET90012, DOM14021 and Qingzhen. Glass compositions, including Cl, were measured using a Cameca SX5 FEG electron probe at the University of Oxford. F, Cl and Br were measured on a Cameca IMS 1280-HR SIMS and the CRPG, Nancy. Our EPMA data find Cl concentrations in chondrule mesostasis up to 5 wt.%. We do not find any correlation between the P and Cl content of mesostasis, as would be expected if apatite was the carrier phase. Cl and Br are well correlated with Na, suggesting NaCl or sodalite as a precursor. If halogens are carried by alkali salts rather than apatite, the T_c condensation temperature would be reduced, pushing the halogen condensation line away from the Sun [2,3]. Djerfisherite contains alkali metals and could also explain the correlation with Na.

Our SIMS data find the maximum and minimum concentrations of halogens are respectively: F, 1000 - 152 $\mu g.g^{-1}$; Cl, 42000 – 11 $\mu g.g^{-1}$; Br, 161 – 0 $\mu g.g^{-1}$. The Br/Cl ratio in glass from both chondrules in LAR12252 is super-chondritic. This is unlikely to be the result of terrestrial alteration because there is no change in Br/Cl with radius. The high Br/Cl ratio could be an artifact of evaporation during chondrule heating. We will investigate the competing effects of heat and material diffusion through diffusion modelling.

[1] J. Filiberto, et al. *Chemical Geology*, 2009, **263**:60. [2] B.J. Wood, et al. *American Mineralogist*, 2019, **104**:844. [3] H. Palme, et al. in *Treatise on Geochemistry: Second Edition*, 2013, **2**:15.

Keywords: Enstatite Chondrite, Chondrule mesostasis, Halogens, Diffusion

3. Bulk H2O abundance and D/H ratios of unequilibrated ordinary chondrites

Grant, Helen; Tartèse, Romain. Jones, Rhian. Marrocchi, Yves. Piani, Laurette.

Presenting author institution: University of Manchester

The origin and transport of water in the early Solar System is an important topic in both astrophysics and planetary science, with applications to astrobiology, planetary formation, and protosolar disk evolution. One of the most practical and efficient ways to investigate early Solar System processes is through the study of chondrites, stony meteorites that originate from asteroids formed within a few million years of the start of Solar System formation. Of particular interest are the unequilibrated ordinary chondrites (UOCs), which have been affected by very limited alteration since their formation. In addition, OC parent bodies formed in the inner protoplanetary disk [1], making OCs, and hence their parent bodies, ideal targets for understanding the origin(s) and distribution of water in the region where terrestrial planets formed. Despite being less aqueously altered than some of the carbonaceous chondrites (CCs), such as the CI, CM and CR groups, mineralogical evidence for aqueous alteration has nevertheless been found in both UOCs [e.g. 2-4] and their parent asteroids [5]. In addition to hydration, previous studies of the least altered UOCs reported very high D/H isotope ratios relative to other bodies in the Solar System, including CCs and terrestrial planets [6-7]. To investigate how this observation holds up with a wider sample set, and how water abundance and H isotope compositions vary with metamorphism, we measured the bulk H_2O content and D/H ratios of 21 UOCs (15 falls and 6 finds), spanning from petrologic subtypes 3.00 – 3.9 using isotope ratio mass spectrometry (IRMS) [7]. UOC falls of the lowest subtypes contain ≥ 1 wt.% water, and water abundance globally decreases with increasing thermal metamorphism. In addition, UOC falls of the lowest subtypes have elevated D/H ratios as high as the outer Solar System comets [6 & refs. within]. This does not easily fit with existing models of water in the protoplanetary disk, which suggest D/H ratios were low in the warm inner Solar System and increased radially [8]. This suggests that OC parent bodies accreted an additional D-rich icy component from either the outer protosolar nebula or injection of molecular cloud streamers [9]. The sharp decrease of D/H ratios with increasing metamorphism above subtypes 3.5 - 3.6 suggests that this D-rich component is subsequently destroyed through thermal alteration.

References: [1] Vernazza P. et al. (2015) *Asteroids IV*:617–634. [2] Hutchison R. et al. (1987) *GCA* 51:1875–1882. [3] Alexander C.M.O'D. et al. (1989) *GCA* 53:3045–3057. [4] Dobrică E. et al. (2019) *GCA* 244:292–307. [5] Jin Z. & Bose M. (2019) *Sci. Adv.* 5:1–9. [6] Alexander C.M.O'D. et al. (2012) *Science* 337:721–723. [7] Vacher L. et al. (2020) *GCA* 281:53-66. [8] Hallis L. (2017) *Philos. Trans. A Math. Phys. Eng. Sci.* 375:20150390. [9] Piani L. et al. (2021) *EPSL* 567:117008.

Keywords: Chondrites, D/H ratios, Unequilibrated ordinary chondrites, Water

4. Investigating Chondritic Clasts in Cumberland Falls Achondrite

Davies, Faye; Daly, Luke; Hallis, Lydia; Lee, Martin

Presenting author institution: University of Glasgow

Aubrite meteorites are brecciated fragments of the crust and/or mantle of a differentiated parent body which was composed of highly reduced material, [1;2]. Aubrites are of particular interest as there are no good candidates for the original parent body in our Solar System suggesting that many of the early formed planets did not survive the embryo-embryo collision during the Solar System formation [3]. Several aubrite meteorites have been noted to contain chondritic inclusions with Cumberland Falls being one of the more well-known as a polymict breccia containing both chondritic and achondritic fragments [4].

The techniques applied during this study are scanning electron microscopy (SEM) imaging, and quantitative energy-dispersive X-ray spectroscopy (EDS) analysis that were conducted at the University of Glasgow in the Imaging Spectroscopy and Analysis Centre to allow for the extraction of quantitative textural and chemical information as well as microstructural information of the sample.

The Cumberland Falls sample has three distinct lithologies that can be distinguished using EDS and SEM images. Each lithology is separated by a sharp boundary from the other lithologies, these lithologies are referred to as brecciated, shocked and chondritic sections throughout this study. The brecciated lithology exhibits the classic brecciated texture often associated with aubrites [1]. The brecciated lithology contains uniform euhedral pure enstatite pyroxene grains with an Mg# of 1.0 with an average grain size of 0.8 mm set in a finer-grained matrix with little to no signs of shock and/or deformation. The shocked lithology is also predominantly comprised of nearly pure enstatite pyroxene with an Mg# of 1.0 across the section with an average grain size of 0.4 mm. There is a greater abundance of shock related microstructures in this region with pyroxene grains containing abundant fractures. The chondritic lithology within Cumberland Falls consists of the main chondritic fragment that contains both barred olivine-pyroxene chondrules and Fe-metal, as well as four smaller clasts containing chondrules (~0.7mm) or Fe-rich metal blebs (0.17-0.3 mm) that are found within shocked lithology, the chondrules are predominantly composed of pyroxene and the Mg# ranged between 0.70-0.97. This large range of Mg# indicates that the chondritic lithology is unequilibrated and overlaps with several chondrite groups. Olivine present in the chondritic lithology had a Mg# of 1.00 this is constant with EH/EL chondrites [2]. Both the shocked and chondritic lithologies exhibit microstructures such as planar fractures within pyroxene that are consistent with shock stage three are heavily shocked to shocked stage three [5].

This presentation will explore the petrology and microstructures of each of the lithologies in more detail and aims to classify the chondritic component to provide further insight into the Cumberland Falls aubrite and the nature of chondritic material impacting the aubrite parent body.

[1] Gaffey, M.J. and Kelley, M.S, 2004 In Lunar and Planetary Science Conference [2] Weisberg et al., (2006) MEISSII [3] Raymond, S.N, O'Brien, D.P, Morbidelli, A. and Kaib, N.A (2009) Icarus [4] Binns, R. (1969) Meteorite research, Springer [5] Stöffler, D, et al. (1991) Geochimica et Cosmochimica Acta

Keywords: Achondrites , Aubrites, Cumberland Falls , Chondrites

5. History of Magmatism on the Angrite Parent Body

Rider-Stokes, Ben; White, Lee; Anand, Mahesh; Darling, James; Tartèse, Romain; Whitehouse, Martin; Franchi, Ian; Greenwood, Richard & Degli-Alessandrini, Giulia

Presenting author institution: The Open University

Introduction: Angrites consistute a group of alkali-delpeted, basaltic achondrites that are amongst the oldest igneous rocks in the Solar System. Based on their isotopic characteristics and clinopyroxene Fe/Mn ratios, it is suggested that they formed inward of Jupiter's orbit and that the angrite parent body (APB) was similar in size to asteroid 4 Vesta. Angrites have been divided into two subgroups, the rapidly cooled quenched angrites, which may in fact represent impact melts, and the slower cooled plutonic angrites. There are some angrites, however, that do not fit into either subgroups. In this study, we demonstrate how coupling quantified microstructural analysis through electron backscatter diffraction (EBSD) with radiometric ages (U-Pb & Pb-Pb) of angrites, the timing and severity of planetary processes on the APB can be empirically quantified, providing insights into its chronological evolution.

Methods: Electron microscope observations were undertaken using a Zeiss EVO MA10 LaB_6 scanning electron microscope at the University of Portsmouth and using a Zeiss Crossbeam 550 with an Oxford Instruments Symmetry 2 EBSD detector at The Open University. *In situ* Pb-Pb isotopic compositions of phosphates were measured using a CAMECA IMS 1280 ion microprobe equipped with a RF-plasma oxygen ion source at the NordSIMS facility in the Swedish Museum of Natural History, Stockholm. Quantitive mineral major element geochemistry was collected using a Cameca SX100 electron microprobe using a beam current of 20 nA, and an accelerating voltage of 15 kV at the Open University. *In situ* trace element abundances of olivine, pyroxene, and plagioclase were measured using a Teledyne Excite+ 193 nm ArF excimer laser ablation system coupled to an Agilent 8900 triple quadrupole ICP-MS at The University of Manchester.

Results: EBSD mapping of NWA 8535 (dunite) revealed simple microstructures and single orientations for the entirety of the sample. Band contrast images demonstrate strong diffraction with little degradation. Ca silico-phosphates within NWA 8535 yields an average Pb-Pb date of 4515 ± 30 Ma (2σ) with a MSWD of 0.111 (n = 4). The representative rare earth element (REE) abundances in NWA 8535 clinopyroxene are similar to other plutonic angrites, exhibiting a negative Eu anomaly (0.37). Olivine REE abundances also display similar patterns to other plutonic angrites.

Discussion and Summary: It was suggested that Angra Dos Reis, previously the youngest angrite, with an age of 4556.60 ± 0.26 Ma (2σ), constrained the timing of disruption of the APB, resulting in the dispersion of multiple smaller bodies. However, the Pb-Pb crystallisation age determined here for NWA 8535 implies prolonged magmatism for at least a further 40 Ma. The complete lack of deformation in NWA 8535 suggests that the Pb-Pb age records crystallisation and not an impact-reset age. Moreover, the similarities between REE abundances in NWA 8535 and other angrites implies that it is not a contaminated impact melt rock. Prolonged magmatism on the APB supports the proposition that the parent body was large, similar to/or larger than 4 Vesta. Other angrite meteorites have also been investigated using similar techniques, results of which will be presented during the meeting.

Keywords: Angrite, Achondrite, Early Solar System, EBSD, Chronology

6. The petrogenesis and isotopic composition of augite-rich basalt Northwest Africa (NWA) 13467: implications for martian crust and mantle processes

Staddon, Leanne; Darling, James; Righter, Minako; Lapen, Thomas; Dunlop, Joseph; Stephen, Natasha

Presenting author institution: University of Portsmouth

Martian meteorites currently represent the only direct samples of the martian crust, and have increased significantly in both number and petrological diversity in the last decade [1]. Despite this, the martian meteorite record remains heavily biased towards geologically young (< 0.6 Ga) shergottites, with meteoritic sampling of crust older than 2 Ga presently restricted to four lithologies that are petrologically distinct from younger samples: orthopyroxenite Allan Hills (ALH) 84001, regolith breccia Northwest Africa (NWA) 7034 and pairs, and two augite-rich shergottites NWA 7635 and NWA 8159 [2-5]. Thus, investigation of martian meteorites with unique petrological characteristics may provide critical insights into the long-term evolution of the martian crust and mantle, and potentially sample an important window of declining surface activity and habitability. Here, we report the petrogenesis of NWA 13467, a single, fusion-crusted stone purchased in Morocco in 2020. NWA 13467 possesses petrographic and geochemical features distinct from late Amazonian shergottites, but shares numerous physiochemical characteristics with previously described ~2.4 Ga augite-rich shergottites NWA 7635 and NWA 8159 [4,5].

NWA 13467 is an evolved (pyroxene Mg# ≤58) basalt derived from a mantle source characterised by depletion in incompatible trace elements (La/Yb_{CI} <0.3). The section analysed here possesses a variably equigranular to intergranular texture, and is composed of subhedral augite (~40 %), plagioclase (now diaplectic glass; ~42 %), olivine (~12 %) and silica (~4 %). Pigeonite is completely absent. Oxide assemblages are diverse, including pyrrhotite, ZnO-bearing chromite, ferric iron-poor ilmenite, trellis-exsolved titanomagnetite, and near endmember magnetite (< 1 wt.% TiO_2). Augite and olivine major and trace element compositions highlight a protracted magmatic history; our data indicate that early augite crystallisation and magmatic assimilation of sulphide-rich material [*e.g.,* 6] occurred at depth within the martian crust, prior to subsequent emplacement of the NWA 13467 melt at or near the martian surface. Subsoldius oxidation and chemical exchange are suggested by ubiquitous orthopyroxene-magnetite symplectites within olivine, olivine-augite Fe-Mg disequilibrium, and calculated Fe-Mg thermometry temperatures of 506-670 °C for olivine-chromite pairs. We propose that these signatures were likely produced by low-temperature modification (< 500 °C) at or near the martian surface, though note that investigation is ongoing. NWA 13467 therefore provides a new record of high- and low-temperature processes in the martian crust.

Ongoing work will employ Sm-Nd and Lu-Hf isotope systematics to elucidate the magmatic crystallisation age of NWA 13467, provide further insights into its mantle source, and confirm or preclude a genetic link with previously described augite-rich shergottites NWA 7635 and NWA 8159.

[1] Udry, A. *et al.* (2020) *JGR: Planets, 125*, e2020JE00652. [2] Lapen, T. J. *et al.* (2010) *Science 328,* 347-351. [3] Humayun *et al.* (2013) *Nature 503*, 513-516. [4] Lapen, T. J. *et al.* (2017) *Science Advances, 3,* e1600922. [5] Herd, C. D. K. *et al.* (2017) *GCA, 218,* 1-26. [6] Humayun *et al.* (2021) *52nd Lunar and Planetary Science conference,* abstract #1390.

Keywords: Mars, Shergottite, Geochemistry, Petrology, Isotope

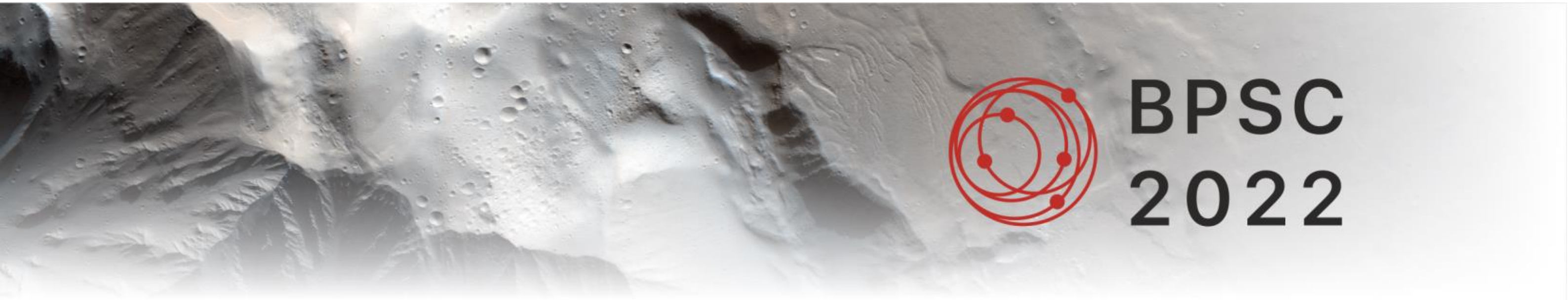

Session 2:

Lighting talk group 1a

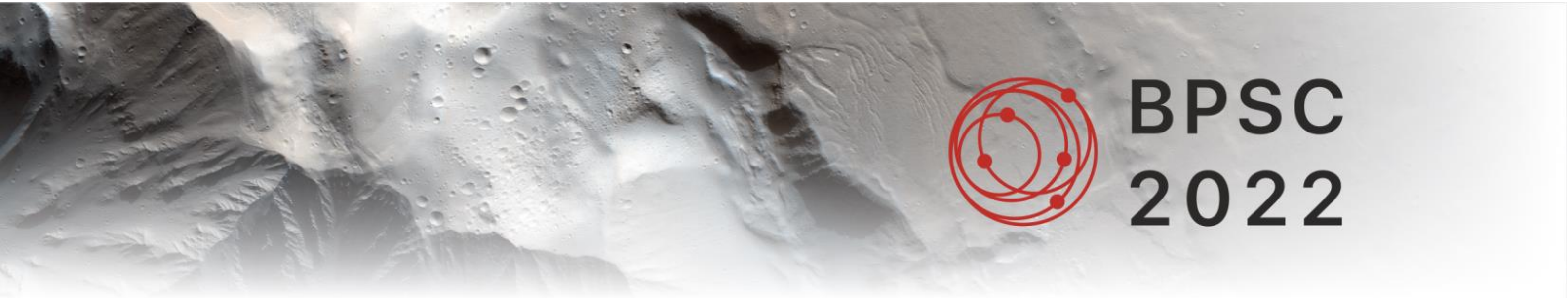

7. Fossil micrometeorites from residues of Devonian rocks from the Ural Mountains: New insights from old collections.

Gerallt Hughes; Sara Russell, Paul Schofield, Martin Suttle, C. Giles Miller, Natasha Almeida, Epi Vaccaro

Presenting author institution: Planetary Materials Group, Department of Sciences, Natural History Museum, London

Cosmic dust is the most voluminous type of extraterrestrial material which comes to Earth, and typically fall as micrometeorites (50-2000 µm). Modern micrometeorites can be found in urban environments, polar regions, and the deep seas; but increasingly are being recognised in the geological record as fossil micrometeorites (e.g., Onoue et al., 2011; Tomkins et al., 2016; Suttle and Genge, 2017). Fossil micrometeorites, incorporated into ancient sediments, can provide a record of past extraterrestrial flux to Earth and allow us to investigate post-depositional and diagenetic processes as well as provide insights into past atmospheric processes (Genge et al., 2008). In this project we used acid-digestion residues from a suite of late Silurian, Devonian to early Carboniferous rocks from the Ural mountains, (approx. 420-350 Ma). The well-constrained chronostratigraphy from previous micropalaeontological studies of this section provide insights into the extraterrestrial flux during this period. These deep-sea limestones have been processed and resistant I-type micrometeorites have been extracted and analysed. A total of 40 micrometeorites have been extracted and confirmed by textural analysis so far, and chemical analysis shows that these micrometeorites are typically composed of magnetite and Mn-bearing magnetite, similar to previous studies of fossil micrometeorites in ancient sediments (e.g., Cretaceous Chalk, Suttle and Genge, 2017). Further textural and geochemical analysis will be used to infer changes in the atmospheric oxidation during this crucial period in Earth's history; when the evolution of land plants led to increase in atmospheric O2 concentrations and decrease of CO2 in the atmosphere. This could provide novel insights and potentially a new climate proxy based on micrometeorites. Comparison between these fossil micrometeorites, and pristine Antarctic micrometeorites and geologically modern samples will provide constraints on the poorly understood processes during storage on the seafloor and during lithification (e.g., Suttle and Genge, 2017). Developing this fossil micrometeorite collection will enhance an existing world-leading repository of extraterrestrial material at the NHM and use previously overlooked samples from palaeontological collections, enhancing both collections simultaneously. Future sample return missions such as Hayabusa2 and OSIRIS-REx (Tachibana et al., 2014; Lauretta et al., 2017) will also return small particulate material from asteroids, and hence there is a necessity to establish a dedicated collection to study both modern and fossil micrometeorites and prepare protocols for future sample return material.

References Genge, M.J. et al., 2008. The classification of micrometeorites. Meteoritics & Planetary Science 43 (3), 497–515. Lauretta, D. S. et al., 2017. OSIRIS-REx: Sample return from asteroid (101955) Bennu. Space Science Reviews 212, 925–984. Onoue, T. et al., 2011. Composition and accretion rate of fossil micrometeorites recovered in Middle Triassic deep-sea deposits. Geology 39 (6), 567-570. Suttle, M.D. and Genge, M.J, 2017. Diagenetically altered fossil micrometeorites suggest cosmic dust is common the geological record. Earth and Planetary Science Letters 476, 132–142. Tachibana, S. et al., 2014. Hayabusa2: Scientific importance of samples returned from C-type near-Earth asteroid (162173) 1999 JU3. Geochemical Journal 48, 571–587. Tomkins, A.G. et al., 2016. Ancient micrometeorites suggestive of an oxygen-rich Archaean upper atmosphere. Nature 533, 235–238.

Keywords: Micrometeorites, Alteration, Curation, Cosmic Dust, Atmospheric Processes

8. Halogen Budget of Enstatite Chondrites

Peter Mc Ardle; Patricia L. Clay; Romain Tartese; Brian O'Driscoll; Ray Burgess

Presenting author institution: The University of Manchester

Enstatite chondrites (EC) are a rare class of meteorite which formed under extremely reducing conditions within the protoplanetary disk [1]. Their composition and mineralogy reflect these formation conditions, including Mg-endmember silicates and lithophile-bearing metal and sulfides. Based on their similar chemical and isotopic compositions, EC were likely a major contributing component during Earth's accretion [1]. Despite their inner Solar System origin, they also contain significant quantities of volatiles [2]. EC formed broadly contemporaneously with other chondrite groups and some were subject to very early shock and/or thermal metamorphism (4.50 Ga) [3, 4] and some to much later shock and/or thermal metamorphism (2.10 Ga) [3]. The oldest ages have been obtained from the I-Xe (4.56 Ga) [4] and Mn-Cr (4.55 Ga) [5] isotopic systems, with Rb-Sr and Ar-Ar generally recording younger ages [6]. At a high level, this variability is controlled by both variable isotopic closure temperatures and retentivity of host phases [6].

This study includes a correlated halogen and multi-system geochronology analysis of selected EC meteorites. Djerfisherite, a K- and Cl-bearing-sulfide, is the primary target. It contains the highest potassium concentration of any phase occurring within enstatite chondrites and is also an important halogen carrier. When present, djerfisherite is expected to exert a considerable control on the Rb-Sr and Ar-Ar dating systems.

EH3 meteorites with a low shock stage and weathering grade have been targeted. Four EH3 meteorites, Klein Glacier 98300, Dominion Range 14021, Larkman Nunatak 12252, and Miller Range 07028 were selected for analysis. Most of these meteorites have been the subject of only limited study to date. Therefore, their mineralogy and chemistry will be used to aid detailed characterisation studies. Djerfisherite has been identified in DOM 14021, LAR 12252 and MIL 07028, but is absent in KLE 98300. Results from this study have confirmed the petrologic type of each of these meteorites, however initial results indicate additional complexity in the characterisation of KLE 98300.

Rb-Sr dating of terrestrial djerfisherite via LA-ICP-MS as per [7] is in progress, prior to the analysis of the meteorite samples. Whole rock meteorite samples are being prepared for neutron-irradiation for Ar-Ar dating and quantification of halogens via CO2 laser stepped heating and noble gas mass spectrometry [8]. A later stage of the study will apply in situ halogen quantification and Ar-Ar dating to djerfisherite and other phases. The correlated in situ dating and halogen quantification approach in this study will prove a valuable means to further our understanding of volatile distributions and processes in the early inner Solar System.

References**:** [1] Weisberg M.K. and Kimura M. (2012) Chemie der Erde 72:101-115. [2] Piani L., et al. (2020) Science 369:1110-1113. [3] Torigoye N. and Shima M. (1993) Meteoritics 28:515-527. [4] Hopp J., et al. (2016) Geochimica et Cosmochimica Acta 174:196-210. [5] Hopp J., et al. (2021) Geochimica et Cosmochimica Acta 310:79-94. [6] Hopp J., et al. (2014) Meteoritics & Planetary Science 49:358-372. [7] Gorojovsky L. and Alard O. (2020) Journal of Analytical Atomic Spectrometry 35:2322-2336. [8] Ruzié-Hamilton L., et al. (2016) Chemical Geology 437:77-87.Chondrites,

Keywords: Early Solar System, Volatiles, Geochronology, Geochemistry

9. Applications of FIBSEM TOFSIMS: trace chemistry and isotope distribution in non-terrestrial samples analysis

Johnson, Diane; Bramley Kris, Kimpton Christine, Pope Steve

Presenting author institution: Cranfield University

Introduction: Time Of Flight Secondary Ion Mass Spectrometry (TOFSIMS) is a highly sensitive surface analysis technique, that produces highly reproducible data, with generation of large amounts of data on a timescale of minutes and has been established as a useful technique in cosmochemistry (1,2). When combined as a fully integrated detector within a dual beam Focused Ion Beam Scanning Electron Microscope (FIBSEM), the SEM is used to identify features of interest and the FIB used as the primary ion source to generate secondary ions from the sample surface. The FIB scans across a defined number of frames, each subsequent frame containing data representing a slightly greater depth of sample than the previous because of the slight milling effect of the FIB. When operated with small beam currents it results in very limited sample destruction or used with higher beam currents can be used to produce topographic 3D datasets, where x, y and z resolution can easily be achieved on a nm scale (3).

In this study we show FIBSEM TOFSIMS data from a range of meteorite sample types to illustrate the microstructural chemistry and isotope distributions in 2 and 3 dimensions with supplementary and complimentary SEM-EDS data.

Method: A range of meteorite samples from iron meteorites to carbonaceous chondrites were prepared into polished resin blocks and gold coated. SEM was used to examine the samples to identify target features of interest to explore in detail, SEM-EDS was performed producing element maps to define these sites of interest, TOFSIMS data was then recorded from these same areas. This analysis was performed on a Tescan Solaris X with integrated Tofwerk TOFSIMS detector collectively producing secondary electron image data stacks, corresponding TOFSIMS 3D data, mass spectra and depth profiles produced for selected elements as required.

Discussion and Results: The SEM-EDS data gave insightful results, but in structures such as fine intergrowths, small inclusions, trace level concentration elements and isotopes the TOFSIMS gave exceptional quality data uniquely defining the sample. The TOFSIMS data was also recorded to show these structures in 3 dimensions, this data being subsequently examined by tomographic reconstruction to further interrogate the dataset giving insight to microstructural formation processes.

Conclusions: FIBSEM TOFSIMS systems are incredibly useful technology in application to planetary science samples, they can resolve structures on a sub-micron scale, including light elements, trace chemistry and isotopes. The technique is typically very data rich, during a single experimental run it can produce a secondary electron image stack, TOFSIMS 3D data, mass spectra and if appropriate this data can be easily interrogated to show depth concentration profiles of any given element detected.

References: (1). Stephan T., Planetary & Space Science, 49, 9, Aug 2001, 859-906, (2). Stephan etal. Earth & Planetary Science Letters, 128, 3-4, Dec 1994, 453-467, (3). Pillatsch L., Ostlund F., Michler J., Progress in Crystal Growth and Characterization of Materials, 65, 1, Feb 2019, 1-19.

Keywords: TOFSIMS, FIBSEM, trace chemistry, isotopes, meteorite

10. Constraining Pre-Imbrian Bombardment History With Comparative In-Situ Chronometry of Accessory Minerals

Černok Ana; Dürr, Tobias; Vanderliek, Dennis; Becker, Harry; Rocholl, Alexander; Schwarz, H. Winfried; Whitehouse, Martin; Cayron, Cyril; Darling, James; White, Lee; Anand, Mahesh

Presenting author institution: Freie Universität Berlin, Germany

Introduction: The surface of the Moon provides a unique record of the impact history of the inner Solar System. Through the measurements of CSFD and isotopic dating studies of ancient Apollo impact breccias, lunar crater-chronology is best established for the period between 4 and 3 billion years ago (Ga). However, absolute chronologies based on CSFD and isotopic dating have been subject to interpretative biases and remain poorly constrained for ages >3.9 Ga. To address these caveats we aim at better understanding when the oldest known basins on the Moon formed and in which samples to find evidence for them. Our goal is to refine evidence for ancient impacts predicted by melt distribution in the lunar near-surface (SPA, Serenitatis, and Crisium) at the Apollo 14–17 sites and resolve this from the predominating and omnipresent Imbrium melt.

Approach and samples: Ancient basin-forming events are mostly preserved in complex impactites. However, multiple events can sometimes be resolved within a single sample. For instance, recent studies of Apollo 15–17 impactites revealed complex ages: different mineral isochrons yielded ~4.2 Ga (A16, A17) while U-Pb ages of zircon and baddeleyite (re-)crystallized by impact-induced processes yielded ages ≥4.2 Ga (A15, A16). Both these geochronometers contrast with the Ar-Ar dates, which make up the ~3.9 Ga impactite age peak reflecting resetting by the Imbrium impact (dated at 3922 ± 12 Ma). It is therefore essential to avoid geochronological bias by performing comparative dating using multiple chronometers. In particular, the ancient ages of impactites are most robustly revealed by in situ dating of accessory minerals baddeleyite, zircon, or phosphates. We performed a comparative analysis of Apollo 16 (60035 and 67415) and Apollo 17 (78235 and 78236) impactites. Complex Apollo 16 breccias rich in highland material have been targeted to reveal lithostratigraphic relationships of Cayley Plains (60035) and Descartes (67415) formations. Shocked norites from Apollo 17 have been targeted to understand if ages clustering at 4.33 Ga is associated with impacts or magmatic emplacement.

Methods: In situ U-Pb and Pb-Pb dating of accessory minerals was performed by SIMS at GFZ Potsdam, HIP Universität Heidelberg, and at NordSIMS in Stockholm. In addition, lattice orientation, internal microstructure, and structural disorder of selected baddeleyite grains were studied by EBSD at the University of Portsmouth and at the Open University. The obtained EBSD microstructural data were analyzed through ARPGE and GenOVa phase reconstruction packages.

Results and outlook: Analyses of polymict anorthositic breccia 60035 (Cayley Plains) revealed dominant pre-Imbrium material in all accessory phases (~4.2 Ga), and minor heating at Imbrium recorded by phosphates (agreeing with previous Ar-Ar data). On the other hand, noritic anorthosite breccia 67415 (presumably Descartes Formation) shows that dominant and omnipresent Imbrium ejecta (recorded by phosphates and previously by Ar-Ar) was mixed with 4.2 Ga material (recorded by zircon and baddeleyite). This suggests that in situ U-Pb ages obtained on complex breccias may record previous impact events and cannot be used to constrain the ages of ejecta units. Regarding Apollo 17 norites, detailed microstructural analyses imply that 4.33 Ga ages can be associated with a basin-forming impact.

Keywords: pre-Imbrian, accessory mineral, In situ dating, lunar , breccia

11. Thermophysical properties of the OSIRIS-REx sample site

Rozitis, Ben; Ryan, Andrew J.; Emery, Joshua P.; Nolan, Michael C.; Green, Simon F.; Christensen, Phil R.; Hamilton, Victoria E.; Daly, Mike G.; Barnouin, Olivier S.; Lauretta, Dante S.

Presenting author institution: School of Physical Sciences, The Open University

NASA’s OSIRIS-REx (Origins, Spectral Interpretation, Resource Identification, and Security – Regolith Explorer) spacecraft successfully sampled asteroid (101955) Bennu on 20 October 2020 and will return the sample to Earth in 2023. Before sample collection, the OSIRIS-REx Thermal Emission Spectrometer (OTES; 6 to 50 µm) mapped variations in brightness temperature across the Nightingale sample site at high spatial resolution (2 to 9 m per spectrometer spot). To interpret this temperature dataset, we applied the Advanced Thermophysical Model (ATPM) to the 20-cm-scale digital terrain models of Nightingale derived by the OSIRIS-REx Laser Altimeter (OLA). From model-to-measurement comparisons, we find that the observed brightness temperatures depend strongly on small-scale topography, the observation phase angle, and local variations in thermal inertia. Subsequent thermal inertia mapping finds evidence of cm-scale particles mixed with porous boulders within the sample site, and identifies boulders of different porosity and surface texture surrounding it. Diurnal and seasonal temperature modelling of the site sampled indicates that the collected material will have likely undergone only minimal alteration by heating from the Sun. We predict that the OSIRIS-REx sample will have unique thermophysical properties in comparison to the existing meteorite collection.

Keywords: OSIRIS-REx, Bennu, Sample site, Temperature, Thermal inertia

12. Exploration of Spectral Unmixing Algorithms to Estimate Asteroid Surface Composition

Brown, Eloïse C.; Bowles, Neil; Donaldson Hanna, Kerri; Shirley, Katherine; Lowry, Vanessa

Presenting author institution: University of Oxford

Introduction: Linear spectral mixing is currently the most widely used model in compositional analysis of mineral mixtures using thermal infrared (TIR; 5-25um) spectroscopy. Under the linear mixing assumption, spectral features from the individual component minerals (end-members) sum together linearly (weighted by their abundances) to form the spectrum of their mixture [1,2]. This forms the basis of the inverse problem (spectral unmixing) to try and retrieve composition of a mixture given a library of end-member spectra (the spectral library). Spectral unmixing is a powerful concept, but the current choice of model and algorithm combination most widely used is known to be insufficient for several applications, such as those where mixtures are dominated by fine grains (<60um). Thus, this raises the question: do we need a new/different model, or just a new/different algorithm?

My project: The main goal of this project has been to explore unmixing algorithms, particularly adopting a Bayesian approach. To do this I have experimented with a variety of different techniques and settled on developing three spectral unmixing algorithms: the weighted least squares with abundance sum constraint and iterative library reduction (this replicates the currently used Frequentist methods, e.g., [2], to form a baseline of comparison for other algorithms), a Markov Chain Monte Carlo (a fully Bayesian method that allows clear exploration of the parameter space), and optimal estimation with abundance sum constraint and iterative library reduction (also a Bayesian technique, but has similarities to the Frequentist least squares method, to provide a meeting point between Frequentist and Bayesian techniques). As an additional tool I have also used principal component analysis (PCA) to explore the similarities between end-member spectra as a source of degeneracy, and thus assess the validity of the linear mixing assumption.

Data used: The OSIRIS-REx Blind Test study presented spectral measurements of materials thought to be compositionally analogous to target asteroid (101955) Bennu [3]. For my project I have used these Blind Test data of mixtures, meteorites and end-members, as these are well characterised, making this an ideal dataset to compare a selection of algorithms. In the absence of end-member spectra, appropriate data were obtained from the online USGS and RELAB spectral libraries, and through private correspondence with Dr. Donaldson Hanna.

Key results so far: From my work with the three chosen algorithms, I have found that they performed roughly equally (based on fit quality metrics and retrieved abundance accuracy), suggesting that the underlying model of linear mixing is at the core of the problem and cannot be compensated for with increasingly sophisticated algorithms. This has led me to conducting a spectral morphology vs grain size study in order to work towards an empirical parameterisation of the linear mixing model which will form an improvement for finer grain sizes whilst retaining computational efficiency.

This proposed presentation aims to outline my thesis, highlighting key results.

References: [1] Lyon R. J. P. (1964) NASA Contractor Report CR-100. [2] Ramsey M. S. and Christensen P. R. (1998) JGR 103:577-596. [3] Donaldson Hanna K. L. et al. (2019) Icarus 319:701-723.

Keywords: Spectral Unmixing, Asteroid Composition, TIR Spectroscopy, Algorithms, PhD Thesis

13. The pursuit of elusive extraterrestrial liquid water in astromaterials

Krizan, Peter A.B.; Chan, Queenie; Gough, Amy; Papineau, Dominic

Presenting author institution: Royal Holloway, University of London

Since the breakthrough discovery of the first samples of liquid extraterrestrial water in the Zag and Monahans (1998) ordinary chondrites [1], there has been great speculation as to whether any additional direct water samples exist in other astromaterials. We now understand that transient water is present and significantly abundant throughout the Solar System - predominantly in the form of solid ice - an observation which lies consistent with the extensive evidence of aqueous alteration seen in primitive meteorites [2]. Nonetheless, it still remains unknown if any more of these extraterrestrial liquid water samples exist, but also why they continue to evade detection, despite the apparent widespread influence of hydrothermal alteration in the Solar System. Recent studies concerning extraterrestrial liquid water and its evolution throughout the Solar System have attempted to gather inferences on the hydrothermal histories of parent asteroid bodies by utilising different proxies (such as magnetite grains, hydrous minerals, and degree of thermal metamorphism). Such studies have only highlighted the lack of direct water samples used within research and the need to determine whether further extraterrestrial liquid water fluid inclusions exist.

Here, we present our findings from our initial assessments of previous unsubstantiated claims of fluid inclusions within a wide range of meteorites and their likelihood of containing true liquid water. We analysed one achondrite meteorite (Allan Hills A77256) and eight chondrite meteorites (Allan Hills 84029, Bells, Lonewolf Nunataks 94101 & 94102, Mighei, Santa Cruz, Sutter's Mill, Sayama). We show that both petrographically primary and secondary fluid inclusions are observed to be hosted within olivine crystals, as well as the initial compositional analyses of the trapped fluids in suitable inclusions (diameter >1μm) - using a combination of Raman spectroscopy and SEM-EDS. In addition to this, we also present evidence for an unexpected discovery of cosmic diamonds within the Bells meteorite and the observable evidence to support their legitimacy and relative age. Overall, this research highlights that numerous factors can affect the probability of a fluid inclusion hosting liquid water.

[1] Zolensky, M. E., Bodnar, R. J., Yurimoto, H., Itoh, S., Fries, M., Steele, A., ... & Ito, M. (2017). The search for and analysis of direct samples of early Solar System aqueous fluids. *Philosophical Transactions of the Royal Society A: Mathematical, Physical and Engineering Sciences*, *375*(2094).

[2] Tsuchiyama, A., Miyake, A., Okuzumi, S., Kitayama, A., Kawano, J., Uesugi, K., ... & Zolensky, M. (2021). Discovery of primitive CO2-bearing fluid in an aqueously altered carbonaceous chondrite. *Science Advances*, *7*(17).

Keywords: Fluid Inclusions , Extraterrestrial Water , Raman Spectroscopy , Astromaterials , Cosmic Diamonds

14. Aqueous alteration on carbonaceous asteroids – insights from hydrothermal experiments

Suttle, Martin; King, Ashley; Ramkissoon Nisha; Bonato, Enrica; Franchi, Ian; Malley, James; Schofield, Paul; Najorka, Jens; Salge, Tobias; Russell, Sara

Presenting author institution: The Open University

We performed long duration hydrothermal alteration experiments to simulate early solar system geological activity on water-rich C-type asteroids. This investigation explored how environmental variables (water-to-rock ratio and temperature) affected the style and extent of aqueous alteration. Whole rock chips of carbonaceous chondrite (CO3.2 Kainsaz) were used as the anhydrous protolith. These were mixed with pure water and sealed in Teflon reaction vessels for 175 days. A series of 11 experimental runs tested a range of water-to-rock ratios (W/R: 0.2 to 0.8) at two different temperatures (50°C and 150°C). In addition, isotopically doped ^{17}O-rich heavy water ($\delta^{17}O$: +64.5‰) was used in five experiments, adding an isotopic perspective. Slow gas escape from the reaction vessels affected all runs and resulted in partial open system conditions.

Our experimental products record an oxidizing Fe-alkali metasomatic environment whose mineral assemblages, textures and isotopic properties are relevant to the CM and CV chondrite parent bodies. The main secondary minerals formed were Fe-oxyhydroxides (goethite) and Fe-oxides (magnetite), with lesser quantities of Fe-sulphides. Minor phases formed include fayalite, sulphates (gypsum and Fe-sulphate) and calcite. Limited amounts of low crystallinity phyllosilicates were generated at 150°C. Mg-rich anhydrous silicates were chemically unaltered but show evidence of hydrothermal fracture. Meanwhile chondrule mesostases were unaffected. The first phase to react was kamacite which readily dissolved, donating Fe and Ni to the fluid phase. Nanophase Fe-sulphides formed within the matrix, while pre-existing pyrrhotite group sulphides experienced Ni enrichment (<3 at.%). Among the high temperature samples sulphides were also partially oxidized, lowering their (Fe+Ni)/S ratio. Furthermore, Ni-rich pyrrhotites (Ni >10 at.%) were formed in the 150°C samples by sulphidation of taenite.

Alteration of the fine-grained matrix reduced porosity and increased the average atomic weight. A striking feature of our experiments was the presence of minimally altered fine-grained matrix found in direct contact with zones of heavily altered matrix. We suggest pregnant fluid solutions readily reacted with unaltered matrix resulting in efficient depletion of dissolved ions (Fe^{2+} and S^{2-}) and leading to the development of highly localized alteration fronts. These formed large ~100µm wide networks that reveal zones of preferential fluid movement through the rock. These textures resemble features previously described in some CM chondrites and the ungrouped CO-like chondrite MIL 07687.

The effects of open system loss notwithstanding, our experiments demonstrate that more advanced alteration is correlated with higher initial W/R ratios. The use of ^{17}O-rich water allowed the isotopic effects of aqueous alteration to be tracked. Bulk rock compositions evolved towards the initial water composition, reflecting the incorporation of heavy oxygen into hydrated minerals. However, altered samples shifted in $\delta^{18}O$ space, reflecting the competing effects of water-mineral fractionation and mass fractionation due to the preferential escape of isotopically light water.

Keywords: Carbonaceous Chondrites, Aqueous Alteration, Experimental, Geochemistry

15. Relict forsterite in unequilibrated enstatite chondrites

L. C. Zenie, N. V. Almeida, I. A. Franchi, M. Grady, A. J. King, T. Salge, P. F. Schofield and S. S. Russell

Presenting author institution: Planetary Materials Group, Natural History Museum

Introduction: Enstatite chondrites (ECs) are thought to represent the material present in the accretion regions of the terrestrial planets [1]. However, ECs contain unique mineral assemblages which indicate that they formed under much more reduced conditions than Earth. It has long been assumed that ECs formed from material condensed at supersolar C/O ratios, however, recent trace element work suggests that ECs may have instead formed from precursors that formed in a more oxidising environment [2]. Later processing of these precursors in an unusually S (and other volatile)-rich and O-poor environment may then explain the highly reduced nature of ECs [2, 3]. ECs may, therefore, record an evolving nebular composition from oxidising to reducing conditions. Several relict forsterites in primitive unequilibrated ECs have been analysed to explore this hypothesis.

Method: Polished sections of Dominion Range 14021 (EH3; section #11) and Larkman Nunatak 12156 (EH3; section #6) were studied using a ZEISS Evo 15LS SEM. Large area elemental mapping was carried out with an Oxford Instruments Aztec EDS system to locate olivine grains. High-resolution cathodoluminescence (CL) imaging has been performed with a Gatan ChromaCL system, at 10kV accelerating voltage, 3nA beam current and at a distance of ~1 mm from the CL detector.

Findings: Anhedral to subhedral forsterite grains poikilitically enclosed in enstatite were identified and imaged in DOM 14021,11 and LAR 12156,6 with the abundance and largest grain in each sample measuring (~2-30%; ~0.2×0.2 mm) and (~2-15%; ~0.26×0.33 mm) respectively. The size and morphology of the forsterite grains enabled the prioritization of porphyritic olivine-pyroxene (POP) chondrules for CL imaging. All chondrules analysed for CL are type I, FeO-poor with $Fo_{(>98.7)}$. Red and blue CL observed in the chondrules of both samples indicate varying concentrations of trace elements in the forsterite grains.

Implications: Several isolated dusty forsterite grains in DOM 14021,11 and LAR 12156,6 exhibit blue CL, in disequilibrium with their host chondrule, thus suggesting a relict origin [4]. Forsterite grains with red-CL cores surrounded by blue-CL rims were also identified and are indicative of relict cores with an overgrowth of a chondrule melt enriched in trace elements [5]. The identification of relict grains within the chondrules of ECs supports the hypothesis of an evolving solar nebula. Our work will advance to the analysis of trace element concentrations and oxygen isotopic variations of the relict grains. This analysis will provide further understanding of the origin and history of relict grains and subsequently the evolving composition of the EC formation region.

References [1] Bizzarro M., et al. (2017) In: Pessah M. and Gressel O. (Eds) Formation, Evolution, and Dynamics of Young Solar Systems. Switzerland; Springer. [2] Jacquet, E., et al. (2018) In: Russell, S. S., Connolly Jr, H. C. and Krot, A. N. (Eds) Chondrules: Records of Protoplanetary Disk Processes. Cambridge, UK: Cambridge University Press. [3] Weisberg, M. K. and Kimura, M. (2012) Chemie der Erde, 72, 101-115. [4] Steele, I. M. (1986) Geochim. et Cosmochim. Acta 50, 1379-1395. [5] Kita, N. T., et al. (2010) Geochim. et Cosmochim. Acta 74, 6610-6635.

Keywords: Chondrite, Chondrule, Forsterite, Relict, Cathodoluminescence

Session 3:

Lighting talk group 1b

16. The Redistribution of Sulphur in Secondary Minerals of Winchcombe and other CM Chondrites

Bridges, John; Hicks, Leon

Presenting author institution: University of Leicester

The rapidly recovered Winchcombe CM chondrite regolith breccia fall gives the opportunity to analyse the secondary alteration phases of this meteorite type in great detail, without the effects of terrestrial contamination. A key part of determining the record of parent body water-rock reactions is studying the mineralogy of phyllosilicates with SEM, (S)TEM-EDX and XAS to determine their structure and cation site occupancies including Fe^{2+}/Fe^{3+}. Linked to the secondary alteration and phyllosilicate mineralogy is the redistribution of sulphur, a process which has been linked to the extent of hydrous alteration [1]. Here we consider the identity and assemblages of secondary S-bearing phases - serpentines and tochilinite - in a polished section of Winchcombe in order to better understand the alteration histories of CM chondrites and the nature of their serpentine-like phases. We are also studying these phases of interest in a set of other fresh CM meteorites including the recent fall Aguas Zarcas.

As part of the Winchcombe analytical team, we have analysed clast and matrix in the section P30543 [1] at the University of Leicester Advanced Microscopy Facility. An initial investigation identified various locations of interest for further FIB-TEM analysis and XAS. FIB lift-out sections measuring up to 15 × 8 µm were extracted using a FEI Quanta 200 3D FIB-SEM, and thinned to ~100 nm attached to TEM Cu-grids for TEM analysis. High-resolution TEM imaging and STEM EDX was performed using JEOL 2100 TEM's. Fe K XANES and EXAFS were performed at Beamline I18 of Diamond Light Source on P30543 using the techniques described in [3,4] to quantify Fe^{3+}/SFe.

Although the hydrated sulphide tochilinite is present in small amounts as needle-like crystalline patches in this section, the dominant S-bearing low temperature phase is a S-bearing 1:1 structure serpentine. This can be distinguished from the tochilinite in composition, as tochilinite is ~43 wt% SO_3 whereas the S-serpentine is typically ~6-10 wt% SO_3. The S-bearing serpentine can in turn also be distinguished from S-poor serpentine in the same section by d_{001} spacings which are 0.62-0.70 and 0.70-0.74 nm respectively. The relatively scarce tochilinite has d-spacings of 0.54 nm. The S-poor and S-rich serpentine phases are both ferric, having Fe^{3+}/SFe 0.5-0.75. In contrast the tochilinite is more ferrous. We are studying the relative abundances and textural characteristics of S-bearing serpentine compared to bona fide tochilinite in Winchcombe and other CM's in order to provide fresh insights into the record of progressive water-rock reactions in their parent bodies.

[1] Suttle M. et al. 2022 MAPS in prep. [2] Daly L. et al. 2022 MAPS in prep. [3] Hicks L. J. et al. (2020) MAPS 55, 2599–2618. [4] Piercy J.D., Bridges J.C. and Hicks L.J. (2022) GCA 326: 97-118.

Keywords: Winchcombe, Cm chondrite, Mineralogy, Serpentine

17. Formation Conditions of Calcium-Aluminium-Rich Inclusions in Carbonaceous Chondrites: An Experimental Approach

Hammett, Megan; Jones, Rhian; Tartèse, Romain

Presenting author institution: The University of Manchester

Introduction: Calcium-aluminium-rich inclusions (CAIs) are the oldest solids (~4.567 Ga) in our Solar System, providing evidence of early protoplanetary disk processes and conditions [1]. Most CAIs formed by evaporation, condensation and aggregation of refractory mineral grains within a hot gas of solar composition, likely near the protosun [1]. Some CAIs were also melted [1], however, thermal constraints on melting conditions are not well understood. This has hindered agreement on models of CAI formation and how CAI melting relates to the formation conditions of chondrules. The best studied melted CAIs are Type B, found almost exclusively in CV (Vigarano-like) chondrites [2]. Type Bs mainly comprise of spinel, melilite, Ti-Al-rich pyroxene and anorthite, and have experienced multiple melting episodes [2]. Previous experiments on Type B analogues have established their equilibrium crystallisation sequence [3], and general constraints on the peak temperature and cooling rates based on the texture [4] and zoning patterns of melilite [5]. However, experiments with non-linear cooling rates or multiple stages of heating have not been explored. We aim to further constrain the formation conditions of Type Bs by reproducing the texture and mineralogy of natural CAIs, using experimental analogues.

Methods: Dynamic crystallisation experiments are performed in a Deltech one-atmosphere furnace. Starting materials were prepared from a mix of oxides (SiO_2, MgO, Al_2O_3, CaO, TiO_2) and trace element solutions (V, Cr, Mn, Li, Be, REEs) as outlined by [6]. The bulk composition is an average value of natural Type B bulk compositions obtained from [7,8]. Scanning electron microscopy (SEM) including imaging and elemental X-ray mapping was conducted on a FEI Quanta 650 FEG SEM.

Results: Experiments with a peak temperature of 1400°C and linear (constant) cooling rates between 1.5-50°C/hr exhibit a similar texture and mineralogy to natural Type Bs, consistent with [4,5]. We also produced good Type B analogues in a multi-stage experiment consisting of two heating cycles to peak temperatures of 1400°C and 1350°C, with cooling in both cycles at 11°C/hr. Experiments that did not successfully reproduce Type B textures include i) experiments at these same linear cooling rates (<50 °C/hr) from peak temperatures >1400°C, ii) experiments with faster linear cooling rates (60-150°C/hr) from a peak temperature of 1400°C, iii) a non-linear cooling rate experiment, varying from 1000°C/hr at 1400°C to ~350°C/hr at <800°C.

Conclusion: Our results support slow cooling of Type B CAIs from a peak temperature of 1400°C, consistent with literature values. We also show that faster cooling rates (>100 °C/hr), comparable to chondrule cooling rates [9], do not produce analogue Type B CAIs, indicating a different heating mechanism for CAIs and chondrules.

References: [1] Krot, A. (2019) *MAPS* **54**:1647-1691. [2] MacPherson, G. et al. (2022) *GCA* **321**:343-374. [3] Stolper, E. (1982) *GCA* **46**:2159-2180. [4] Stolper, E. and Paque, J. (1986) *GCA* **50**:1785-1806. [5] MacPherson, G. et al. (1984) *JG* **92**:289-305. [6] Beckett, J. et al. (1990) *GCA* **54**:1755-1774. [7] Beckett, J. (1986) *PhD Diss. UChicago.* [8] Srinivasan, G. et al. (2000) *MAPS* **35**:1333-1354. [9] Jones, R. et al. (2018) Chondrules: Records of Protoplanetary Disk Processes 57-90.

Keywords: refractory inclusions, calcium-aluminium-rich inclusions, chondrites, protoplanetary disk, experimental petrology

18. Curation Of The Winchcombe CM Chondrite Fall

Almeida, Natasha V.; Bates, Helena C.; King, Ashley J.; Smith, Caroline L.; Russell, Sara S.; UK Fireball Alliance; Winchcombe Consortium

Presenting author institution: Natural History Museum

Introduction: The Winchcombe meteorite fell on 28th February 2021. At 21.54, the fireball was witnessed across the UK and recorded by 16 stations operated by the six meteor camera networks of the UK Fireball Alliance (UKFAll), allowing for calculation of its strewn field and main belt source [1]. The event was widely observed by eyewitnesses and soon attracted considerable media attention. The first carbonaceous chondrite recovered in the UK, Winchcombe joins a short list of only 17 British falls for which material is known [2].

Recovery: The recovered material was initially examined by team members in the field, conducting home visits to potential finds and systematically searching the local area. Permission for minimally destructive analysis on the material was sought from all landowners. The quick response of UKFAll and associated media campaign was critical in raising awareness of how to identify a meteorite and how to handle specimens appropriately, resulting in many enquiries from the public. In total, approximately 602 g have been recovered from sites across an 8.5 km strewnfield.

Immediate curation: The first samples were received and placed into a desiccator at the NHM on the 4th. Samples were quickly curated, and are stored in glass vials with polyethylene lids, with fragments > ~100 mg individually weighed. Twenty-three of the largest fragments have been encased in high purity Al foil, placed in acid-free cardboard trays and stored in heat-sealed Escal enclosures with Mitsubishi RPK system oxygen scavengers.

Two stones (BM.2022,M1-85 and BM.2022,M1-86) were taken directly from the field to the Open University to facilitate swift oxygen isotope measurements and are stored in a nitrogen cabinet in a class 100 cleanroom, under long-term loan from the NHM.

Tracking subsamples: A total of 518.3 g have now been donated into the NHM collection. Specimens have been designated according to their find location and collection date. The subsamples are tracked with sequential numbers, similar to the NASA curatorial numbering system. The subsample relationship of any given fragment can be provided upon request to the curator. Thus far, 47 loans, a total of approximately 80 g (including non-destructive analyes) and 20 polished sections have been made available to the Winchcombe consortium, covering analyses including bulk properties, mineralogy and petrology of the different lithologies, fusion crust, organics, magnetics, reflectance spectroscopy, and terrestrial alteration, as well as C, N, O, Ti, Cr, H, Ne isotopic systems.

Long term curation: A nitrogen glove box (MBraun Labstar) with built-in microscope is on order and will be used for the permanent storage of the Winchcombe meteorite, funded by the Science and Technology Facilities Council (STFC), UK. Samples of the mud, lawn, and the original collecting vessels are all available as witness material. We welcome requests for scientific loans once the initial consortium work is published in a special issue of *Meteoritics and Planetary Science*.

References: [1] King A.J. et al., (submitted) *Science Advances* [2] Grady, M. M. (2000) Cambridge University Press. [3] Russell S.S. (in preparation) et al. *Meteoritics and Planetary Science*

Keywords: Curation, Carbonaceous chondrite, Meteorite fall

19. Investigating CM chondrite precursors in Lonewolf Nunataks 94101

R. Findlay; I. A. Franchi, R. C. Greenwood, M. Anand and M. D. Suttle

Presenting author institution: The Open University

Introduction: The water-rich CM chondrites are complex, heterogeneous breccias [1], containing clasts that have been altered to different degrees by the action of water [2, 3]. A pertinent question with regards to understanding the process of alteration is the nature, distribution and oxygen isotopic composition of the hypothesised CM precursor [2, 3]. Such a precursor would be 'pristine', unaltered and therefore of petrologic type 3.0 with a 'light' oxygen isotopic composition and spatial / geochemical evidence for a relationship to the extensively altered CM2s [2, 3]. Here, we present a petrographic and oxygen isotopic study of a large, near unaltered clast in the Antarctic find LON 94101. Our aim is to examine this clast to establish its link to CM2 material and related meteorites to further understand the nature of aqueous alteration on the CM parent bodies.

Methods: A large block (~100 g) of LON 94101 was examined using a Zeiss Crossbeam 550 FIB-SEM and the unusual clast was mapped in high-resolution mode. Approximately 350 µg of material was microsampled using a New Wave Instruments MicroMill, to be analysed for oxygen isotopes via laser fluorination in 'single shot' mode. A homogenized bulk sample (~300 mg) of LON 94101 was also analysed.

Results and Discussion: The clast shows little evidence of aqueous alteration and is sharply juxtaposed against a highly altered (~ CM2.2) lithology rich in phyllosilicates. It consists of metal rich, porphyritic olivine and olivine/pyroxene chondrules; fragments of both zoned type II fayalite grains; and fragments of barred olivine chondrules. Sulphide and metal are evenly distributed throughout the clast in and between chondrules as rounded blebs. The matrix is fine grained and is mostly anhydrous, evident by high analytical totals (> 95 %). However, very thin (10s µm) veins of iron rich phyllosilicate cross cut the matrix throughout the whole clast, suggesting incipient alteration occured. The oxygen isotope composition of bulk LON 94101 plots in the CM2 field at the moderately / heavily altered end [4,5], consistent with its CM2 classification. However, the clast is approximately 6 ‰ lighter in $\delta^{18}O$ and plots on the opposite end of the array, close to the CCAM, in a space that is occupied by both the Asuka CMs (the most pristine CM chondrites yet analysed) [6] and a cluster of C2-ung measurements [5]. This clast preserves evidence of an early and potentially short-lived episode of alteration and represents a novel spatial relationship between altered and unaltered CM material. This finding suggests that CM precursors may be more akin to weakly altered C2-ungrouped meteorites than CO chondrites [e.g. 7].

References: [1] Bischoff A. et al., (2006) *MESS II* 679-712. [2] Rubin A. et al., (2007) *GCA 71*, 2361-2382. [3] Suttle M. et al., (2021) *GCA* 299, 219-256. [4] Clayton R. N. and Mayeda T. K. (1999) *GCA 63*, 2089-2104. [5] Greenwood R. C. et al., (2019) *LPSC 50* abst #3191. [6] Kimura M. et al., (2020) *PS* 26 100565. [7] Torrano Z. A. et al., (2021) *GCA* 301, 70-90

Keywords: Chondrite , CM, Aqueous Alteration , Asteroid , Carbonaceous

20. Functional chemistry and morphologies of pristine organic matter within the Winchcombe meteorite

C.L. Bays, A.J. King, P.F. Schofield, C. Vollmer, J. Leitner, T. Araki, A.B. Mosberg, D. Kepaptsoglou, Q.M. Ramasse, Q.H.S Chan, and A.J. Dickson.

Presenting author institution: Planetary Materials Group, Natural History Museum, London, UK

Introduction: The Winchcombe meteorite was observed to fall in February 2021, becoming the first CM ("Mighei-like") chondrite to be recovered in the UK. It records early solar system fluid-rock reactions and contains ~2 wt.% carbon, with some present in organic matter (OM) [1]. The OM in carbonaceous chondrites is morphologically diverse, containing isotopic anomalies related to interstellar, nebula, and parent body processes [2]. It contains both soluble organic species and concentrated C- and N-rich regions, with globule-like morphologies in the matrix [1]. Due to Winchcombe's rapid recovery, it contains some of the most pristine OM in our collections.

Methodology: Carbonaceous materials were identified in the matrix using an FEI Quanta 650 scanning electron microscope (SEM). Regions of interest in intermediately and highly altered lithologies were then extracted and prepared as ultra-thin sections (~10 x 10 µm diameter, ~100 nm thickness) using a focused ion beam (FIB) system. A series of X-ray transmission images (STXM) across carbon (280-310 eV) and nitrogen (390-430 eV) K-edges were obtained from the carbonaceous materials, at a spatial resolution of ~50 nm on beamline I08 at Diamond Light Source, UK.

Results: STXM C K-edge spectra of all carbonaceous materials show strong absorption features indicative of aromatic/olefinic carbon (C=C, ~285 eV) and aldehyde/ketone (C=O, ~286.6 eV). Other features observed in some spectra include weak carboxyl functional groups (-COOH, ~288.5 eV) and, in a few cases, CO_3 (~291 eV) from the presence of carbonates. Several carbonaceous areas also showed strong N K-edge absorption features just below the main edge at ~400 eV, suggestive of C=N (imine) and/or C≡N (nitrile).

Discussion: Carbon functional chemistry of the OM is dominated by C=C and C=O bonding, similar to previously studied OM in other carbonaceous chondrites [2]. In the CM chondrites, OM in minimally altered lithologies often comprises a higher aliphatic:aromatic content [3, 4], with aromaticity increasing with progressive hydration. The presence of aromatic and carboxyl functional groups in the Winchcombe meteorite is, therefore, consistent with its classification as a partially altered CM2 chondrite.

The C=N and C≡N functional groups of some carbonaceous materials in Winchcombe are comparable to those identified in the CM2.6 chondrite Maribo but differ from typical meteoritic OM [5]. In Maribo, which overall is less aqueously altered than Winchcombe, a few organic particles are associated with nitrogen isotopic compositions ($\delta^{15}N \sim -200$ ‰) that may indicate an interstellar heritage [6]. Evidence of highly reactive [7] double and triple bonding within the nitrogen functional groups (imine and nitrile) supports observations of the pristine nature of OM within Winchcombe. Future work will therefore combine our initial results with the isotopic composition of OM in the Winchcombe meteorite to determine its origin and evolution.

References: [1] King, et al. (2022) *MetSoc* 85:6443. [2] Alexander, et al. (2017) *Chem. der Erde.* 77:227. [3] Vollmer, et al. (2014) *PNAS* 111:15338. [4] Vinogradoff, et al. (2017) *GCA* 212:234. [5] Vollmer, et al. (2020) *Meteorit. Planet. Sci.* 55(6), 1293–1319. [6] Vollmer, et al. (2020), *Sci. Rep.* 10:20251. [7] Cody and Alexander (2017) *LPSC* 48:A2747.

Keywords, Meteorites, Winchcombe, Organics, Carbonaceous Chondrite

21. Noble gases of the Apollo 16 'soil-like' regolith breccia suite.

M. Nottingham, N. M. Curran, J. F. Pernet-Fisher, R. Burgess, J. D. Gilmour, I. A. Crawford, K. H. Joy

Presenting author institution: University of Manchester

Regolith breccia samples collected by the Apollo 16 mission have so-far been grouped into 'ancient', and 'young' regolith breccia groups (consolidated between ~3.8 – 3.4 Ga and ~2.5 – 1.7 Ga, respectively), and a further possible 'soil-like' regolith breccia group (hypothesized to have consolidated <2 Ga) [1-3]. Noble gas measurements support the distinctions between the 'young' and 'ancient' regolith breccia groups but, so far, no noble gas measurements have been reported for the 'soil-like' regolith breccias.

We visually identified ten 'soil-like' breccia samples from the Apollo 16 sample suite. The samples represent a range of surface exposure (i.e., maturity), based on reported Is/FeO indices [1], and textural classification types [4]. The samples were step heated, and the concentrations and isotopic ratios of each noble gas element were analysed separately using a Thermo Fisher Helix Multi-collector Mass Spectrometer running in static mode, after cryogenic separation. Heavy (Kr, Xe) and light (He, Ne, Ar) measurements were made on two separate chips of different masses, from the same parent sample chip.

Noble gas concentrations in eight 'soil-like' breccias studied here are comparable to those reported for Apollo 16 soils, and are higher than the 'ancient' and 'young' regolith breccias [2,5]. Two samples allocated appear texturally to be impact melt samples (rather than regolith breccias), this was supported by their gas-poor nature.

Cosmic ray exposure ages were calculated using literature bulk sample data [4] and the theoretical cosmogenic nuclide surface production rate model of [6]. The 'soil-like' regolith breccias show CRE ages of T3 = 2 - 5 Myr, T21 = 2 - 16 Myr, T38 = 30 - 150 Myr, and T126 = 10 - 35 Myr, and the impact melt breccias have short CRE durations (<100,000 years across all isotope systems). Using the calibration of [3] and reported sample bulk chemistries [4], we calculated 40Ar(parentless)/36Ar(trapped) antiquity ages for each regolith breccia [3,7] (see [6] for details). Model-dependent antiquity ages have large uncertainties, but they can still establish an estimated timeline between the formation of each breccia. Two samples show higher antiquity ages of 2.33 and 2.51 Ga, four samples formed between 1.76 to 2.04 Ga, and two samples show ages of 0.86 and 1.33 Ga. These are consistent with ages reported for the Apollo 16 'young' regolith breccias, suggesting that the breccias were consolidated within the lower Eratosthenian period.

In summary, our new data support the theory of [1], that these regolith breccias formed from soils that resemble soils found at the Apollo 16 landing site (i.e., they formed from regolith that had been exposed on, or near, the lunar surface for a relatively long time).

[1] Jerde E.A., et al. (1987) *17th LPSC, Part 2.*, *JGR. 92*,B4,E526-E536. [2] McKay D.S., et al. (1986) *17th LPSC, Part 2.*, *JGR. 91*,B4,D277-D303. [3] Joy, K.H., et al. (2011) *GCA*, 75(22), [4] Curran N. (2017) *PhD Thesis, Univ. of Manchester* [5] Curran N.M., et al. (2020) *PSS, 182*,104823. [6] Hohenberg C.M., et al. (1978) Proc. 9th LPSC, 2,2311–2344 [7] Eugster et al. (2001) *MaPS*, *36*,1097-1115.

22. A fragment of the Lunar mantle?

Downes, Hilary; Bhanot, Krishan; Jennings, Eleanor; Wotton, Steve

Presenting author institution: Birkbeck University of London

An unresolved problem of lunar science is the nature and composition of the lunar mantle. No samples of the lunar mantle have yet been unambiguously identified in the Apollo collection, although a dunite clast in a brecciated meteorite may be from the lunar mantle. Thermodynamic modelling suggests that the lunar mantle is primarily composed of olivine and orthopyroxene with lesser amounts of clinopyroxene and garnet. Here we discuss a possible fragment of the lunar mantle collected by Apollo 17 astronauts.

Apollo samples 72415–72418 are cataclastic dunites composed of 93% olivine (Fo_{86-89}), 4% plagioclase (An_{85-97}) and 3% pyroxene ($En_{84}Wo_{3}Fs_{10}$ and $En_{50}Wo_{42}Fs_{4}$). They are formed of olivine clasts in a very fine-grained olivine matrix. All olivines have similar Fo values of 88. Most olivine clasts are angular, but some have rounded edges. They often show fractures which terminate at their edges, together with undulose extinction and mosaicism, probably a result of shock.

Different textures involving Cr-spinel have been identified, varying in size, mineral associations and relative abundances. Micro-CT investigations of the 3D interiors confirm that Cr-spinel occurs in distinct textural types. One common texture (**Type A**) is a ~0.3 mm ellipsoidal symplectite of Cr-spinel + diopside ± enstatite ± Fe-Ni metal, with cpx>>opx. It occurs as individual clasts formed by clusters of Cr-spinel and pyroxene. **Type A** spinel-pyroxene clusters show randomly orientated intergrowths of highly vermicular spinel within pyroxenes. Individual clusters generally have rounded edges but can be fractured. In contrast, **Type B** is an association between spinel + anorthite, closely associated with olivine with maximum dimension 1.4 mm. Spinel forms both blocky and elongate grains, and shows a branching structure. **Type B** clusters are highly complex intergrowths with blocky or elongate spinel. Spinel branches are elongate and form linear features which display a weak parallel orientation and often terminate in very flat plate-like structures.

Type A Cr-spinel-pyroxene clusters originated at a depth of 420 km as a result of a metamorphic transformation of garnet brought on by decompression following the reaction of ol + gt $\rightleftharpoons$ cpx + opx + sp. The reconstructed garnet composition is unusually Cr-rich. The garnet to spinel transition pressure (around 20 kbar) provides a minimum constraint on the ultimate depth of origin of the **Type A** symplectites. However, LMO crystallisation modelling indicates that garnet would only have fractionated much deeper, close to the lunar core-mantle boundary at 4 GPa. The presence of these symplectites at the Moon's surface therefore implies an overturn in the lunar mantle that has moved material through its entire depth. They were moved by the overturn to a depth of ca. 70 km, equivalent to 8 kbar pressure in the lunar mantle where anorthite is stable. The anorthite-rich **Type B** clusters were probably formed at this depth, perhaps by melting during the Serenitatis impact.

Keywords: Moon, mantle, petrology, Apollo 17, mineralogy

23. The effect of pre-impact surface conditions on the efficiency of giant impact atmospheric loss

Lock, Simon J.; Stewart, Sarah T.

Presenting author institution: University of Bristol

Earth is thought to have acquired its inventory of volatile elements during the main stage of its accretion. The atmospheres of at least some of the planetary embryos that accreted to form Earth must therefore have survived the giant impacts (collisions between planet-sized bodies) that dominate the end of the main stage of Earth's accretion. In this work we use 1D hydrodynamic simulations to investigate how efficiently the atmosphere and ocean of proto-planets can be removed during giant impacts. In particular, we quantify the effect that pre-impact surface conditions (such as surface temperature, atmospheric pressure, and ocean mass) have on the efficiency of loss. We find that the degree of loss is relatively insensitive to the composition and temperature of the atmosphere, but strongly dependent on the relative mass of the ocean and atmosphere. In cases where the ocean is substantially more massive than the atmosphere, a large range of giant impacts could remove a substantial fraction of the pre-impact atmosphere of a planet. To allow our results to be combined with 3D giant impact simulations, we develop a scaling law that relates the surface conditions to the efficiency of atmospheric and ocean loss. Our results show that the final volatile budgets of planets are critically dependent on the thermal and oxidation state of their surfaces during the final stages of accretion. Stochastic differences in the parameters and timing of giant impacts may therefore be responsible for substantial diversity in the atmospheres of terrestrial planets.

Keywords: Impacts, Accretion, Atmospheres, Earth, Volatiles

24. Mineral records of magma storage and crystallization in basaltic systems on the Moon

Ravy, Divyareshmi; Bell, Samantha; Joy, Katherine; Neave, David; Hartley, Margaret

Presenting author institution: University of Manchester

Lunar lavas mainly erupted between 4.35 to 3 billion years ago with some areas of the Moon thought to have been volcanically active as recently as a billion years ago **[1]**. With the Chang'e 5 mission returning lunar mare basalts as young as two billion years, the youngest reported to date **[2]**, questions about magma genesis and evolution on the Moon remain as prominent as ever. Although different lunar magmas are thought to have reached the surface via a range of storage and crystallization mechanisms **[3]**, the pressures and temperatures governing these processes remain uncertain.

This project aims to address the following questions: (i) Did lunar magmas stall and crystallize in crystal mush chambers or did they ascend rapidly from melting region to surface? (ii) At what temperatures and pressures did crystals nucleate? (iii) What can crystal records tell us about the subsurface magmatic systems and volcanic eruption styles on the Moon? This is done by the principles of geothermobarometry which helps determine the P-T conditions of magmatic storage and crystallization by understanding the equilibrium constant (K) of chemical reactions in unique mineral assemblages **[4]**. Many mineral thermobarometers have been calibrated for terrestrial magmatic systems, but may be of limited applicability to lunar systems, owing (i) to the low-pressure gradients (~4.5 MPa/km) on the Moon, (ii) lunar melt chemical characteristics which differ from terrestrial systems (eg: lunar higher-Ti, -Fe and Na poorer basalts), and (iii) the more reducing nature of the Moon.

As an initial approach, the application of the cpx-liq thermobarometric model on the low-Ti Apollo 15 mare basalts produced a series of pressures and temperatures for the lunar clinopyroxene compositions. The model was modified by replacing the terrestrial value of 0.28±0.08 **[5]** with the lunar value of 0.349 ± 0.035 **[6]**. The Na-poor nature of the lunar pyroxenes could be one of the multiple reasons for no P-T values for the majority of the compositions. Therefore, further calibration of these models is essential with respect to lunar mare basalts for their better understanding.

Hence, through this work, we aim to compile and review published experimental data to investigate element partitioning into lunar minerals and conduct experiments to refine the mineral-mineral and mineral-melt thermobarometers calibrated specifically for lunar magma compositions. We will apply these further by refining the calibrations for high-Ti mare basalt samples returned from the Apollo 17 mission. We, therefore, aim to integrate the experimental, petrological and computational outputs to better understand what crystal records can tell us about subsurface magmatic systems and volcanic eruption styles on the Moon.

References: [1] Schultz P. H. and Spudis P. D (1983) *Nature* [2] Tian H. C. et al. (2021) *Nature*. [3] Neal C. R (2018) *LPSC*. [4] Powell R. and Holland T. J. B (2008) *Journal of Metamorphic Geo*. [5] Putirka K. D (2008) *Rev. in Min. and Geochem*. [6] Barr, J. A., & Grove, T. L. (2013). *GCA*.

Keywords: Lunar volcanism, Mare basalts, Thermobarometry, Crystallization, Mineral Assemblages

25. X-ray Computed Tomography and Diffraction for Basic Characterisation of Mars2020 Samples

Adam, Lukas; Bridges, John; Holt, John

Presenting author institution: University of Leicester

Basic Characterisation (BC) is a set of non-contact measurements to identify the basic physical and geological characteristics of a returned Mars sample in order to inform its later, detailed analysis. It will be performed on all returned Mars2020 samples. Strict contamination control measures must be taken for planetary protection and to prevent contamination of the samples by Earth's environment, so BC will be carried out under high containment. It will include X-ray computed tomography (XCT) and possibly X-ray diffraction (XRD); performed on sealed sample tubes as well as later extracted samples [1]. These techniques will offer our first view of the collected extraterrestrial material, without having to breach the containment of the sample tubes and start the clock for time-sensitive investigations. These data will be used to inspect tube seal integrity, examine sample shape and state, search for morphological biosignatures, check for signs of contamination, map geological features like grain size and shape, aid in preliminary mineralogical identification, and provide early recognition of high science-priority features. X-ray diffraction would enable direct compositional and mineralogical characterisation before sample tubes need to be opened, while the samples are still fully pristine. We are investigating the feasibility and instrument requirements of CT and XRD for Basic Characterisation. Four Mars sample analogues have been prepared for this: basaltic fluvio-lacustrine sediment collected for the SAND-E Mars analogue mission from Iceland; and drill-cores of Old Red Sandstone, fluvial mudstone, and basalt. Mars2020 sample tube analogues made out of grade 5 titanium alloy have also been manufactured. CT scans performed on the analogues using Nikon XTH 225 and XTH 320 microtomography scanners have been compared against a proposed set of minimum BC measurement requirements. Samples were scanned inside and outside sample tubes, and minimum requirements met for both cases. We are also measuring the decrease in scan quality caused by beam attenuation due to the sample tube walls and investigating how scan parameters should be adjusted to counteract this. The sample porosity has also been derived from these scans. XRD on sample analogues inside and outside sample tubes was tested using Diamond Light Source's I12 beamline. Synchrotron radiation is required due to the size of the samples. Bulk compositional measurements and 2D spatially resolved diffraction scans were carried out, with a range of beam sizes and sample-detector distances. This is being compared to compositional data from a conventional Rigaku lab powder diffractometer. These data will help to determine feasibility of XRD analysis of sealed Mars2020 sample tubes and the effect the titanium walls have on phase identification. Preliminary results indicate that overlap between tube wall and mineral diffraction peaks is small. We are currently testing whether these titanium peaks can be subtracted completely from the diffraction spectra.

Acknowledgements: The project was partly funded by ESA and the lead author's studentship by STFC. This work was carried out with the support of Diamond Light Source, instrument I12-JEEP (proposal MG30591).

References: [1] MSPG 1, Meyer, M., et al., (2019), "Science in Containment". Unpublished report, 05/05/22 at https://mepag.jpl.nasa.gov/reports.cfm.

Keywords: Mars, Sample Return, Instrumentation

Session 4:

Icy Satellites

26. Exploring the outer solar system with space robots

Howett, Carly

Presenting author institution: University of Oxford

Space robots have revolutionised our understanding of the outer solar system. For example, Cassini showed us that Saturn's small moon Enceladus was active, and New Horizons showed us that Pluto is too. We will discuss what we know about this activity, its implications, and the bumps along the way in discovering them. We will also look ahead to two upcoming missions, and what they will teach us about activity, habitability and the history of our solar system: Lucy and Europa Clipper.

Keywords: Icy Moons, Trojan Asteroids, Instrumentation

27. Compositional Mapping of Ganymede with VLT/SPHERE using Markov Chain Monte **Carlo Spectral Analysis**

King, Oliver; Fletcher, Leigh

Presenting author institution: School of Physics and Astronomy, University of Leicester, Leicester

Datasets: We acquired observations of Ganymede using the SPHERE instrument on the ground-based Very Large Telescope (VLT) in an observing campaign in summer 2021. Multiple observations enabled coverage of the majority of Ganymede's surface, with spatially resolved infrared spectra from 0.95 to 1.65μm (R~30) and simultaneous dual band imaging at 2.11 and 2.25μm. VLT/SPHERE has a high spatial resolution (7.46 mas/px), allowing features <150km across to be resolved on Ganymede's surface. We have also analysed spacecraft-based Galileo/NIMS observations with similar spatial and spectral coverage to our SPHERE data.

The SPHERE observations were reduced and cleaned to produced mapped spectral cubes of Ganymede's near-IR solar reflectance spectrum. The Oren-Nayar photometric correction (Oren & Nayar, 1944) enables mapping to high latitudes, allowing our SPHERE observations to provide global-scale ~100km spatial resolution mapping covering >80% of Ganymede's surface.

Spectral modelling: We analyse the mapped cubes by fitting to laboratory spectra from reference cryogenic libraries. The reference spectra include water ice, hydrated salts, sulphuric acid, and a spectrally flat darkening agent. We model the spectra using a Markov Chain Monte Carlo technique (King et al., 2022) which produces a posterior abundance distribution for each endmember and combination of endmembers. These posterior distributions can be sampled to calculate the best estimate abundance for each endmember, and the uncertainty on this fitted abundance.

Results: Modelling results show strong contrasts between Ganymede's young bright terrain, which has a high water ice abundance, and old dark terrain (e.g. Galileo Regio) which is dominated by the spectrally-flat darkening agent. The modelled water ice distribution shows global-scale trends in ice grain size, with larger grains at low latitudes, likely due to the latitudinal thermal gradient. There is also a longitudinal trend in ice grain size which may be caused by varying irradiation with longitude. The darkening agent appears to have a relatively uniform low albedo, but the lack of distinct spectral features makes identification difficult.

Sulphuric acid has a low abundance, and appears spatially correlated with plasma bombardment, where Ganymede's poles are exposed to the external Jovian magnetic field. Best-estimate abundances suggest a mixture of chlorinated and sulphate salts are present, although uncertainties make it difficult to confidently detect individual salts. Some salts (sodium magnesium sulphate and magnesium chlorate) appear correlated with exogenic plasma bombardment, while others (magnesium chloride and sulphate) appear correlated with younger terrain, suggesting a potential endogenic origin.

Keywords: Icy Moons, Remote Sensing, Spectroscopy, MCMC Modelling, Ganymede

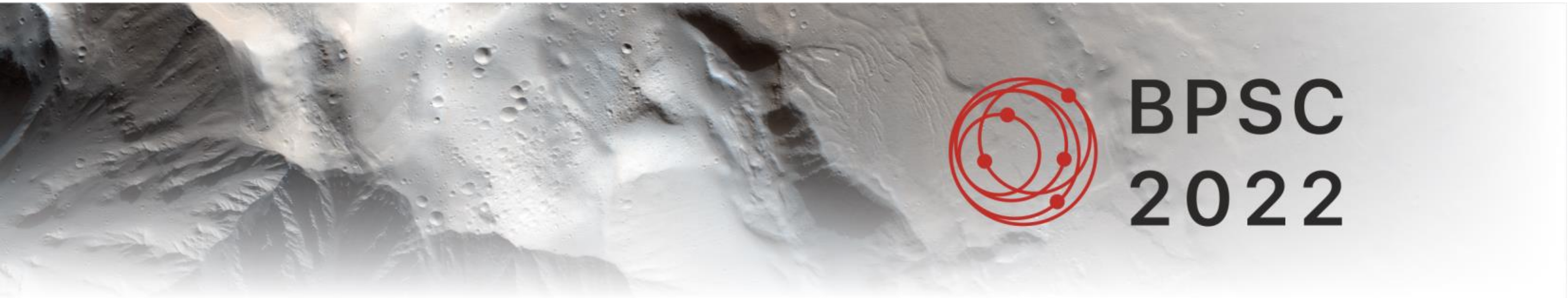

28. Looking for hotspots on Enceladus outside the South Polar Terrain

Miles, Georgina; Howett, Carly; Spencer John

Presenting author institution: Oxford University

We use the 12 years of Enceladus observations by the Cassini Composite InfraRed Spectrometer (CIRS) to evaluate whether endogenic "hotspots" might exist outside of Enceladus' South Polar Terrain (SPT). Such additional hotspots if present are expected to be small and by their nature challenging to detect, but their presence would have implications for our understanding of the energy budget and evolution of Enceladus. Current models of the tidal heating explain much of the cryovolcanic activity in the SPT but do not preclude hotspots elsewhere.

We use a passive thermal model to estimate expected surface temperatures and investigate departures from these values. In order to establish anomalous temperatures both model and observation error must be well characterised. We have improved the representation of temperature error for CIRS spectra for very cold scenes by examining the statistics of how spectral noise is conferred on temperature uncertainty. We perturbed the model input thermal parameter space to characterise a time and location dependent model error. We find excellent model agreement for the majority of observations but identify a limited number of cases where they do not agree well and warrant further investigation. We will present the preliminary results of this study and highlight what future observations would be desirable to further constrain our understanding of Enceladus' energy budget.

Keywords: Enceladus, Icy moons, Thermal modelling

29. Seismic detection of differing interior structures on Enceladus

Dapré, Kat; Irving, Jessica C. E.

Presenting author institution: University of Bristol

Saturn's icy moon Enceladus is a high-priority target for future life-seeking missions due to its accessible subsurface ocean and predicted hydrothermal seafloor vents [1]. However, its small 252km radius means it lacks a clear mechanism from available data for thermally sustaining this ocean through its history. A seismological mission to Enceladus, such as the proposed Orbilander [2], could take advantage of anticipated seismic sources including plume regions and significant faulting around the south pole [3] in order to gather information on the interior structure. This work investigates whether diagnostic differences between candidate structural models could be measured with a single landed seismometer, and examines the reliance of these results upon the location of such a mission.

Current theories of Enceladus' interior structure have drawn primarily on data collected by Cassini-Huygens, and have made use of orbital dynamics, shape data, and heat budgets, as well as surface observations and compositional data from plume samples at the south pole. These studies agree on the broad layered structure of an ice shell and global subsurface water ocean totalling 50-70km thick, overlying a rocky core between 200-180km thick. Some degree of unconsolidated or porous upper core is also often suggested, while the ice shell is strongly axisymmetric, becoming thinner at the poles and particularly towards the south. However, the relative thicknesses of these layers vary widely between different proposed models, with significant implications for composition, partitioning of tidal heating, and consequent astrobiological potential.

Models selected for analysis [4,5,6] are simplified to be laterally homogeneous for computation and to enable more direct comparison between models. Ray theoretical travel times are calculated for each model using the TauP Toolkit [7], and are used to identify phases of interest in subsequent full-waveform modelling using AxiSEM [8]. Ice shell thickness is shown to have significant impact on the maximum propagation distance of ice phases, while core-transmitted phases key to examining any potential porous upper layer are observable only at large distances from source. Seismic attenuation is also predicted using data from terrestrial analogues and laboratory studies to relate temperature and quality factor; attenuation is found to have a negligible effect on the amplitudes of phases of interest.

[1] National Academy of Sciences, Engineering and Medicine. 2022. *Origins, Worlds, Life: A Decadal Strategy for Planetary Science and Astrobiology 2023-2032* https://doi.org/10.17226/26522. [2] MacKenzie, S. M. et al. (2021) *Planet Sci. J., 2(2)*, 77. [3] Olsen, K. G. et al. (2021) *JGR: Planets, 126*, e2021JE006862. [4] Čadek, O. et al. (2016) *Geophys. Res. Lett., 43*, 5653-5660. [5] Vance, S. D. et al. (2018) *JGR: Planets, 123*, 180-205. [6] Neumann, W. and Kruse, A. (2019) *ApJ., 882*, 47. [7] Crotwell, H. P., Owens, T. J., and Ritsema, J. (1999) *SRL, 70*, 154-160. [8] Nissen-Meyer, T. et al., (2014) *Solid Earth, 5*, 425-445.

Keywords: Icy Moons, Enceladus, Seismology, Future Missions

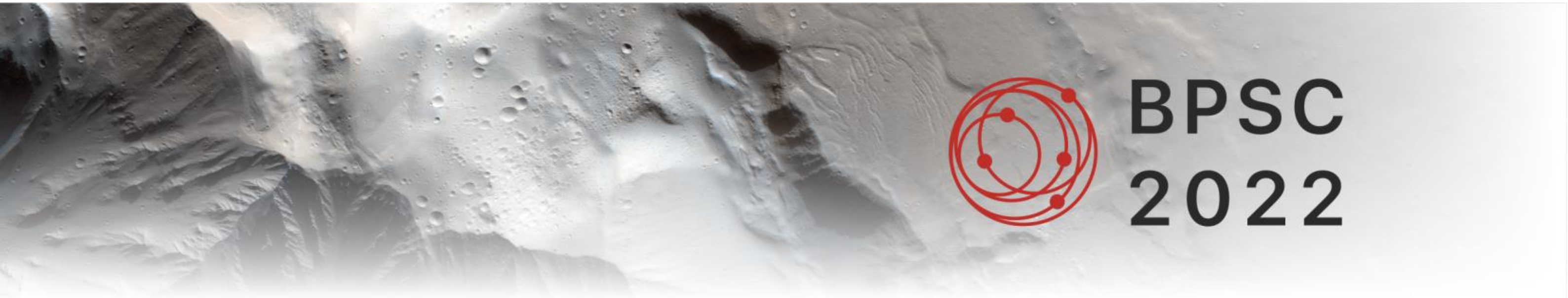

30. Geochemical cycling of the subsurface environment of Enceladus

Hamp, Rachael; Schwenzer, Susanne; Olsson-Francis, Karen; Pearson, Victoria

Presenting author institution: The Open University

Enceladus, an icy moon of Saturn, is a potentially habitable environment. Its South Polar Region hosts active plumes that eject material from the subsurface into space. Plume material was analysed by the Cassini spacecraft, which confirmed the presence of a global subsurface ocean, active hydrothermal activity, and the presence of bio-essential elements (carbon, nitrogen, and hydrogen). Data from the plumes provided a snapshot of the subsurface chemical environment, however, could not fully constrain the composition of the silicate interior or specific ocean chemistry.

A modern-day ocean composition was determined by thermochemical modelling using CHIM-XPT, where hypothetical starting compositions for the ocean interact with the silicate interior to produce a modern-day fluid. This fluid is then both cooled and frozen to study changes in the chemical composition as water ascends from the water-rock interface on Enceladus. The fluid composition generated through thermochemical modelling was then critically compared to Cassini's plume data. This study found that a CI chondrite and cometary ice composition are suitable analogues for the silicate interior and icy exterior of a proto-Enceladus. The results from modelling simulations found the ocean is likely dominated by salts and carbonates, with a pH of 8.5-9.5. Geochemical cycles for carbon, silica and sulfur occurring in a modern Enceladus have been defined and the availability of different chemical species that could be utilised by life have been assessed, which enhanced the prospect of Enceladus as a habitable environment.

Keywords: Icy moons, Geochemistry, Habitability, Enceladus

31. Exploring Europa's biological potential using laboratory simulations

del Moral, Álvaro; Siggs, Dominic; Fox-Powell, Mark G.; Pearson, Victoria K.; Olsson-Francis, Karen

Presenting author institution: AstrobiologyOU, The Open University, Milton Keynes, MK7 6AA, UK.

Jupiter's moon Europa contains a liquid water ocean under its thick ice layer which could contain chemical disequilibria capable of supporting microbial life. Even though its composition has yet to be measured directly, modelling suggests a pH of between 6.22 to 12.88, a salinity of between 20 g/L and >500 g/L with sodium chloride, sodium bicarbonate or magnesium sulfate being the dominant salts[1–3], and a temperature range of 0°C, near the ice shell, to 90°C at its 100km deep ocean floor. These conditions are not to be considered very extreme as there are numerous microbial communities on Earth living in similar situations[4].

Using bespoke environmental simulations, the aim of this project was to understand the functional and physiological adaptations required to survive in Europa's sub-surface ocean by subjecting communities of microorganisms to simulated Europa ocean conditions over multiple generations. For this work, we prepared several growth media based on the results of models of Europa's ocean composition[1–3] and inoculated them with microbial communities from environments on Earth with matching chemical properties, from saline lakes and abandoned quarries, to subglacial lakes, identified by our random forest algorithm[5]. The surviving community, sampled originally from Basque Lake, Canada and grown in a carbonate-chloride Europan chemistry, was then transferred to an environmental simulation chamber capable of reaching 300 bars of pressure to simulate the physical conditions found in the upper region of the moon's ocean. They were exposed to incremental steps of pressure, from 20 bar to 100, 200 and 300 bar to allow the communities to adapt and to track pressure-induced changes in the community composition and physiology. Chemical changes in the media were monitored using Ion Chromatography and Inductively Coupled Plasma Optical Emission Spectroscopy. Microbial community growth was monitored through fluorescence cell microscopy and composition using 16s rRNA sequencing. Pressure-induced morphological changes in cell structure were investigated using Transmission Electron Microscopy. Preliminary results demonstrate that microorganisms from Europa-analogue environments on Earth grow well under simulated Europa ocean conditions under the pressure regimes found below the moon's ice shell. In future work, the selected microorganisms will serve as model organisms to study putative biosignature formation in the Europa ocean.

References: 1. Melwani Daswani, M., Vance, S. D., Mayne, M. J. & Glein, C. R. A Metamorphic Origin for Europa's Ocean. *Geophysical Research Letters* **48**, (2021). 2. Zolotov, M. Y. & Kargel, J. S. *On the Chemical Composition of Europa's Icy Shell, Ocean, and Underlying Rocks*. (2009). 3. Kargel, J. S. *et al.* Europa's Crust and Ocean: Origin, Composition, and the Prospects for Life. *Icarus* **148**, 226–265 (2000). 4. Russell, M. J., Murray, A. E. & Hand, K. P. The possible emergence of life and differentiation of a shallow biosphere on irradiated icy worlds: The example of Europa. *Astrobiology* **17**, 1265–1273 (2017). 5. del Moral, A., Pearson, V., Fox-Powell, M. & Olsson-Francis, K. Using supervised machine learning methods to improve the selection of analogue sites for studying habitability of the sub-surface ocean of Europa. **14**, 10–12 (2022).

Keywords: Icy Moons, Earth Analogues, Microbiology, Extremophiles

Session 5:

Lighting talk group 2

32. Optimising Filter Bandpass Selection for the Thermal Infrared Imager on ESA's Comet Interceptor Mission

Shirley, K. A.; Warren, T. J.; Faggi, S; Villanueva, G. L.; Protopapa, S; Donaldson Hanna, K. L.; Kohuts, T.; Bowles, N. E.; Nasila, A., Thirumangalath

Presenting author institution: University of Oxford

ESA's upcoming Comet Interceptor (CI) mission will be the first to visit a long period, potentially dynamically new, comet that will consist of some of the most primitive material from the beginning of our Solar System. Part of CI's payload includes the Modular InfraRed Molecular and Ices Sensor (MIRMIS) which will map the thermal and compositional variation of the comet's nucleus and coma. Here we focus on how to maximise the science return of MIRMIS's thermal imager (TIRI, 6-25 µm). TIRI's instrument design includes one central broadband thermal imaging channel (6-25 µm) and 2 identical sets of eight narrow-band channels situated orthogonal to each other to accommodate the instrument orientation as it changes upon closest approach to the comet. To optimise TIRI's narrow-band filter set, we used both synthetic nucleus spectral targets and laboratory measured analogue minerals and meteorite spectra to understand TIRI's detection capabilities at retrieving both temperature and composition. Several filter sets were proposed that consisted of band-centres evenly spaced along TIRI's range; band-centres concentrated near 9-11 µm (a region rich in silicate features); or a mix of the two.

Synthetic Spectral Analysis: Twelve synthetic spectra were generated with the Planetary Spectrum Generator (PSG) [Villanueva et al., 2018] that included six featureless spectra made of single or mixed temperature blackbodies and six spectral mixtures composed of crystalline and amorphous silicates convolved with single or mixed temperature blackbodies. The silicate endmembers were chosen based on identified minerals of comets Tempel 1 and Hale-Bopp [Lisse et al., 2007].

We used the Retrieval Module of the PSG to test the ability of each filter set to retrieve a sequence of information about the temperature and composition of each original synthetic spectrum. These retrievals showed that temperature of the featureless spectra was always reliably determined independent of the filter set. For the silicate spectra, temperature was always retrieved (±1 K) if >250 K, but spectral shape determination had a dependence on filter set.

Laboratory Spectral Analysis: We examined laboratory spectra of minerals and meteorites likely to be present/analogous to the anticipated primitive comet including minerals used in the OSIRIS-REx collection and carbonaceous meteorites. From these, we identified several key features for composition determination centred within 8-12 µm. Additionally, we examined a set of mineral mixtures with known amorphous content and a set of hydrated/altered meteorites. Differences were subtle at low amorphous content and unlikely to be captured at this spectral resolution. The overall spectral shape of the meteorite composition was well captured, and including longer wavelengths (12-15 µm) improved differentiation of hydrous alteration.

The synthetic analysis showed that filters covering a large range are necessary to capture both temperature and spectral shape of the target comet. The laboratory analysis showed that, while a concentrated filter set was better at distinguishing minute differences between compositions, a wider range of filters can still provide adequate qualitative spectral information to achieve TIRI's science objectives. We, therefore, propose a filter set covering 8-22 µm to retrieve temperatures and to better capture mid-range compositional features.

Keywords: Infrared Spectroscopy, Comet, Comet Interceptor, MIRMIS, Spectral Retrieval

33. MIRMIS – The Modular Infrared Molecules and Ices Sensor for ESA's Comet Interceptor.

Bowles, Neil; A. Näsilä, T. Kohout, G. L. Villanueva, C. Howe, G. H. Jones, C. Snodgrass, K. L. Donaldson Hanna, B. T. Greenhagen, P. G. J. Irwin, S. B. Calcut, R. Evans, K. Shirley, T. Warren, A. Akujärvi, A. Penttilä, A Kokka, S. Faggi, S. Protoppa, K. Nowicki, D. Korda, H. Eshbaugh, S. Ogborne, R. Curtis, C. Tubiana, and the Comet Interceptor team.

Presenting author institution: Department of Physics, University of Oxford.

The Comet Interceptor mission was selected by ESA as the first of its new "F" class of missions in June 2019. Comet Interceptor (CI) aims to be the first mission to visit a long period comet, preferably, a Dynamically New Comet (DNC), a subset of long-period comets that originate in the Oort cloud and may preserve some of the most primitive material from early in our Solar System's history. CI is scheduled to launch to the Earth-Sun L2 point with ESA's ARIEL [2] mission in ~2028 where it will wait for a suitable DNC target.

The CI mission is comprised of three spacecraft. Spacecraft A is the main spacecraft that will pass by the target nucleus at a distance of ~1000 km to mitigate against hazards caused by dust due to the wide range of possible encounter velocities (e.g. 10 – 70 km/s). As well as acting as a science platform, Spacecraft A will deploy and provide a communications hub for two smaller spacecraft, B1 (supplied by the Japanese space agency JAXA) and B2 that will perform closer approaches to the nucleus. Spacecraft B1 and B2 will make higher risk/higher return measurements but with the increased probability that they will not survive the whole encounter.

This presentation will provide details of the Modular InfraRed Molecular and Ices sensor (MIRMIS) instrument that is currently baselined as part of the CI Spacecraft A scientific payload. The MIRMIS consortium includes hardware contributions from Finland (VTT Finland) and the UK (University of Oxford) with members of the instrument team from the University of Helsinki and NASA's Goddard Space Flight Centre.

MIRMIS will map the spatial distribution of temperatures, ices, minerals and gases in the nucleus and coma of the comet using three modules covering a spectral range of 0.9 to 25 microns. An imaging Fabry-Perot interferometer will provide maps of composition at a scale of ~180 m at closest approach from 0.9 to 1.7 microns. A Fabry-Perot point spectrometer will make observations of the coma and nucleus at wavelengths from 2.5 to 5 microns and finally a thermal imager will map the temperature and composition of the nucleus at a spatial resolution of 260 m using a series of multi-spectral filters from 6 to 25 microns.

The MIRMIS instrument is compact (548.5 x 282.0 x 126.8 mm) and low mass (<8.8 kg) and has single mechanical and electrical interface to the spacecraft, making the design also suitable for remote sensing mission from small satellites in LEO or other targets in the Solar System.

References: [1] Snodgrass and Jones, 2019, Nature Comms. 10, 5418. [2] Tinetti et al. 2018, Exp. Astron. 46, 135-209.

Keywords: Comet Interceptor, Spectroscopy , Instrumentation

34. High Resolution Observations of Titan's Equatorial Dynamics using Cassini CIRS Spectra

Wright, Lucy; Teanby, Nicholas; Irwin, Patrick; Nixon, Conor; Mitchell, Dann

Presenting author institution: University of Bristol

The Cassini spacecraft explored the Saturn system for over 13 years, performing 127 close fly-bys of Titan from 2004 to 2017. One of Cassini's 12 instruments, the Composite InfraRed Spectrometer (CIRS) (Flasar *et al.,* 2004; Jennings *et al*., 2017) acquired over 8 million Titan spectra at spectral resolutions from 0.5 - 15cm^{-1}. Here, we analyse low spectral resolution (~15cm^{-1}) nadir observations from CIRS FP3 and FP4 focal planes, which are sensitive to mid-infrared ranges 600-1100cm^{-1} and 1100-1500cm^{-1} respectively. These low spectral resolution observations require shorter scan times, so can be performed at a closer approach distance to Titan, thus achieving higher spatial resolution. This allows small spatial variations in atmospheric constituents to be resolved. However, we found that the correlated-k approximation, often used to decrease retrieval computation time in spectral analysis, is not accurate for these low spectral resolution observations. Furthermore, performing accurate line-by-line inversions of these spectra is computationally expensive.

We present a radiance ratio method for approximating latitudinal distributions of stratospheric HCN. Radiance ratios can be a useful tool for approximating gas contributions to a spectrum. They do not have the reliability of full spectral retrievals, but are much more computationally efficient, allowing a greater number of observations to be analysed rapidly. First, we construct a radiance ratio to approximate HCN abundance from CIRS infrared spectra. Second, we assess the reliability of our radiance ratio by comparison to full line-by-line retrievals of HCN latitudinal distributions for a subset of CIRS observations using the NEMESIS radiative transfer and retrieval code (Irwin *et al.*, 2008). A key parameter in line-by-line modelling is the underlying spectral grid spacing. Finer grid spacing produces higher accuracy but at a greater computational cost. Therefore, during these tests, we also determined an optimal grid spacing to achieve the required accuracy as efficiently as possible. After confirming the reliability of the radiance ratio, we applied it to the entire low resolution CIRS dataset to determine the evolution of Titan's equatorial chemistry. We use the results of this study to investigate dynamical processes at Titan's stratospheric equator and how it evolves over the entire Cassini mission.

References: Flasar, F. M., *et al.* (2004). Exploring The Saturn System In The Thermal Infrared: The Composite Infrared Spectrometer. Space Science Reviews, 115 (1-4), 169–297. https://doi.org/10.1007/s11214-004-1454-9; Irwin, P., *et al.* (2008). The NEMESIS planetary atmosphere radiative transfer and retrieval tool. Journal of Quantitative Spectroscopy and Radiative Transfer, 109 (6), 1136–1150. https://doi.org/10.1016/j.jqsrt.2007.11.006;Jennings, D. E., *et al.* (2017). Composite infrared spectrometer (CIRS) on Cassini. Applied Optics, 56(18), 5274. https://doi.org/10.1364/AO.56.005274

Keywords: Titan, Atmosphere, Radiative Transfer, Dynamics

35. Comparing atmospheric cloud models of Jupiter, can we reduce the degeneracy of this problem?

Alexander, Charlotte; Irwin, P.G.J.

Presenting author institution: University of Oxford

The grand appearance of Jupiter's banded atmosphere, coloured with many shades from white to red, currently remains elusive with no clear single cloud structure model responsible for this varied appearance. With a general pattern of alternating bright cloudy zones and darker belts, as well as unique regions such as the Great Red Spot, finding a way to model all of these differing appearances with a single model has proven difficult. Jupiter's atmosphere provides continual challenges when attempting to characterise its cloud structure due to its frequently varying appearance. This leads to differences between every observation meaning that models are constantly having to adapt to be explain these changes.

Recent work by Braude et al. (2020), Pérez-Hoyos et al. (2020) and Dahl et al. (2021), among others, have all attempted to model Jupiter's atmosphere using a universal chromophore (cloud colouring compound). These works have all been able to model the atmosphere successfully but it has currently not been possible to determine between different set ups as to which is the most likely representation of the atmosphere. As all the different sets ups have several ways to vary cloud structure and chromophore properties among other parameters, they have been able to fit the changes in the observations. Therefore keeping each set up as a viable set up even as the atmosphere changes. The current inability to conclude on a favoured cloud structure highlights the highly degenerate nature of this problem.

Utilising new observations and techniques to analyse the data highlights the delicacy of these results as the previous set ups have to be altered in order to produce the desired fit to the new observations once the input have varied slightly. Introduction of a limb viewing technique, which attempts to fit multiple viewing angles simultaneously also begin to question the robustness of these results, due to an inability of nadir set ups to reproduce the multiple observations as successfully.

Therefore in this work we have begun to attempt to reduce the degeneracy of the problem before utilising the NEMESIS retrieval algorithm (Irwin et al. 2008), to fit an atmospheric setup to our observations. It is hoped that reducing one of the degenerate parameters before fitting will allow us to constrain the atmospheric set up more decisively. Furthermore combining this with the limb darkening technique will hopefully allow us to rule out some of the solutions to this highly degenerate problem to find more confidence in the proposed models.

In this work we will present the preliminary results taken from the application of these methods to observations to derive a new atmospheric set up which can be compared with past work. Additionally we will present the use of new techniques to determine the ability of previous models to adapt to new observations to see if they are still viable.

Keywords: Atmospheres, Giant Planets, Cloud Retrievals

36. Constraining the composition of Europa's subsurface ocean from water-rock interactions

Ramkissoon, Nisha K.; Schwenzer, S. P., Fox-Powell, M. G., Del Moral, A., Olsson-Franics, K. and Pearson, V. K.

Presenting author institution: The Open University

Constraining the composition of Europa's ocean would help us to understand whether it could be capable of supporting life, and provide an insight into its evolution. In this study we have taken a "bottom-up" approach to assess potential ocean compositions for Europa. This approach assumes Europa's subsurface ocean is in contact with a silicate mantle, which would facilitate water-rock interactions that would liberate solutes that could be found in the ocean. Previous investigations have taken a similar approach [1–4], however, these studies have predominantly explored the influence of mantle compositions based on carbonaceous chondrites. This is despite computer modelling indicating a composition between a L and LL type ordinary chondrite correlated with Europa's moment of inertia and, thus, may also be candidate composition for the europan silicate interior [5]. Furthermore previous investigations have also focused on the aqueous alteration of the mantle by pure H2O or HCl fluids [1, 3, 4, 6], which may have been accreted as Europa formed. However, this ignores the potential contribution of ices that may have been captured since Europa's formation. Specifically, cometary ices are thought to be responsible for 90% of impact craters found on the europan surface today [7] and may have influenced the europan ocean composition.

Thermochemical modelling was employed to simulate water-rock interactions that could be occurring within Europa's silicate mantle to assess potential ocean compositions. Mantle compositions were based on L, LL and CV chondrites (both oxidised and reduced endmember compositions). These four candidate mantle compositions were reacted with either pure H2O or a fluid based on cometary ices (using data from 67P/Churyumov-Gerasimenko [8]) which reflect the two endmember fluid compositions that may have contributed to Europa's initial water inventory. Models were run at a pressure and temperature of 250 MPa and 333.15 K, which are the conditions anticipated in regions where hydrothermal alteration would occur within the mantle [9]. The resultant fluid from this initial model was then cooled and depressurised to conditions expected at the mantle ocean interface [9], to mimic the ascent of the hydrothermal fluids from depth to the ocean reservoir.

Here, we will present the modelled ocean compositions and describe their implications for habitability of the europan ocean.

References: [1] Zolotov & Shock (2001) *J. Geophys. Res. E Planets*, vol. 106, pp. 32815–32827. [2] Daswani et al. (2021) *Geophys. Res. Let*, vol. 48, e2021GL094143. [3] Kargel et al. (2000) *Icarus*, vol. 148, pp. 226–265. [4] Zolotov & Mironenko (2007) Ices, Oceans, and Fire: Satellites of the Outer Solar System, *Abstract# 6065*. [5] Kuskov & Kronrod (2005) *Icarus*, vol. 177, pp. 550–569. [6] Zolotov (2012) *Icarus*, col. 220, pp. 713-729. [7] Zahnle et al. (1998) *Icarus*, vol. 136, pp. 202–222. [8] Rubin et al. (2019) *Mon. Not. R. Astron. Soc.*, vol. 489, pp. 594–607. [9] Vance et al. (2007) *Astrobiology*, vol. 7, pp. 987–1005.

Keywords: Europa, Geochemistry, Icy moons, Modelling

37. Viable metabolisms in a simulated martian chemical environment

Macey, Michael C., Ramkissoon, Nisha K., Pearson, Victoria K., Schwenzer, Susanne P., Olsson-Francis, K.

Presenting author institution: The Open University

Introduction: The surface of modern-day Mars cannot support liquid water almost everywhere, but liquid water was present on the surface of Mars during the Noachian (4.1 - 3.7 Gya) (Martín-Torres et al. 2015, McEwen 2011). Local lithologies would have exerted a strong influence on the fluid chemistries, in turn effecting the redox-oxidation reactions that could drive microbial metabolisms (Ramkissoon et al. 2021). To identify metabolisms that could support persistent growth in martian aqueous environments, a microbial enrichment series with material from an analogue environment was performed using a simulated martian chemical environment.

Methodology: The simulated martian environment was established using a simulant based on Rocknest (Ramkissoon et al. 2019) and a thermochemically modelled fluid (Ramkissoon et al. 2019, Ramkissoon et al. 2021). This environment was inoculated using sediment from the Colne estuary (UK) that was shown to contain a microbial community with diverse metabolisms (McKew et. al. 2013, Curtis-Harper et al. 2018). Enrichments were established by adding 5 g of anoxic sediment to 40 ml of the modelled brine and 5g of simulant. A headspace of 1 bar of H_2/CO_2 (80:20) was added to the tubes. The enrichment was incubated for 28 days, after which 1 % was transferred into 10 ml of the modelled brines containing 10 g of simulant material. This provided a 1:1 ratio, akin to the water to rock ratio in rock pore spaces. The enrichment was subcultured seven times to dilute any estuarine nutrients and select for microbes growing only on the simulated chemical environment. The chemistry of the resultant brines was determined using ICP-OES. Changes in the microbial community were determined by sequencing 16S rRNA gene amplicons.

Results: Growth was observed in every stage of the enrichment, confirming the simulated chemical environment was able to support microbial growth. The diversity and abundance of the microbial communities decreased over the course of the enrichment, with sulfate-reducing bacteria ($SO_4^{2-} + H^+ + 4H_2 \rightarrow H_2S + 4H_2O$) and acetogens ($2\ CO_2 + 4\ H_2 \rightarrow CH_3COOH + 2H_2O$) dominating the enriched community at the end of the enrichment and additional heterotrophic anaerobes also persisting.

Implications: Results produced here indicate the chemistry of the ancient martian aqueous environments like Rocknest may have supported specific metabolisms, specifically sulfate reduction and acetogenesis. Given the persistence of additional generalist heterotrophic anaerobes, this work also shows community dynamics may be enhancing survival (i.e., syntrophy).

Future work: Growth dynamics will be investigated using a continuous culture approach to simulate lacustrine environments more accurately. This will enable the identification of microbially – induced geochemical changes that could be used as biosignatures, and would therefore, inform future life detection missions.

References: Curtis-Harper et al. (2018) *Microorganisms*, 6, 1-19 Martín-Torres et al. (2015) *Nat Geosci*, *8*, 357-361 McEwen (2011) *Science, 333*, 740–743. McKew et al. (2013) *FEMS Microbiol Ecol, 84*, 495-509. Nixon et al. (2013). *Astron Geophys, 54*, 13 – 16. Ramkissoon et al. (2019) *Planet Space Sci, 179*, 104722. Ramkissoon et al. (2021) *MAPS*, 1-19. Schwenzer et al. (2016) *Meteorit and Planet Sci, 51*, 2175-2202.

Keywords: Simulation, Mars, Sulfate

38. First insights into the chemistry and microbial community composition of salt plains in a potential Mars analogue site

Ilieva, Velislava; Stephens, B.P.; Goodall, T.; Ori, G.G.; Read, D.; Pearson, V.K.; Olsson-Francis, K.; Macey, M.C.

Presenting author institution: The Open University

The identification of novel terrestrial sites that are analogous for other planetary bodies is an active area of research within astrobiology, as a result of the logistical and financial difficulties in obtaining direct samples for analysis. Characterisation of potential analogue sites is undertaken to assess how accurately they represent a specific extraterrestrial environment. Analysing their physicochemical conditions and microbial communities are key components of these studies.

One such novel analogue environment is the salt plains of Western Sahara. Western Sahara represents one of the driest regions on Earth. It is located in the northwest coast of West Africa and is characterised by high levels UV exposure, low annual precipitation, low water activity, subsurface water and high annual temperatures. These features make Western Sahara a potential analogue site for Mars during the Noachian-Hesperian transition period (3.5 – 3.8 Ga) on Mars, when the atmosphere began to thin and surface water started evaporating (Warner et al., 2010). Late Noachian to Hesperian climate change on Mars: Evidence of episodic warming from transient crater lakes near Ares Vallis (Warner et al., 2010), similar to other deserts, such as the Atacama Desert and the McMurdo Dry Valleys.

In this study, molecular and geochemical techniques were used to give the first insights into the Western Sahara salt plains. The microbiology was investigated through cultivation-independent and culture-dependent analyses of salt crystals, sediment and water samples obtained at three sites near Llaayoune. The chemical nature of the samples was analysed through ion chromatography (IC) and inductively coupled plasma - optical emission spectrometry (ICP-OES).

The geochemical characterisation confirmed the high salinity of the samples and identified that sodium, potassium, magnesium and sulfur were the most enriched elements within all samples. 16S rRNA amplicon sequencing of the samples identified a high relative abundance of sulfate reducing bacteria (SRB), Cyanobacteria, and *Bacillus*. To complement the 16S rRNA gene amplicon sequencing, enrichments were established to isolate aerobic heterotrophs, phototrophs and SRBs. The enrichments from the salt were dominated by strains of *Bacillus*, whereas sulfate-reducing strains of *Clostridium* were isolated from the sediment samples. Microscopic analysis of phototroph-selective media also indicated that algae and Cyanobacteria were successfully enriched from the samples.

Future characterisation of this environment will involve metagenomic analysis of the samples and genome sequencing of the isolates to identify the key metabolisms underpinning the survival and viability of the microbial community. Comparative studies with other Mars analogue environments will then be undertaken to identify metabolisms that may have been thermodynamically viable in ancient martian aqueous environments.

References: Warner, N., Gupta, S., Lin, S.-Y., Kim, J.-R., Muller, J.-P., & Morley, J. (2010). Late Noachian to Hesperian climate change on Mars: Evidence of episodic warming from transient crater lakes near Ares Vallis [https://doi.org/10.1029/2009JE003522]. Journal of Geophysical Research: Planets, 115(E6). https://doi.org/https://doi.org/10.1029/2009JE003522

Keywords: Earth Analogues, Mars, Microbiology, Western Sahara

39. Entombment of microbial biomass within rapidly frozen fluid droplets relevant to the plumes of Enceladus

Fox-Powell, M .G; del Moral, Á, Cousins, C. R., Stephens, B., Slade, D., Dazley, C., Richards, G., Olsson-Francis K.

Presenting author institution: Open University

The plumes emanating from the south polar region of Saturn's moon Enceladus were studied by the Cassini mission, and have revealed evidence for ongoing hydrothermal activity, organic chemistry, and redox conditions favorable for microbial metabolism in the ocean below. Salt-rich icy particles encountered by Cassini were interpreted to originate as rapidly frozen droplets of ocean spray. If extant microbial communities exist within Enceladus's ocean, cells may become incorporated into these particles and ejected into space where they can be sampled by future spacecraft. However, the potential fate of biomass within frozen icy particles is not understood. Here, we used cryogenic imaging and sublimation-extraction techniques to study the interaction of microorganisms with inorganic phases during freezing of simulated Enceladus ocean fluids at contrasting cooling rates. Cells, harvested from four phylogenetically and morphologically distinct pure cultures, and a mixed community from an Enceladus-analogue environment in Iceland, were suspended in simulated Enceladus ocean fluid. Droplets were then cooled at two contrasting rates: rapid quench cooling (10^1-10^2 K s^{-1}), simulating the ejection of droplets into the ultra-cold Enceladus surface environment, and gradual cooling (0.01 K s^{-1}).

Under both freezing scenarios, ice crystallisation within the droplet produces an interconnected network of solidified solute-rich brine veins accumulated at ice grain boundaries. The presence of microbial cells leads to the formation of additional isolated inclusions of brine fully encased by ice, which are disconnected from the main brine vein network. Crystallisation microtextures, which under abiotic conditions are diagnostic of cooling rate, are modified by the presence of biomass, with distinct differences arising between brine veins and isolated inclusions. Mineralogical analyses of cryogenic salt phases shows that the presence of microbial biomass kinetically favors the precipitation of nahcolite, which is inhibited under abiotic conditions. This finding provides a route by which the presence of biomass at Enceladus could influence the mineralogy of icy particles in the plumes. Given that mineralogy is also sensitive to cooling rate and fluid pH, analyses of mineralogy within plume particles at Enceladus should be prioritized in future observations.

Our results demonstrate how microbial biomass may be preserved within icy particles relevant to the Enceladus plumes, revealing complex, cooling rate-dependent interactions between microbial biomass and rapidly precipitating solid phases. The association of microbial cells with specific inorganic phases has implications for interpreting secondary ion fragments in spacecraft impact-ionization mass spectra, and in the planning for future plume sampling missions that target in situ analyses, or more ambitiously, cryogenic sample return.

Keywords: Icy moons, Enceladus, plumes, biosignatures, astrobiology

40. Two Novel Halobacillus Species were Isolated from the Laboratory Enrichments of Epsomite Crystal from Basque Lakes, BC, Canada

Srivastava, Anushree; Macey, Michael Christopher; McGenity, Terry J; Toubes-Rodrigo, Mario; Pontefract, Alexandra; Pearson, Victoria K; and Olsson-Francis, Karen.

Presenting author institution: The Open University

The Basque Lakes (BLs) are sulfate-rich playas in the Pacific Northwest that serve as analogues for Mars' ancient hypersaline sulphate lakes (~4 Gya in early Noachian) and could serve as a proxy to constrain the putative martian microbiome. Here, two novel bacterial species isolated from epsomite ($MgSO_4.7H_2O$) crystal enrichments have been reported and taxonomically described. Such bacteria residing in extreme terrestrial epsomic habitats are the exemplar of the microbial life deemed to be associated with hypersaline ancient martian paleolakes.

Epsomite crystals collected from the margins of the lake were subsequently dissolved in a low-nutrient, $MgSO_4$-rich brine medium (2.5 M; ionic strength 12.099 mol L^{-1}), which was prepared anaerobically. Two pure cultures were obtained by repeated streaking onto agar plates and were assigned as strains A1 and A5. The genomes were sequenced by MicrobesNG using Illumina HiSeq technology with a 250-bp paired-end protocol. Draft genome sequences were submitted to a high-throughput genome description tool called Protologger and Type (Strain) Genome Server for whole 16S rRNA gene and genome-based taxonomic analyses. Phenotypic and chemotaxonomic analyses were conducted to provide a complete taxonomic description of the isolates.

The whole 16S rRNA gene and genome-based phylogenetic analysis indicated that strains A1 and A5 belong to the genus *Halobacillus* with 100% sequence similarity to multiple *Halobacillus* species, including the type species *Halobacillus halophilus*. The digital DNA-DNA relatedness (dDDH), and average nucleotide identity (ANI) values of strains A1 and A5 were significantly lower (dDDH ranged from 18.6 to 22.3% and 18.5 to 21.4% respectively; ANI 78.6% and 78.15%, respectively) than the threshold values (>70% and >90%, respectively). Furthermore, the dDDH, ANI, and Average Amino acid Identity (AAI) scores between the two new strains were 19.1%, 76.63%, and 78.76%, respectively, supporting the delineation of two novel species of the genus *Halobacillus*. Physiological and chemotaxonomic variations were observed between the two novel *Halobacillus* strains and across phylogenetically closely related *Halobacillus* strains.

The strains appear to be epsotolerant, which means that can grow at $MgSO_4.7H_2O$ concentration up to 2.7 M, but do not require it to grow. This is in line with their habitability in a rare natural habitat with high levels of dissolved Mg^{2+} and SO_4^{2-} ions. The novel species announcement paperwork is underway. The findings of the new bacterial species from the natural sulfate crystal associated brine medium may offer important insights into the habitability of the similar environmental pockets on Mars that could be enriched with or have preserved detectable biosignatures.

Keywords: Bacteria, Halophiles, Sulfate, Taxonomy

41. The ExoClock Project: an open integrated platform for maintaining the Ariel target ephemerides with contributions from the public

Kokori, Anastasia

Presenting author institution: UCL-CSED

The ExoClock Project (www.exoclock.space) is an open, integrated, and interactive platform, designed to maintain the ephemerides accuracy of the Ariel targets. Ariel is ESA's medium class space mission prepared for launch in 2029. The main aim of the mission is to characterise a large number of exoplanets to better understand their nature. ExoClock aims to provide transit mid-time predictions for Ariel by collecting all currently available data (literature observations, observations conducted for other purposes, both from ground and space) and by efficiently planning dedicated efforts to follow-up the Ariel targets. ExoClock is open to contributions from a variety of audiences professional, amateur astronomers, university students and industry partners aiming to make the best use of all available resources towards delivering a verified list of ephemerides for the Ariel targets before the launch of the mission. In this presentation strategies, tools and the current status of the ExoClock project will be described. In addition, the results will be presented from almost three years of operation of the project. Finally, showcases of particular targets will be discussed.

Keywords: exoplanets, transit observations, open science, ephemerides , Ariel space mission

Session 6:

Lighting talk group 3a

42. Development of a CubeSat system to supplement lunar prospecting missions

Levy, Victoria; Cullen, David; Morse, Andrew; Sheridan, Simon

Presenting author institution: The Open University

In Situ Resource Utilisation (ISRU) is key to the future of lunar exploration, where the ability to make use of the widely available lunar surface material, will allow for a reduction in both mission launch and operations costs. It has been demonstrated that regolith-type material can be utilised in the creation of infrastructure, the extraction of useful metals, and the production of oxygen. For example, recent studies at the Open University have demonstrated that oxygen can be produced from the reduction of lunar analogues and samples [1], representing a variety of terrains across the lunar surface. The potential resource of water at the lunar poles has also been discussed in detail and provides a target for many upcoming missions [2].

This study looks to the successful research into ISRU systems such as PROSPECT [3] and LUVMI [4] and considers the feasibility of a new miniaturised sampling and analysis system. The aim is to develop a system centred around a small-scale magnetic-sector mass spectrometer, compatible with the CubeSat form factor. The device would be cost effective and easily replicable, allowing deployment across the lunar surface to provide initial data for future ISRU missions. Additionally, as it is vital in the context of longer-term lunar exploration that ISRU activities be sustainable and make best use of the access to pristine lunar material. This research will consider scientific outcomes that can be achieved alongside prospecting activities, especially in the key areas lacking 'ground-truth' data, such as the lunar poles. It is hoped that the developed system could provide measurements of the volatile abundance and D/H isotope ratio within a sample, addressing questions about the type and origin of water at the lunar surface.

A breadboard demonstration model will be developed at the Open University to simulate the system from end to end. Using standard reference equipment, the limits of the system will be determined, and optimisation implemented to increase accuracy and precision. Samples will be heated within an oven to release volatile species, which will then be passed for analysis. A miniature magnetic-sector mass spectrometer will be used to analyse samples which are intended to be representative of mare, highland, and polar material.

References: [1] Sargeant, H. et al., Hydrogen reduction of lunar samples in a static system for a water production demonstration on the Moon (2021) in Planetary and Space Science, 205 (105287), [2] Hurley, D. M. et. al., Lunar Polar Volatiles: Assessment of Existing Observations for Exploration (2016). Available at https://ssed.gsfc.nasa.gov/dream/docs/PolarVolatiles_HEOMD_Hurley.pdf, [3] Heather, D. et al., The ESA PROSPECT Payload for Luna 27: Development Status (2021) in Lunar Planet. Sci. Conf., LPI, Abs #. 2548, [4] Gancet, J. et al., Lunar Volatiles Mobile Instrumentation (LUVMI) Project Results (2019) in Proc. Int. Astronaut. Congr. IAC, Vol. 2019-October

Keywords: ISRU, mass spectrometry, lunar regolith, lunar water, volatiles

43. Low Power Microwave Heating of Icy Lunar Simulants

Cole, James; Morse, Andrew; Lim, Sungwoo; Anand, Mahesh; Sheridan, Simon; Sargeant, Hannah

Presenting author institution: The Open University

Water ice deposits exist in Lunar polar regions of permanent shadow at temperatures as low as 30 K. These deposits could be a crucial resource required to sustain a human presence on the lunar surface. Recent work has shown microwaves efficiently heat lunar simulants, with promising results for the extraction of water from icy simulants. Through funding from The Open University's Space SRA initiative, and ESA's Off-Earth Manufacturing and Construction Campaign, we have heated lunar simulants doped with water cooled down to initial temperatures of < 120 K in a microwave heating unit (MHU). The MHU supplies microwaves, adjustable in power from 0 to 1 kW, to samples in a cavity capable of operating at pressures from 1 atm down to 10-5 mbar.

Samples were created using 3 lunar simulants: OPRL2NT, LHS-1, and OPRH3N which represent high-Ti mare, and highland materials respectively. Each 50 g sample was desiccated at 230 °C for 24 hours in a vacuum oven. Deionized water was then added to make 5 or 10 wt % water content samples. The samples were placed in a cryogenically chilled N2 gas environment for 90 minutes until the sample had reached < 120 K. The samples were then put under vacuum in the microwave cavity. Once stable pressures were achieved at ~ 1 mbar, the MHU was turned on for 30 minutes producing 250 W, 2.45 GHz microwaves.

Extraction efficiency is defined as the quantity of water extracted compared to the total initially added. Preliminary work for samples with 5 and 10 wt % water content samples suggests the extraction efficiency is lower for highland simulants than for mare simulants. The reason for this is still being explored, however it is probably due to the differing chemical compositions or water absorption characteristics. For 5 wt % LHS-1 samples, it was found that the extraction efficiency increased from 10 % at 35 minutes to over 95 % at 65 minutes whereupon the extraction efficiency began to plateau. Further investigations will take place to explore how the optimum heating time is affected by a selection of variables such as input power, simulant type, and initial water content.

Keywords: ISRU, Lunar Water, Microwave Heating, Icy Simulant

44. The Lunar Trailblazer mission: Understanding the Moon's water

Bowles, Neil; Ehlmann, Bethany; Klima, Rachel, Calcutt, Simon; Evans, Rory; Klesh, Andrew; Howe, Chris; Warren, Tristram, Shirley, Katherine, Curtis, Rowan; Bennett, Lee; Scire, Elena; Fogg, Robert; Furlan, Elise; Llamas, Jake; Seybold Calina; Elkington, Nicholas; Blaney, Diana; Dickson, Jay; Donaldson Hanna, Kerri; Edwards, Christopher; Green, Robert; House, Martha; Pieters, Carle; Thompson, David

Presenting author institution: Department of Physics, University of Oxford

Lunar Trailblazer is a pioneering NASA SIMPLEx mission to investigate the presence and form of water on the Moon. The mission was selected in June 2019 and will be ready for launch in 2023 as an ESPA Grande class ride-along. This presentation will describe Lunar Trailblazer's science and the status of the mission as the spacecraft and instruments are tested and integrated

Lunar Trailblazer targets understanding of the Moon's water: its form (ice, H_2O, or OH), abundance, and distribution as well as the Moon's potential time-varying lunar water cycle. A Lockheed Martin integrated smallsat will carry the JPL High-resolution Volatiles and Minerals Moon Mapper (HVM^3) shortwave infrared imaging spectrometer and the UK-contributed, University of Oxford-built Lunar Thermal Mapper (LTM) infrared multispectral imager, which simultaneously measure composition, temperature, and thermophysical properties. From ~100-km polar orbit, Lunar Trailblazer will detect and map water on the lunar surface at key targets with 4 science objectives: (1) determine its form (OH, H_2O or ice), abundance, and local distribution as a function of latitude, soil maturity, and lithology; (2) assess possible time-variation in lunar water on sunlit surfaces; (3) use terrain-scattered light to determine the form and abundance of exposed water in permanently shadowed regions; and (4) understand how local gradients in albedo and surface temperature affect ice and OH/H_2O concentration, including potential identification of new, small cold traps..

This mission provides unprecedented sensitivity for direct detection of lunar water at key targets. HVM^3 builds upon the demonstrated ability of M^3 to detect lunar water even in permanently shadowed regions with enhanced spatial and spectral resolution, SNR, and spectral range. LTM brings enhanced spectral and spatial resolution relative to Diviner. Understanding the lunar water cycle and determining the abundance, local distribution and form of water will support exploration and utilisation of the Moon and its resources. Identification and characterization of water and its forms is critical knowledge as lunar exploration moves forward. Reconnaissance of potential landing zones will also be possible.

The mission has recently (May 2022) passed its system integration review, and assembly, test, and calibration of the LTM and HVM^3 instruments is currently underway.

Keywords: Lunar , Water, Remote sensing

45. Radiometric Calibration for the Lunar Thermal Mapper on NASA's Lunar Trailblazer.

Elkington, Nicholas; Bowles, Neil; Calcutt, Simon; Warren, Tristram; Shirley, Katherine; Evans, Rory; Eshbaugh, Henry; King, Greg; Temple, Jon; Hoe, Jordan.

Presenting author institution: University of Oxford

Lunar Trailblazer is a NASA SIMPLEx program mission to investigate the form and abundance of water on the surface of the Moon, launching in 2023. Trailblazer will carry JPL's High-resolution Volatiles and Minerals Moon Mapper (HVM^3) and the Lunar Thermal Mapper (LTM) from the University of Oxford. As a thermal infrared radiometer accurate knowledge of the instrument's internal temperature and calibration targets is essential to understanding the radiometric accuracy of the instrument during ground testing and in flight. This poster will describe the temperature sensor circuit performance and the implications for the accuracy of LTM for mapping the Moon's surface temperature and composition.

LTM is an imaging thermal radiometer that will map the lunar surface with 4 broad bands between 6 and 100 mm and 11 narrow bands between 7 and 10 mm. HVM^3 is a shortwave infrared imaging spectrometer operating between 0.6 and 3.6 mm. HVM^3 is optimised for the detection of volatiles to map ice, OH and bound H_2O. The instruments will produce complimentary datasets with the LTM broad bands providing high accuracy (<1 K uncertainty) surface temperature measurements (110-400K) to allow accurate thermal corrections to be made to the HVM^3 spectra, and the narrow bands providing information on surface physical properties and silicate composition. LTM takes design heritage from the Diviner Lunar Radiometer and is very similar in design to The Modular Infrared Molecules and Ices Sensor (MIRMIS) which will fly on ESA's Comet Interceptor in 2029. The testing and ground support described in this presentation will apply to both LTM and MIRMIS.

As a radiometer LTM's detector measures the intensity of radiation falling on its surface, this measurement must be converted to a radiance by means of in-situ calibration views falling on either side of target observations. Deep space is used as one calibration view and an on-board blackbody target is the other. Considerable ground testing calibration work is done prior to launch to inform the in-flight calibration process. Knowledge of the on-board blackbody temperature is crucial to correct flight calibration and constrains the accuracy of the instrument.

The temperatures of components within LTM are measured by platinum resistance thermometers (PRTs) which are monitored by circuitry contain on LTM's Housekeeping Board. In order to establish the accuracy of these temperature measurements the circuitry has been tested under varying thermal environments representative of lunar orbit.

A combined radiometric model has been created to simulate the radiance at the detector as the temperature of each component within LTM changes. This model has been used to evaluate the instrument temperature requirements and will here be used to contextualise the uncertainties introduced into LTM's data and calculate the effect temperature uncertainty will have on final measurements.

The LTM testing regime is currently underway, in preparation for Lunar Trailblazer to launch in 2023.

Keywords: Lunar Ice, Radiometric Calibration, Radiometry, Remote Sensing, Ground Support

46. Spectroscopic Analysis of Askival, an Aqueously Altered Cumulate in Gale Crater

Bowden, D. L.; Bridges, J.C., Cousin, A., Rapin, W., Pinet, P., Semprich, J., Payre, V., Sautter, V., Gasnault, O., Forni, O., Gasda, P., Das, D., Schwenzer, S. P., Wiens, R. C., Bedford, C. C.

Presenting author institution: University of Leicester

Introduction: Askival is a highly altered feldspathic cumulate sample investigated by the Curiosity rover in Gale crater, Mars. Between sols 2015-2021, Curiosity performed a series of geochemical analyses and generated accompanying imagery of Askival at the Bressay site, which contains several float samples.

Methods: Analysis was performed using the Chemistry and Camera (ChemCam) [1], Alpha-Particle X-Ray Spectrometer (APXS) [2] and Mars Hand Lens Imager (MAHLI) [3] instruments. The ChemCam instrument is a geochemical remote sensing instrument that employs laser induced breakdown spectroscopy (LIBS) to assess the abundance of major elemental components in geological targets on Mars. LIBS uses a high-powered laser to induce a short-lived micron-scale plasma on the surface of a target, producing characteristic atomic spectra as the plasma returns to the ground state. ChemCam is able to analyse targets up to approximately 7 m away from the rover using this technique. For a coarse-grained target such as Askival, individual phases can be analysed separately due to the small scale of the analysis spot. The ChemCam Remote Micro-Imager (RMI) camera provides accompany images that allow LIBS spot analyses to be mapped onto the target's texture. We use APXS and MAHLI data as a complementary dataset to the ChemCam LIBS analyses performed on Askival. In addition, ChemCam analysis of a previous feldspar cumulate target, Bindi, provides a useful geochemical comparison.

Results: Askival's texture consists of 4 distinct phases; The most abundant phase comprises approximately 65% of the visible sample and consists of light-toned, subhedral crystals with some cases of elongation. This phase is separated and sometimes enclosed by a secondary dark-toned phase which comprises approximately 30% of the sample. The remaining portion of the sample contains a fibrous grey/brown phase which appears a couple of times on the surface texture as well as a second light-toned phase that occurs as small veins in interstitial areas. Geochemically, the primary light-toned phase trends away from a stoichiometric feldspar composition, in particular being enriched in SiO_2, in some cases up to 80% by mass. This enrichment is correlated with an increase in H, depleted alkali elements and enrichment in Mg, suggesting aqueous alteration producing a leached layer and precipitation of Mg-phyllosilicates under low temperature acidic conditions [4]. Other float samples at the Bressay site lack geochemical evidence of similar alteration and do not have the same cumulate texture as Askival, suggesting a diverse range of sources for material transported to the site. The secondary phase presents a range of mafic chemistry, indicating a matrix of fine-grained mineral endmembers. Normative composition models suggest the matrix consists of Fe/Mg silicates including pyroxenes and amphibole, supporting a model of formation under an upper crustal setting.

References: 1. Maurice, S., et al., Space Science Reviews, 2012. 170(1-4): p. 95-166. 2. Gellert, R., et al., Journal of Geophysical Research: Planets, 2006. 111(E2): p. n/a-n/a. 3. Edgett, K.S., et al., Space Science Reviews, 2012. 170(1): p. 259-317. 4. Yuan, G., et al., Earth-Science Reviews, 2019. 191: p. 114-140.

Keywords: Mars, Spectroscopy, Geochemistry, Aqueous Alteration

47. Raman Spectroscopy of Mars Analogue Samples from Þórisjökull, Iceland

Bowden, D. L.; Bridges, J. C., Bedford, C. C., Hutchinson, I., McHugh, M., Lerman, H.

Presenting author institution: University of Leicester

Introduction: Raman spectroscopy represents a new opportunity for planetary geochemistry, with two currently operational instruments (SuperCam [1] and SHERLOC [2]) on board the Mars 2020 *Perseverance* rover and the ongoing preparation of the Raman Laser Spectrometer (RLS) instrument [3] for the planned ExoMars rover mission. By providing comparative spectra with data sent back from Mars, terrestrial analogue samples allow the assessment and optimization of instrument performance and help to analyse mineralogical components in Martian samples.

We analyse a set of samples taken from the Þórisjökull glacio-fluvio-aeolian sedimentary system in southwest Iceland. These samples were provided by the NASA-funded SAND-E Mars analogue mission [4] and are comprised of unconsolidated basaltic sediments gathered from a series of sites within a 10 km transect of the Þórisjökull area. These samples have similar mineralogical compositions to Martian sediments encountered by current and previous surface missions, and the site represents a mineralogical analogue to geological units within the Jezero crater and Oxia Planum landing sites.

Methods: We employed a Horiba benchtop Raman spectrometer and optical microscope system to analyse the sediment samples, both as unmodified sediment and as crushed material. We also doped a set of test samples derived from a single sediment sample location with additional siderite and Fe-clay minerals, which are of particular relevance to astrobiological studies and habitable paleo-environments. The benchtop spectrometer system uses two lasers; 532 nm, which is the same wavelength as SuperCam and RLS, and 784.75 nm. The spot size, laser power at the sample and spectral range are also similar to that of the RLS system.

Results: We present the results of these analyses, including comparison to mineralogy determined through X-ray diffraction, and analyse the detection constraints of the carbonate and clay-doped samples. Basaltic mineral components including pyroxene and feldspar are identified throughout the SAND-E samples and we examine the detectability of the siderite and clay within doped samples at 5%, 10% and 15% proportions by mass. Further work will make use of an RLS simulator unit which replicates the capabilities of the RLS instrument even more closely.

[1] Wiens, R., et al. in *Proceedings of the 48th Lunar and Planetary Science Conference*. 20172 [2] Beegle, L.W., et al.. in *AGU Fall Meeting Abstracts*. 2014 [3] Fernando, R., et al.,. Astrobiology, 2017. **17**(6-7): p. 627-654 [4] Bedford, C., et al., LPI Contributions, 2021. **2595**: p. 8091.

Keywords: Mars, Raman Spectroscopy, Analogue Samples, Geochemistry

48. Carbon speciation in Martian magma chambers

Rinaldi, Michele; Sami Mikhail

Presenting author institution: University of St Andrews

The chemistry of the Martian atmosphere results from a combination of several processes, including, but not limited to, volcanism, weathering, meteoritic influx, and biological processes. Considerable attention has been given to disequilibrium carbon species detected in the atmosphere, such as methane (CH4), because the origin is either geological or biological. We contribute to this quandary by addressing a simple question: is methane an equilibrium phase in Martian magma chambers?

The Martian landscape preserves a record of large bodies of superficial fluids, but little is known about deep fluids. Recently, macro-molecular and gaseous organic carbon components have been found in sedimentary rocks associated with mafic minerals (Blamey et al., 2015), leading to the notion that an inorganic source of hydrocarbons is a feature of Martian geology. Unlike Earth, Mars does not have plate tectonics and subduction zones; therefore, the origin of these enigmatic fluids may be related to lithospheric gravitational instabilities at the crust-mantle boundary (Breuer and Spohn, 2003).

We utilise the Deep Earth Water Model (DEW) to run thermodynamic models simulating fluid-rock metasomatism in a hypothetical magma chamber located at the crust-mantle boundary (40 km depth ca., 0.5 GPa). We employ different temperatures (from 200 to 1000 ºC) to match plausible geothermal gradients within a range of oxygen fugacity compatible with Martian meteorites' data (from 0 to -4 ΔFMQ). The geological model involves a fluid, initially in equilibrium with a peridotite, moving along an isothermal and isobaric path and finally interacting with a set of Martian mafic rocks (peridotites and pyroxenites). Our results show that the fluid speciation during a metasomatic event is strongly related to the environmental parameters, with methane formation feasible over a broad range of conditions. Therefore, the abiotic formation of methane in the Martian interior is expected and is not enigmatic.

References; Blamey, N.J.F., Parnell, J., McMahon, S., Mark, D., Tomkinson, T., Lee, M., Shivak, J., Izawa, M., Banerjee, M., Flemming, R. (2015) - Evidence for methane in Martian meteorites - Nature Communications; Breuer, D., Spohn, T. (2003) - Early plate tectonics versus single-plate tectonics on Mars: evidence from magnetic field history and crust evolution - J. Geophys. Res. Planets 108 (E7)

Keywords: Mars, metasomatism, carbon speciation, modelling

49. The Department of Planetary Sciences at the University of Aberdeen

Martin-Torres, Javier, **Nazarious, Miracle Israel**

Presenting author institution: University of Aberdeen

The Department of Planetary Sciences, School of Geosciences of the University of Aberdeen, was recently created in 2020 and is focused on studying Earth and planetary sciences and developing instruments for Earth and planetary exploration. The Department adds to previous planetary and Astrobiology contributions from existing members at the School of Geosciences. We are part of current and future missions to Mars: we are co-Investigators of the NASA's Curiosity and Perseverance rovers on Mars, of the ESA's Trace Gas Orbiter, and we have developed an instrument for the ExoMars mission. The device is called HABIT (HabitAbility: Brine, Irradiation and Temperature) and, among other things, will produce liquid water on Mars to support future exploration of the planet. HABIT will be the first UK In-Situ Resource Utilization instrument on the surface of another planet. We are also interested in comparative planetology and how studying the other planets of the solar system can help us understand our Earth better. Infrastructure: We have two Labs for hardware development and research experiments, including our Space-Q Martian Simulation chamber. Research: We are an interdisciplinarity team, and we can go from idea to instrument design, development, and scientific exploitation. Our primary research topics are Mars Research, Environmental Research, Hardware development, Geophysics, Remote sensing and Radiative Transfer of Earth and planetary atmospheres, and Astrobiology. Education: We educate undergraduates and third-cycle students. Last year we started an MSc of Planetary Sciences; we supervise Bachelor and Master theses and provide education through seminars and several general audience outreach activities. Our pedagogical methodology is founded on cooperative learning to promote individual creativity and initiative. Innovation: We support innovation by producing new methods and instruments and engaging in interdisciplinary subjects. We have international awards for innovation challenges and critical contributions to research. We collaborate with the industrial and academic sectors. Knowledge dissemination: We have a solid international network of collaborations. We publish our technological contributions in open form because we are committed to immediately returning to society. Our research is published in the top-ranking refereed journals and presented at international conferences.

Keywords: Planets, Astrobiology, Research, Education, Innovation

Session 7:

Exploration and Mars

50. Contemporary chemistry in the Martian atmosphere observed with the ExoMars Trace Gas Orbiter

Olsen, Kevin

Presenting author institution: University of Oxford Department of Physics

Since 2018, the ExoMars Trace Gas Orbiter has been collecting science data with the Atmospheric Chemistry Suite (ACS) with the primary objective of detecting trace gases in the atmosphere of Mars. While several target species, including organics and sulphur molecules, remain undetected, we have been able to use the mid-infrared channel (ACS MIR) to detect hydrogen chloride (HCl) and to monitor ozone (O3). With ACS MIR, we are not only able to observe the spatial and temporal variability of such gases, but also their vertical structure, and make detailed comparisons with coincident measurements of water vapour, temperature, and aerosol abundances. These measurements give us new insights into the odd-oxygen and odd-hydrogen photochemistry of the Martian atmosphere. HCl and O3 are both very tightly correlated with water vapour and its photolysis by-products (anti-correlated in the case of ozone) and exhibit strong seasonal cycles that depend on southern spring/summer and the dusty season. HCl is likely formed via reactions with the hydroxyl and hydroperoxyl radicals (OH, HO2), and appears coincidently with dust. The sources and sinks of HCl remain unknown, but are very likely to be related to aerosol activity. Chloride-bearing dust may be its source, while ice condensation may contribute to its rapid removal. On the other hand, hydroperoxyl leads to the removal of ozone by converting odd-oxygen into O2. Therefore, ozone only appears when water is scarce, in the cold and dry aphelion periods. We are observing more than twice the amount predicted by global climate models, but can examine the ratio of ozone to water along the vertical, and note that temperatures have a strong impact on the build-up of ozone. In this presentation, I will highlight the recent results from ACS and show in-depth what we know about the behaviour of HCl and O3, as inferred from our observations.

Keywords: Mars, photochemistry , ozone, atmopsheric physics , atmospheric chemistry

51. Martian ozone and aerosol climatology from MY34 to MY36 as measured by the NOMAD-UVIS spectrometer

Mason, Jonathon; Patel, M.R. Holmes, J.A. Streeter, P. Brown, M. Sellers, G. Marriner, C. Lewis SR. Wolff, M.J. Willame, Y. Depiesse, C. Thomas, I. Vandaele, A.C. Daerden, F. Lopez-Moreno, J.-J. Bellucci, G.

Presenting author institution: The Open University

Near continuous radiance measurements of the martian atmosphere by the Ultraviolet and VISible spectrometer (UVIS), in the 200-650 nm wavelength range (Patel *et al*., 2017), provides a powerful dataset for investigating the ozone and aerosol climatology, and by extension the water cycle, from the well-established photochemical anti-correlation between water vapour and ozone. UVIS forms the UV/visible channel of the NOMAD instrument on the ExoMars Trace Gas Orbiter (TGO) (Vandaele, *et al*., 2018). TGO is in a near-circular 74° inclined orbit with a periapsis of 380 km and apoapsis of 420 km and an orbital period of approximately 2 hours allowing 12 dayside nadir passes per day. Near complete coverage of the surface achieved after 373 orbits (approximately 1 month) when the orbit 'closes' (repeats the same ground track). The repeatable ground track allows UVIS to make repeated measurements at the same location and because the orbit is not sun synchronous these measurements are at different local times.

We perform iterative radiative transfer modelling of the martian atmosphere using the discrete ordinates DISORT package (Stamnes *et al*., 1988) to derive the total column abundances of ozone in the martian atmosphere. Our retrievals also provide derived column abundances for dust and ice aerosols as well as an estimate of the surface albedo. Atmospheric fields outputted by the OpenMars atmospheric data set for Mars (Holmes *et al*., 2020) are used to define our *a priori* and atmospheric state for each UVIS observation.

In this work we describe the spatial and temporal variation of ozone and aerosols in MY34 through to MY36. The uniqueness of the TGO orbit, allowing measurements at different local times, provides the capability to investigate the diurnal cycle of ozone and aerosols. Our results show the characteristic and repeatable O_3 distribution with peak ozone abundances, >30 µm-atm, observed in the colder and dryer spring, winter and autumn seasons in both hemispheres, associated with reduced solar insolation and low atmospheric water vapour content (Crismani *et al.,* 2021). The warmer and dustier perihelion season (L_s = 210°– 330°), with increased atmospheric water content and solar insolation sees ozone abundances reaching a minimum, typically around 1 µm-atm from -74° S to 50° N. Beginning around L_s = 30° and ending around L_s = 120° (MY35) an ozone enhancement is observed in both MY35 and MY36 at mid-latitude, with ozone values between 2-4 µm-atm, and coincides with a cooling atmosphere, a lower hygropause (the altitude at which water vapour condenses) and s the formation of the aphelion cloud belt. The decay of the aphelion ozone band precedes that of the aphelion cloud belt, likely from an influx of H_2O rich air from the sublimating southern pole being transported towards equatorial latitudes and an increasingly higher hygropause.

Keywords: Mars, Remote sensing, Radiative transfer modelling, Atmosphere, Climatology

52. Impacts of Heterogeneous Chemistry on Vertical Profiles of Martian Ozone

Brown, Megan; Patel, Manish; Lewis, Stephen; Holmes, James; Sellers, Graham; Streeter, Paul; Bennaceur, Amel; Liuzzi, Giuliano; Villanueva, Geronimo; Vandaele, Ann-Carine

Presenting author institution: The Open University

Ozone gas is found in small quantities in the martian atmosphere; about 1% of the average ozone column on Earth. It is highly variable temporally and spatially, ranging from < 0.01 pppmv in the warmer, perihelion season, up to 20 ppmv during the colder aphelion season. Ozone abundance is controlled by photochemical reactions involving hydroxyl radical species, which do not have strong spectral signatures at infrared or ultraviolet wavelengths. Two main ways ozone is destroyed in the martian atmosphere are by: 1. absorbing ultraviolet sunlight; 2. reacting with hydroxyl radicals, which are highly reactive chemical species formed by the photolysis of water vapour. The latter leads to a well-known anti-correlation between ozone and water vapour.

In Global Climate Models (GCMs), an underprediction of ozone implies that chemical reactions are missing or incorrect. We investigate reactions between hydroxyl radicals and water ice, known as heterogeneous reactions, as a potential explanation for the ozone underprediction by using a 1-D model and observed vertical profiles. The observed profiles are from the ExoMars Trace Gas Orbiter's NOMAD instrument, and cover the first half of Mars Year 35 at high northern and southern latitudes. The heterogeneous reactions used in the model have been adapted from previous GCMs to better represent the physical processes in the atmosphere. We find improving the heterogeneous chemical scheme causes ozone abundance to increase when water ice is present, better matching observed trends. When water vapour abundance is high, there is no consistent vertical correlation between observed ozone and water ice and, in simulated scenarios, the heterogeneous chemistry does not have a large influence on ozone. Hydroxyl radicals, which are by-products of water vapour, dominate ozone abundance and mask the effects of heterogeneous chemistry on ozone. This is consistent with gas-phase-only modelled ozone, showing good agreement with observations when water vapour is abundant.

We find that the influence of heterogeneous reactions on ozone is dependent on the abundance of water vapour, which undergoes seasonal and spatial variation. In the high water vapour abundance simulated scenario, hydroxyl radical abundance only decreased by a factor of 3 when simulated with heterogeneous chemistry. In contrast, hydroxyl radicals in the low water vapour case decreased by an order of magnitude, despite the water ice concentration being three times less than the high vapour scenario. The relationship between the observed ozone and water ice, which is used as a proxy for heterogeneous chemistry, is also expected to vary temporally and spatially. This is due to the water vapour; the higher the water vapour abundance, the less impact the heterogeneous reactions have on ozone abundance, as the amount of hydroxyl radical adsorbed is lower, relative to the total hydroxyl radical abundance. Water vapour abundance is, therefore, a key species to help understand the interaction of heterogeneous chemistry and the impacts this has on ozone. Overall, the inclusion of heterogeneous chemistry improves the ozone vertical structure in regions of low water vapour abundance, which could explain why GCMs underpredict ozone.

Keywords: Mars, GCM, modelling, TGO, Ozone, Atmospheric chemistry.

53. 4D Transport of Hydrogen Chloride in the Martian Atmosphere

Rajendran, Kylash; Lewis, Stephen R., Streeter, Paul M., Holmes, James A., Patel, Manish R.

Presenting author institution: The Open University

Interest in the martian chlorine cycle has been renewed as a result of the recent discovery of hydrogen chloride (HCl) in the martian atmosphere (Korablev et al. 2021, Olsen et al. 2021). Korablev et al. 2021 used the Atmospheric Chemistry Suite (ACS) aboard the ExoMars Trace Gas Orbiter (TGO) and detected HCl quantities in the 1-4 ppbv range in both hemispheres. Subsequent measurements by Olsen et al. 2021 confirmed that HCl appears seasonally, with almost all positive detections occurring in the dusty second half of the martian year and with abundances decreasing rapidly after the dust season. In addition, a significant correlation between the vertical profiles of HCl and water vapour has also been observed (Olsen et al 2021, Aoki et al 2021). These findings have led to speculation that the source of atmospheric HCl arises from a direct coupling between chloride minerals in martian mineral dust with atmospheric water vapour (Korablev et al. 2021).

Studies of martian chlorine chemistry thus far have focused on studying gas-phase and heterogeneous chemical reactions using simplified column models of the martian atmosphere. Whilst these models have advantages, they cannot evaluate the crucial impact of atmospheric dynamics and transport on the chlorine cycle. In this work we present the results of a full 4-dimensional modelling study of the transport and chemical interactions of chlorine and water species in the martian atmosphere, using the UK version of the Laboratoire de Météorologie Dynamique (LMD) Martian Global Climate Model. The model uses a modified version of the LMD photochemistry scheme (Lefevre et al. 2004) that has been augmented with a chlorine sub-model with 11 new gas species, 47 gas-phase reactions and 5 photolysis reactions in order to simulate the major chemical pathways of atmospheric chlorine (Duffy et al. 2014, Duffy 2015). By varying the locations, times and rates at which HCl is introduced and removed from the model, we quantify the impact of both chemical and transport processes on the subsequent horizontal and vertical distribution of HCl. These results are then compared to the reported observations of chlorine, allowing us to constrain the rates of creation and destruction of HCl.

References:

Aoki, S. et al.: Annual appearance of hydrogen chloride on Mars and a striking similarity with the water vapor vertical distribution observed by TGO/NOMAD. Geophys. Res. Lett., 48(11):e2021GL092506, 2021.

Duffy, M.K.D. et al.: Numerical simulations of the possible atmospheric origin of martian perchlorate. In F. Forget et al., editors, Fifth International Workshop on the Mars Atmosphere: Modelling and Observations, 2014.

Duffy, M.K.D.: Studies of ozone and chlorine chemistry in the Martian atmosphere: implications for recent and future missions. PhD thesis, The Open University, 2015.

Korablev, O. et al.: Transient HCl in the atmosphere of Mars. Sci. Adv., 7(7):eabe4386, 2021.

Lefèvre, F. et al.: Three-dimensional modeling of ozone on Mars. J. Geophys. Res.-Planet, 109(E7), 2004.

Keywords: Mars, Atmospheric Chemistry, Trace Gases

54. Seasonal behaviour of Mars' northern polar vortex

Streeter, Paul; Lewis, Stephen; Patel, Manish; Holmes, James; Rajendran, Kylash

Presenting author institution: School of Physical Sciences, The Open University

Like Earth, Mars has polar vortices: regions of cold air above the winter pole, circumscribed by powerful jets. Understanding the nature of Mars' polar vortices, and how they behave under different atmospheric dust conditions, is important for understanding the current and ancient martian climate, including the chemical and aerosol cycles. In this work we present a climatology of eight martian years of the northern polar vortex, constructed via data assimilation [1] of orbital temperature and dust measurements [2] into a Mars global climate model [3]. We show that the large-scale seasonal behaviour and characteristics of the northern vortex are highly interannually repeatable, though with the important exception of dust storm activity. Previous work [e.g. 4] has focused on individual regional or global dust events, and specifically solstice-time for the latter; by investigating a full eight-year period containing two global and numerous regional dust storms, we are able to investigate the potentially crucial effects of dust storm seasonal timing on vortex behaviour, as suggested by previous work [5]. We find that the timing of atmospheric dust events has a critical role in controlling storm dynamical effects on the northern polar vortex. Storms which occur later in Mars' perihelion (dusty) season, such as solstitial global dust storms and C-type regional dust storms [6], have a greater impact in disrupting both the morphology (including latitudinal extent) and intensity of the vortex than those early in the season, such as equinoctial global dust storms and A-type regional dust storms.

References: [1] S. R. Lewis, M. Collins, and P. L. Read, “Data assimilation with a martian atmospheric GCM: an example using thermal data,” Adv. Space Res., vol. 19, pp. 1267–1270, May 1997. [2] D. J. McCleese, J. T. Schofield, F. W. Taylor, S. B. Calcutt, M. C. Foote, D. M. Kass, C. B. Leovy, D. A. Paige, P. L. Read, and R. W. Zurek, “Mars Climate Sounder: An investigation of thermal and water vapor structure, dust and condensate distributions in the atmosphere, and energy balance of the polar regions,” J. Geophys. Res.-Planet , vol. 112, p. E05S06, May 2007. [3] F. Forget, F. Hourdin, R. Fournier, C. Hourdin, O. Talagrand, M. Collins, S. R. Lewis, P. L. Read, and J.-P. Huot, "Improved general circulation models of the Martian atmosphere from the surface to above 80 km," J. Geophys. Res.-Planet, vol. 104, pp. 24155-24175, Oct. 1999. [4] S. D. Guzewich, A. D. Toigo, and D. W. Waugh, "The effect of dust on the martian polar vortices," Icarus, vol. 278, pp. 100-118, Nov. 2016. [5] P. M. Streeter, S. R. Lewis, M. R. Patel, J. A. Holmes, A. A. Fedorova, D. M. Jass, and A. Kleinböhl, "Asymmetric Impacts on Mars' Polar Vortices From an Equinoctial Global Dust Storm," J. Geophys. Res.-Planet, vol. 126, no. 5, p. e2020JE006774, 2021. [6] D. M. Kass, A. Kleinböhl, D. J. McCleese, J. T. Schofield, and M. D. Smith, "Interannual similarity in the Martian atmosphere during the dust storm season," Geophys. Res. Let., vol. 43, p. 2016GL068978, June 2016.

Keywords: Mars, Mars atmosphere, dust storms, data assimilation, atmospheric dynamics

55. Seeing Minerals Clearly: Learning Dimension Reductions on Spectral Reflectance Libraries for Efficient In Situ Multispectral Image Acquisition and Analysis

Stabbins, Roger; Grindrod, Peter; Motaghian, Sara; Allender, Elyse; and Cousins, Claire

Presenting author institution: The Natural History Museum

Vision is critical to the exploration of an environment. Colour vision, the act of sampling light across several distinct spectral bandwidths, encodes the material boundaries and compositional context of an environment into an interpretable low-dimensional representation. The exploration of the surface of Mars by rover platforms has benefitted from multispectral vision systems, that increase the spectral extent and resolution of typical trichromatic systems, and accordingly are able to discriminate an increased number of rock and soil material classes [1]. Here we investigate the problem of choosing and combining a minimal number of colour and near-infrared spectral channels from a multispectral filter suite, to discriminate a given target material against a background, in image products captured by a multispectral imager. Solving this problem can alleviate data-volume requirements and computational and cognitive processing during a given image analysis task, two problems of relevance to ground-in-the-loop time-critical remote planetary surface exploration operations, e.g. with rover platforms or small-body rendezvous missions. This work supports preparations for the operation of the multispectral PanCam Wide-Angle Cameras of the ESA ExoMars rover [2]. PanCam will capture 12-band multispectral panoramic images of the rover surroundings that will be calibrated to units of reflectance, to provide preliminary distinctions of rock and soil classes, prior to further investigations by instruments of greater discriminative power but narrower spatial scope. Here we approach the problem by training a supervised dimension reduction method with the reflectance spectra of minerals expected at the rover landing site, *Oxia Planum*, sourced from publicly available laboratory measured spectral reflectance libraries [3]. After resampling the spectral library entries to the instrument multispectral resolution, we compute, in parallel, the optimal Fisher Ratio for each pair combination of all permutations of the spectral parameters afford by the 12-band filter set. The optimal Fisher Ratio, the inter-class separation over the intra-class variance, is computed with the dimension reduction method of Linear Discriminant Analysis, that finds the linear projection from a high-dimensional feature space to a subspace, such that the Fisher Ratio is maximised [4]. We use the resultant Fisher Ratio scores to rank the effectiveness of the spectral parameter paired combinations at separating the target from background in the projected subspace, providing an efficient method for selecting filter subsets for a given task. Although developed in the context of ExoMars PanCam, this method is applicable to targeted imaging tasks of any multispectral imaging system, provided the task has a well-defined set of expected materials. Current and future multispectral imaging experiments set to benefit from this method include the Mastcam and Mastcam-Z instruments of the NASA Mars Science Laboratory *Curiosity* and Mars 2020 *Perseverance* rovers [5], [6], and the OROCHI instrument of the JAXA Martian Moons Exploration sample return spacecraft [7].

[1] Bell *et al.*, 2019, doi:10.1017/9781316888872.028. [2] Coates *et al.*, 2017, doi:10.1089/ast.2016.1548. [3] St. Clair *et al.*, 2022, https://westernreflectancelab.com/visor/ [4] Duda, Hart, and Stork, *Pattern Classification*, 2001. [5] Bell III *et al.*, 2017, doi:10.1002/2016EA000219.[6] Bell *et al.*, 2021, doi:10.1007/s11214-020-00755-x., [7] Kameda *et al.*, 2021, doi:10.1186/s40623-021-01462-9.

Keywords: Spectral Imaging, Instrumentation, Reflectance Spectroscopy, Mars, ExoMars

Session 8:

Lightning talk group 3b

56. Combining spectral and morphostratigraphic units on Mercury: A case study of the Rachmaninoff basin area

Wright, Jack; Zambon, Francesca; Carli, Cristian; Altieri, Francesca; Pöhler, Claudia M.; Rothery, David A.; van der Bogert, Carolyn H.; Rossi, Angelo Pio; Massironi, Matteo; Balme, Matthew R.; Conway, Susan J.

Presenting author institution: European Space Agency, ESAC, Spain

MESSENGER-era quadrangle geological maps are primarily made by observing Mercury's geomorphology in monochrome MDIS mosaics (Galluzzi et al., 2021), and so might more accurately be called morphostratigraphic maps. Geological maps of Earth incorporate more information, such as rock lithology, composition, and origin (Massironi et al., 2021). Until landed Mercury science begins (Ernst et al., 2022), most bedrock properties will probably remain elusive, hence the convention for planetary geological maps to be descriptive and conservative. MESSENGER did collect spectroscopic data, indicative of composition, but this information has not systematically been incorporated into the planet's geological maps thus far.

Recently, Zambon et al. (2022) produced spectral unit maps of Mercury using MDIS data, including the Hokusai quadrangle. In this work, we combine the morphostratigraphic units of (5) with these spectral units. We focus on Rachmaninoff basin and its surroundings, including Nathair Facula. Our aim was to augment the descriptions and correlation of map units of Wright et al. (2019).

We summarized the spectral unit map, originally produced as a ~450 m/pixel raster, by digitizing new spectral contacts between regions dominated by different spectral units. We observed that these spectral contacts either closely align with morphostratigraphic contacts, indicating spectrally and geomorphically distinct units in contact with each other, or spectral contacts diverge from morphostratigraphic contacts, indicating spectral diversity within a morphostratigraphic unit. We added these diverging spectral contacts to the morphostratigraphic contacts to create a new geostratigraphic map.

By combining spectral and morphostratigraphic datasets, we have been able to distinguish impact melt and volcanic plains deposits within Rachmaninoff, which formerly had to be grouped together (Wright et al., 2019). Our method can be applied retroactively to preexisting morphostratigraphic maps of Mercury (Giacomini et al., 2021) and other planetary bodies (Pöhler et al., 2022), and it produces similar results to maps created from the outset using color data (Semenzato et al., 2020). Our approach brings planetary geologic maps closer to their Earth equivalents.

Galluzzi et al. (2021) Planetary Geologic Mappers Meeting, Abstract #7027. https://www.hou.usra.edu/meetings/pgm2021/pdf/7027.pdf

Massironi et al. (2021) EGU21-15675. https://doi.org/10.5194/egusphere-egu21-15675

Ernst et al. (2022) Planet. Sci. J., 3, 68. https://doi.org/10.3847/PSJ/ac1c0f

Zambon et al. (2022) JGR Planets, 127, e2021JE006918. https://doi.org/10.1029/2021je006918

Wright et al. (2019) J. Maps, 15, 509–520. https://doi.org/10.1080/17445647.2019.1625821

Giacomini et al. (2021) EGU21-15052. https://doi.org/10.5194/egusphere-egu21-15052

Pöhler et al. (2022) 53rd LPSC, Abstract #2094. https://www.hou.usra.edu/meetings/lpsc2022/pdf/2094.pdf

Semenzato et al. (2020) An integrated geologic map of the Rembrandt basin, n Mercury, as a starting point for stratigraphic analysis. Remote Sensing, 12. https://doi.org/10.3390/rs12193213

Keywords: Mercury, Geology, Mapping, Data Fusion

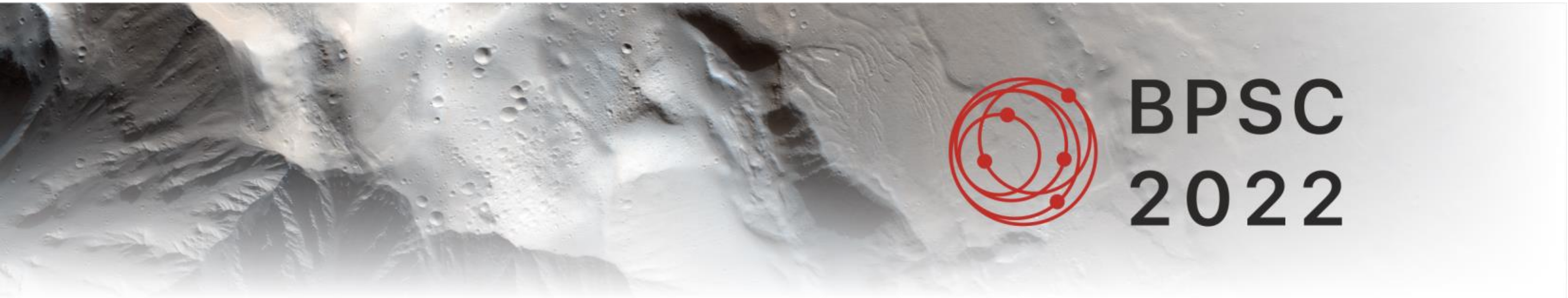

57. Geological Mapping of Mercury's Bach-side (the south polar Bach Quadrangle, H15)

Lennox, Annie; Rothery, David; Balme, Matt; Conway, Susan; Wright, Jack

Presenting author institution: Open University

Introduction: For cartographical purposes, Mercury is divided into 15 quadrangles (H01-H15). Prior to ESA/JAXA's BepiColombo mission reaching Mercury, a comprehensive suite of geological maps of each quadrangle is required to support and provide context for the planned science phase of the mission. Currently, 8/15 quadrangles are completed and 3 more, including H15, are underway at the OU (H11 and H13). Here we review the progress made for H15, the area poleward of -65°.

Methods: We map using: a 166 m/p monochrome primary basemap; high-incidence east and west, and low-incidence angle secondary basemaps; a 665 m/p enhanced color mosaic; and a 665 m/p stereo-derived digital elevation model. Additionally, we use individual narrow-angle camera images at higher resolutions to better investigate important features of interest. All these data are products of MESSENGER's Mercury Dual Imaging System instruments. We map using the south polar projection, digitising at a scale of 1:400k with map publication at 1:3M.

Progress: We have mapped crater rims for large (>20 km), small (5-20 km) and subdued (buried) craters, and this is largely complete. Additionally, we have started mapping tectonic features (lobate scarps and wrinkle ridges). Watters et al. (2015) predicted a transition from N-S to E-W trending scarps occurring at a latitude of around -60°. From our initial mapping, there seems to be an ostensibly equal abundance of N-S and E-W trending scarps.

We have also identified 5 craters in H15 exhibiting lobate ejecta. These are relatively rare on Mercury and represent ejecta flows that are texturally rougher with steeper margins than typically, ballistically emplaced ejecta, and maintain constant thickness across the flow front. Such features can be found on many planetary bodies, with two scenarios for mode of emplacement: a mass-wasting event or a fluidised ejecta flow. Prior to this discovery, only 7 craters with ejecta flows had been compiled on Mercury (Xiao and Komatsu, 2013). Our discoveries, alongside those made by Blance et al. (2022) who are conducting a global survey of such features, will add to this database. When possible, we have mapped: the proximal and distal ejecta; the crater floor, wall, and central uplift features; and impact melt deposits of these 5 lobate ejecta deposits.

References: A. J. Blance et al. (2022) MExAG Ann. Meeting; T. Watters et al. (2015) Geophysical Research Letters, 42(10), 3755-3763; Z. Xiao and G. Komatsu (2013) Planetary and Space Science, 82-83, 62-78.

Keywords: Mercury, Mapping, Geology

58. Mapping Mercury's Discovery Quadrangle

Blance, Alistair; Rothery, David; Balme, Matt; Galluzzi, Valentina; Wright, Jack

Presenting author institution: The Open University

Here we present progress on the mapping of Mercury's H11 Discovery quadrangle, part of a series of maps aiming to cover Mercury globally at 1:3,000,000 scale, ready for BepiColombo's arrival into scientific orbit around the planet in 2025. The quadrangle is in Mercury's southern hemisphere (0–90°W, 22.5–65°S), and is named after Discovery Rupes, a prominent lobate scarp found within the quadrangle. The quadrangle is heavily cratered, with craters and impact basins of various degradation states. A variety of terrain types are found within H11, with crater materials and intercrater plains constituting the majority of the quadrangle. There is also a minor component of smooth plains materials, found mostly within the interior of large craters. In addition, Discovery also contains a chaotic terrain. The largest example of this type of surface morphology on Mercury, the chaotic terrain consists of numerous knobs, pits, and linear grooves, which cut across crater rims, often drastically altering their surface expression.

We are mapping H11 using ArcGIS to digitise features and contacts, based on a variety of MESSENGER derived image and data products. This includes a 116 mpp monochrome basemap, high-incidence and low-incidence angle secondary basemap variants, colour image mosaics, and a digital elevation model. Additionally, we use individual MESSENGER MDIS camera frames to look at features in higher resolution if available. The map is in a lambert conformal conic projection, the standard projection for mid-latitude quadrangles. So far we have mapped all crater rims within the quadrangle, and are now digitising crater fill material contacts.

Features of interest we have identified so far within H11 include the chaotic terrain, which is antipodal to the Caloris basin in the northern hemisphere of Mercury. Previous studies (Schultz and Gault, 1975) have suggested the Caloris impact may have formed the terrain, where seismic shaking and impact ejecta deposition resurfaced the area. This mechanism has also been proposed for chaotic terrains on the Moon. Alternatively, Rodriguez et al. (2020) suggested the Discovery chaos terrain may have been formed from volatile loss. Careful observation of the morphology of the terrain, in addition to seeking evidence for its age, may help in deciphering its origins. Elsewhere in the quadrangle, Discovery Rupes is close to proposed pyroclastic vents, in addition to two proposed ancient impact basins, Andal-Coleridge and b54. This is an area of interest for studying the interplay between ancient basins, faults, and volcanic features, where the presence of ancient basins may influence the propagation of faults (Fassett et al., 2012 and Watters et al., 2001), and pyroclastic pit sites may occur preferentially on impact craters and in highly fractured areas (Klimczak et al., 2018).

Keywords: Mercury, Mapping, Remote sensing, BepiColombo, Geomorphology

59. Global Dust Storms on Mars: The Initialisation, Growth, and Categorisation of Global Dust Storms on Mars

Hyland, Benedict; Amezcua, Javier; McGuire, Patrick

Presenting author institution: University of Reading

This is a dissertation project that looked at the Initialisation, Growth, and Categorisation of Global Dust Storms on Mars.

Martian Global Dust Storms can lead to power failures in solar modules when the surface of Mars is covered in a thick cloud for weeks or months. This dissertation project has used the Ensemble Mars Atmosphere Reanalysis System (EMARS) to distinguish atmospheric features which lead to the largest dust storms on Mars. This has been done by using Empirical Orthogonal Function (EOF) analysis on the EMARS dataset and comparing it to storm data from the Mars Dust Activity Database (MDAD).

The EMARS data was analysed using Singular Value Decomposition (SVD) was used to collect the EOF, principal components, and scores for the variable activity in time, whilst the MDAD data was analysed using Partitioning Around Medoids (PAM), Ordering Points To Identify Cluster Structure (OPTICS), and Iterative Reducing and Clustering using Hierarchies (BIRCH) – all unsupervised machine learning algorithms. This was done with the intention of creating a new method of classification for dust storms, which would not only be dependent on the size and length, but also on the position and time of year.

It was found that the Martian variability is highly dependent upon the solar longitude and opposing baroclinic wavenumber one and two waves. Rapid variation in opposing wavenumber one waves appears to lead to the generation and growth of the largest dust storms on Mars, with 63% of the largest dust storms occurring immediately after a rapid change from a negative score to a positive score.

The optimum number of clusters for dust storm classification on Mars was found to be five, with obvious centroids located dependent upon the maximum area, length, time of year and latitude. Whilst OPTICS and BIRCH clustering found there to be more fuzzy boundaries between the clusters, the centroids were well defined and could be used for future classification of Martian dust storms.

Keywords: Mars, Dust Storms, Principal Component Analysis, Machine Learning, Baroclinic Waves

60. Searching for odd-hydrogen in the atmosphere of Mars with the ExoMars Trace Gas Orbiter

Alday, Juan; Holmes, J. A., Patel, M. R., Mason, J. P., Trokhimovskiy, A, Fedorova, A. A., Belyaev, D. A., Korablev, O., Lefèvre, F., Montmessin F., Baggio L., Braude A. S., Olsen K. S., Irwin, P. G. J., Wilson, C. F.

Presenting author institution: The Open University

Odd-hydrogen (HO_x) species such as OH and HO_2 have a crucial role in regulating the chemistry of the atmosphere of Mars. In particular, they are responsible for maintaining the 96% abundance of CO_2 in the atmosphere and provide key information to understand the seasonal and diurnal cycles of other photochemical species such as CO or O_3. While the abundance of HO_x therefore seems crucial to understand the photochemical processes in the martian atmosphere, there is little information from measurements.

In this study, we search for infrared spectral signatures of OH and HO_2 in the atmosphere of Mars using solar occultation measurements by the Atmospheric Chemistry Suite (ACS) onboard the ExoMars Trace Gas Orbiter (TGO). In particular, the spectral region between 2.78-2.9 µm (3448-3597 cm^{-1}) is monitored in 150 solar occultations from L_S=160 in Martian Year 35 (MY35) to L_S = 60 in MY36. The biggest challenge for the detection of HO_x in this spectral range is the removal of the absorption by CO_2, H_2O and dust to isolate the weak spectral features of OH and HO_2. However, fitting those spectral features allows the derivation of the vertical profiles of pressure, temperature and water vapour abundance, which provide context for any detections of the odd-hydrogen species.

The results from these measurements will be compared with the expectations from the assimilation runs from the Mars Global Circulation Model (GCM) used by the modelling group at the Open University to test whether the measurements can meaningfully constrain Mars' photochemical models. In additions, the expectations from the model will also be used to establish a sensitive search at the times/locations when the abundance of HO_x is highest.

Keywords: Mars, ExoMars, Radiative transfer, Atmosphere

61. Calibration of the HABIT (HabitAbility: Brine, Irradiation and Temperature) instrument

Nazarious, Miracle Israel; Mathanlal, Thasshwin; Ramírez-Luque, Juan Antonio; Zorzano, Maria-Paz; Martin-Torres, Javier

Presenting author institution: University of Aberdeen

The HABIT **(HabitAbility: Brine, Irradiation and Temperature)** instrument consists of two modules that will characterise the present-day habitability at its landing place: (i) EnvPack (Environmental Package) that monitors the thermal environment (air and ground), the incident ultraviolet radiation, the near surface winds and the atmospheric dust cycle; and (ii) BOTTLE (Brine Observation Transition To Liquid Experiment), an In-situ Resource Utilization instrument to produce liquid water for future Mars exploration.

The **EnvPack module** has heritage from previous missions operating on the surface of Mars, and the environmental observations of its sensors will be directly comparable to those delivered, simultaneously, from other sites on the planet, by the NASA missions – Mars Environment and Dynamics Analyzer (MEDA) in Mars2020 Perseverance Rover, Temperature and Winds for InSight (TWINS) in the InSight lander, and the Rover Environmental and Monitoring Station (REMS) in MSL Curiosity rover.

BOTTLE will be used also to investigate the electrical conductivity properties of the Martian atmosphere, the present-day atmospheric-surface water cycle and to evaluate if liquid water can exist on Mars in the form of brines, and for how long. These variables measured by HABIT are critical to determine the present and future habitability of the Martian surface.

HABIT can provide information of the local temperature with ±0.2°C accuracy, local winds with ± 0.3 m/s, surface brightness temperature with ±0.8°C, incident UV irradiance with 10% error of its absolute value in the UV-A, UV-B, UV-C ranges, as well as in the total UV-ABC range, and two additional wavebands, dedicated to ozone absorption. The UV observations can be used to derive the total opacity column and thus monitor the dust and ozone cycles. BOTTLE can demonstrate the hydration state of a set of four deliquescent salts, which have been found on Mars (calcium chloride, ferric sulphate, magnesium perchlorate and sodium perchlorate) by monitoring their electric conductivity.

HABIT weighs 918 g. Its power consumption depends on the operation mode and internal temperature, and it varies between 0.4 W, for nominal operation, and 13.1 W (when heaters are turned on at full intensity). HABIT has a baseline data rate of 683 KB/sol, with extended operations data rate of 1.5 MB/sol. In addition to providing critical environmental observations, this light and robust instrument, will be the first demonstrator of a water capturing system on the surface of Mars, and the first UK In-Situ Resource Utilization instrument on the surface of another planet.

In this paper we will present the main hardware features of HABIT and the calibration process to accomplish its scientific requirements.

Keywords: Space Instrument, Mars, Habitability, Water Cycle, In-Situ Resource Utilisation

62. DNA extraction and sequencing from liquid planetary analogues for in-situ life detection and characterization

Miracle Israel Nazarious, Jyothi Basapathi Raghavendra, Javier Martin-Torres, Maria-Paz Zorzano

Presenting author institution: University of Aberdeen

Methane has been detected in the atmosphere of Mars at ~10 parts per billion (ppb) by some instruments, whilst others have reported upper limits as low as 0.05 ppb and therefore the presence, and potential source or sources, of the gas are still highly debated. One of the proposed production mechanisms is via methanogenic microorganisms within the subsurface, especially given that most atmospheric methane on Earth is produced microbially. No unambiguous evidence for life currently exists for Mars but organic molecules have been detected within sediments in Gale Crater. Additionally, organic material may be transferred with transient water traveling between the surface and subsurface reservoirs that may contain methanogens. Furthermore, water-rock interactions and the composition of salts within the water could further influence the chemistry of subsurface liquid environments. Therefore, the chemistry of the subsurface environment needs to be considered when invoking methanogenesis to reconcile detections of the gas in the martian atmosphere. In order to determine whether methanogens are not just able to survive in the subsurface but are also able to actively metabolise and produce methane, we simulated the chemistry of the subsurface environment of Mars. A brine solution and a simulant regolith were created to be similar to their proposed composition in Gale Crater, and Mars-relevant organics (benzothiophene, oxalic acid or an amino acid mixture) were also added. In combination, these factors offer an approximation of a martian subsurface liquid-water environment based on current knowledge. Within this simulated environment, the hydrogenotrophic (utilises hydrogen and carbon dioxide for metabolism) methanogen Methanothermoccocus okinawensis was grown to determine if the solution was inhibitory to methanogenesis, which would then render methanogens an implausible solution for explaining atmospheric methane. Experiments showed that the combination of an organic, the simulant regolith and the simulant brine were not inhibitory to methanogenesis after 3 days of incubation at the organism's optimal temperature (60°C). This demonstrates that methanogenesis is a plausible metabolism that could be occurring in the subsurface when considering the potential chemistry of the subsurface of Mars and its impact on biotic methane production. Further work is planned to identify whether additional methanogenic volatile organic compounds (VOCs) are also released. Additionally, methanogens that utilise the methylotrophic pathway (requiring a 1-carbon organic with a methyl group for metabolism) could be grown instead, to determine if they directly utilise a Mars-relevant organic for metabolism and produce additional VOCs. These data would be valuable in constraining knowledge of the habitability of martian subsurface environments for methanogenic organisms and inform future missions to ensure maximising detection of atmospheric biosignatures on Mars.

Keywords: Astrobiology, Liquid Planetary Analogues, Ocean Worlds, Life Search, Future Technology

63. Methane production by a hydrogenotrophic methanogen in a simulated chemical martian subsurface environment

Slade, David; Patel, Manish; Olsson-Francis, Karen; McGenity, Terrence; Steinke, Michael

Presenting author institution: Open University

Methane has been detected in the atmosphere of Mars at ~10 parts per billion (ppb) by some instruments, whilst others have reported upper limits as low as 0.05 ppb and therefore the presence, and potential source or sources, of the gas are still highly debated. One of the proposed production mechanisms is via methanogenic microorganisms within the subsurface, especially given that most atmospheric methane on Earth is produced microbially. No unambiguous evidence for life currently exists for Mars but organic molecules have been detected within sediments in Gale Crater. Additionally, organic material may be transferred with transient water traveling between the surface and subsurface reservoirs that may contain methanogens. Furthermore, water-rock interactions and the composition of salts within the water could further influence the chemistry of subsurface liquid environments. Therefore, the chemistry of the subsurface environment needs to be considered when invoking methanogenesis to reconcile detections of the gas in the martian atmosphere. In order to determine whether methanogens are not just able to survive in the subsurface but are also able to actively metabolise and produce methane, we simulated the chemistry of the subsurface environment of Mars. A brine solution and a simulant regolith were created to be similar to their proposed composition in Gale Crater, and Mars-relevant organics (benzothiophene, oxalic acid or an amino acid mixture) were also added. In combination, these factors offer an approximation of a martian subsurface liquid-water environment based on current knowledge. Within this simulated environment, the hydrogenotrophic (utilises hydrogen and carbon dioxide for metabolism) methanogen *Methanothermoccocus okinawensis* was grown to determine if the solution was inhibitory to methanogenesis, which would then render methanogens an implausible solution for explaining atmospheric methane. Experiments showed that the combination of an organic, the simulant regolith and the simulant brine were not inhibitory to methanogenesis after 3 days of incubation at the organism's optimal temperature (60°C). This demonstrates that methanogenesis is a plausible metabolism that could be occurring in the subsurface when considering the potential chemistry of the subsurface of Mars and its impact on biotic methane production. Further work is planned to identify whether additional methanogenic volatile organic compounds (VOCs) are also released. Additionally, methanogens that utilise the methylotrophic pathway (requiring a 1-carbon organic with a methyl group for metabolism) could be grown instead, to determine if they directly utilise a Mars-relevant organic for metabolism and produce additional VOCs. These data would be valuable in constraining knowledge of the habitability of martian subsurface environments for methanogenic organisms and inform future missions to ensure maximising detection of atmospheric biosignatures on Mars.

Keywords: Mars, Methane, Methanogens, Subsurface chemistry, Astrobiology

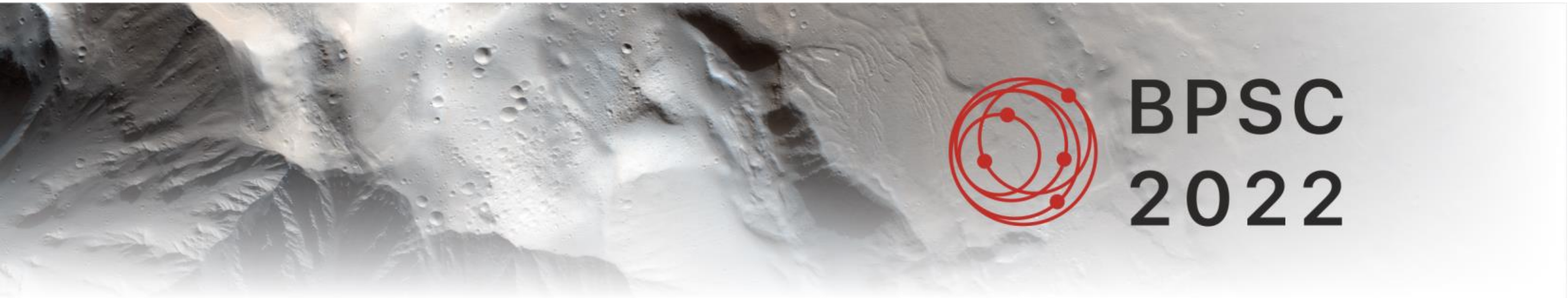

64. Classifying Planetary Surfaces Using Deep Learning, Results From Martian Landing Sites.

Barrett, Alexander; Wright, Jack; Balme, Matthew; Favaro, Elena; Fawdon, Peter; Woods, Mark

Presenting author institution: The Open University

Deep learning convolutional neural networks were used to classify surface textures from 25 cm/pixel HiRISE images. The NOAH-H (Novelty or Anomaly Hunter – HiRISE) system was created to assist in landing site selection for the ESA ExoMars mission. The HiRISE dataset provides a fantastic resource with which to study the martian surface in unprecedented detail. However, the data volume makes studying large areas at HiRISE scale prohibitive. There is a trade-off between coverage and resolution, which can be challenging when studying an area as large as the potential 3-sigma landing ellipse of an upcoming mission.

Classification by semantic segmentation can be used to perform “triage” on unmanageably large datasets, producing maps of surface texture to highlight the distribution and abundance of features, as well as detecting textural changes which could be indicative of geomorphological unit boundaries. This provides a richer data product, which can inform human interpretation of a site, and identify areas of interest at metre scale across large areas. However, it cannot replicate the more interpretive process of formal geological map making.

The Model was trained using images from Mawrth Vallis and Oxia Planum. The classification scheme consists of 14 descriptive textural classes, including 7 that describe surfaces, 6 for different morphologies of aeolian cover, and 1 for boulder cover. These are aggregated into five thematic groups, to form an interpretive layer of the model; 3 classes are considered indicative of non-bedrock surfaces, and 4 of bedrock surfaces. The aeolian classes are divided into large and small bedforms which are interpreted to have different constraints on rover traversability. Finally boulders form their own group.

The model performs well for Oxia and Mawrth, returning high precision and recall when compared to expert labelled data reserved for validation. The mean Intersection over Union across all classes, is 74% for the full list of 14 classes, and 92% after first level aggregation.

The model has since been used to produce terrain maps of Jezero and Gale Craters, the landing sites of NASA’s Perseverance and Curiosity Rovers respectively, as well as the Insight landing site. It performed well, despite not being trained on examples from those sites. The model was most transferable to Jezero Crater. Landforms common at Gale, such as dark dunes, were absent in the training set, preventing a reliable classification at that site. Conversely the interior of Jezero Crater exhibits a very similar variety of landforms to those in Oxia and Mawrth, as does the Insight landing site.

Continuous surface textures generally transferred well, since these are “generic” roughness classes common across the martian surface. Applicability to new sites is instead limited by the variety of aeolian landforms. Irregular bedforms are misclassified at both Jezero and Insight, while the dark dunes at Gale have no analogue from the training sites. These observations provide information about the applicability and transferability of the model, as well as informing what terrain classes generalise well, and which do not. This is providing important information for designing future classification schemes.

Keywords: Mars, Aeolian, Machine-Learning, Classification, ExoMars

65. Subpixel-Scale Topography Retrieval of Mars Using Deep Learning

Tao, Yu; Muller, Jan-Peter; Conway, Susan

Presenting author institution: Imaging Group, Mullard Space Science Laboratory, University College London

High-resolution digital terrain models (DTMs) play an important role in studying the formation processes involved in generating a modern-day planetary surface such as Mars. However, it has been a common understanding that DTMs derived from a particular imaging dataset can only achieve a lower, or at the best, similar effective spatial resolution compared to the input images, due to the various approximations and/or filtering processes introduced by the photogrammetric and/or photoclinometric pipelines. With recent successes in deep learning techniques, it is now become feasible to improve the effective resolution of an image using super-resolution restoration (SRR) networks [1], retrieving pixel-scale topography using single-image DTM estimation (SDE) networks [2], and subsequently, combine the two techniques to produce subpixel-scale topography from only a single-view input image [3]. Here we present our recent work [3] on combining the UCL (University College London) MARSGAN (multi-scale adaptive-weighted residual super-resolution generative adversarial network) SRR system [1] with the MADNet (multi-scale generative adversarial U-net based single-image DTM estimation) SDE system [2] to produce single-input-image-based DTMs at subpixel-scale spatial resolution [3]. Our experimental site is within the 3-sigma ellipse of the Rosalind Franklin ExoMars rover's planned landing site (centred near 18.275°N, 335.368°E) at Oxia Planum. We apply MARSGAN SRR to the 4 m/pixel ESA Trace Gas Orbiter Colour and Stereo Surface Imaging System (CaSSIS) "PAN" band images and the 25 cm/pixel NASA Mars Reconnaissance Orbiter High Resolution Imaging Science Experiment (HiRISE) "RED" band images. Subsequently, we apply MADNet SDE to the resultant 1 m/pixel CaSSIS SRR images and the 6.25 cm/pixel HiRISE SRR images, to produce CaSSIS SRR-DTMs at 2 m/pixel and HiRISE SRR-DTMs at 12.5 cm/pixel, respectively. We show qualitative assessments for the resultant CaSSIS and HiRISE SRR-DTMs. We also provide quantitative assessments (please refer to [3]) for the CaSSIS SRR-DTMs using the DTM evaluation technique that is described in [4], using multiple smoothed versions of the higher-resolution reference DTMs to compare with the lower-resolution target DTMs. The resultant CaSSIS and HiRISE SRR MADNet DTMs have been released through the ESA planetary science archive's Guest Storage Facility (GSF) at https://www.cosmos.esa.int/web/psa/ucl-mssl_meta-gsf.

References: Tao, Y.; Conway, S.J.; Muller, J.-P.; Putri, A.R.D.; Thomas, N.; Cremonese, G. Single Image Super-Resolution Restoration of TGO CaSSIS Colour Images: Demonstration with Perseverance Rover Landing Site and Mars Science Targets. Remote Sens. 2021, 13, 1777.

Tao, Y.; Muller, J.-P.; Xiong, S.; Conway, S.J. MADNet 2.0: Pixel-Scale Topography Retrieval from Single-View Orbital Imagery of Mars Using Deep Learning. *Remote Sens.* **2021**, *13*, 4220.

Tao, Y.; Xiong, S.; Muller, J.-P.; Michael, G.; Conway, S.J.; Paar, G.; Cremonese, G.; Thomas, N. Subpixel-Scale Topography Retrieval of Mars Using Single-Image DTM Estimation and Super-Resolution Restoration. *Remote Sens.* **2022**, *14*, 257.

Kirk, R.L.; Mayer, D.P.; Fergason, R.L.; Redding, B.L.; Galuszka, D.M.; Hare, T.M.; Gwinner, K. Evaluating Stereo Digital Terrain Model Quality at Mars Rover Landing Sites with HRSC, CTX, and HiRISE Images. *Remote Sens.* **2021**, *13*, 3511.

Keywords: Mars, topography, super-resolution, deep learning, digital terrain model

Session 9:

Lightning talk group 3c

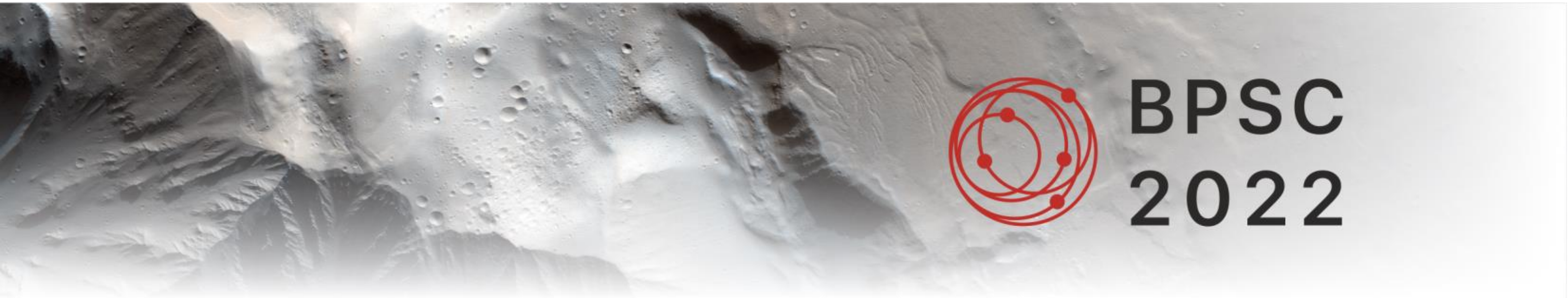

66. Morphological Diversity of Glacier-Like Forms on Mars

Driver, Graham; El-Maarry, Mohamed Ramy; Hubbard, Bryn; Brough, Stephen.

Presenting author institution: Birkbeck University of London

Introduction: Glacier-Like Forms (GLFs) are a sub-group of ice-rich landforms known as Viscous Flow Features (VFFs) that occupy Mars' mid-latitudes [e.g. 1-3]. While GLFs appear similar to terrestrial valley or rock glaciers, observations of the GLF population have shown they can be morphologically varied. This study aims to classify GLFs into distinct morphological forms to reveal regional trends in GLF geomorphology and further our understanding of their formation and evolution.

Methods: 250 GLFs (20% of the total population [3]) were selected for analysis. GLFs were arranged by surface area (km^2) and sub-sampled to provide a representative view of the total population. Analysis was performed using ArcGIS PRO using CTX and HiRISE images. Existing [3] and new geometrics data were used to aid GLF classification.

Results: Seven morphological types of GLF were identified. *Valley GLFs (76.8%)* are morphologically similar to terrestrial valley glaciers. The subgroup is the most numerous and varied type of GLF, having diverse geometries and distributions. *Scarp GLFs (10.0%)* occupy terrains with medium/high slopes and reliefs. They are generally unconstrained and linear, displaying spatulate morphologies. *Lobate Debris Apron GLFs (4.0%)* are somewhat adjoined to existing Lobate Debris Apron deposits and other ice-rich flows, merging with or within them, making their boundaries difficult to define. *Sinuous Valley GLFs (4.0%)* are valley GLFs that are highly sinuous and often multi-lobed. They are commonly found in regions rich in existing fluvial landforms. *Crater Confined GLFs (2.4%)* occupy impact craters. While similar to Concentric Crater Fills, they display GLF morphology such as the flowing of material into or out of cavities through rim breaches, creating directional flow structures. *Lineated Valley GLFs (1.6%)* occupy rift or tectonic valleys and have low sinuosity. They appear in regions where such rifts are common (e.g., Tempe Terra). *Debris Rich Avalanches (1.2%)* are GLFs that appear geomorphologically similar to terrestrial debris rich avalanches, displaying flow bands and lobate depositional morphologies. These GLFs are located on steep crater rims and have heavily sublimated blocky lower (traditional ablation) zones.

Discussion: The spatial distribution and clustering of the different classifications of GLF suggest that they may have evolved differently and that the local geological setting is important to GLF geomorphology and evolution. Northern hemisphere GLFs show more morphological variation than in the south, suggesting that elevation plays a role in GLF evolution. There are geomorphological differences in GLF accumulation zones, where gradients vary between low and high reliefs, suggesting topographic controls and accumulation processes also shape GLF morphology.
It is possible that in the past, GLFs in mountainous regions were carving out their topography, while other GLFs could simply be exploiting existing topography. Some GLFs exhibit a steep terminus, suggestive of recent movement. This is not specific to any one classification, suggesting that despite their similarities, not all GLFs have morphology suggestive of recent activity.

References: [1] Hubbard et al., (2014) *The Cryosphere*, 8, 2047-2061. [2] Milliken et al., (2003) *JGR*,108, 6. [3] Brough et al., (2019) *EPSL*, 507, 10-20.

Keywords: Glacier Like Forms, Mars, Geomorphology, Martian Cryosphere, Glaciology

67. Morphological complexity of Concentric Crater Fills on Mars: insights into glacial history

Cornford, B. T; Ng, F., Butcher, F. E. G. and Bryant, R.G.

Presenting author institution: Department of Geography, University of Sheffield

Impact craters in the Martian mid-latitudes contain ice-rich deposits collectively termed 'Concentric Crater Fills' (CCFs). CCFs are putative debris-covered glaciers, relics of mid-latitude glaciation under higher planetary spin-axis obliquity. Their characteristics reflect the interplay of ice deposition, evolution, removal and preservation factors, and they likely retain unexplored records of Mars' climate and glacial history. Here we investigate the morphology of CCFs with the aim of deciphering such histories. The surfaces of some CCFs exhibit distinct 'tracelines' that form patterns suggestive of ice accumulation and flow, but how these patterns originate and their variable expressions across CCFs remain largely unexamined. We develop a preliminary classification scheme for CCFs, categorising their traceline expressions by their increasing level of complexity. Traceline patterns are found to range from near-circular to considerably more irregular (often with higher-order polygonal geometry with countable 'sides', and cusps). We applied this geometric classification in both hemispheres to an initial subset of ~1000 CCFs and analysed the spatial distribution and frequency of the classes. In the future, we will expand the data collection and integrate this classification study with analyses of host-crater morphology and morphometry, to decipher CCF formation, evolution and preservation. This activity will inform broader efforts of using mid-latitude ice deposits as proxies for Mars's past climate.

Keywords: Concentric Crater Fills, Mars, Mars' climate, Mid-Latitude Glaciation, Mars' glacial history

68. Geomorphological mapping and investigation of a mountain glacier in the Argyre Region, Mars.

Gor, Nisha

Presenting author institution: University College London

Introduction and Aims: MRO data has shown that the equatorial and mid-latitudinal regions (~20-60º) on Mars contain hundreds of viscous flow features (VFFs). Geomorphological and radar studies have confirmed their interiors are composed of nearly pure water ice known as glacier-like-forms (GLFs) [1]. Within these latitudes lie the Argyre Basin which hosts one of the largest VFFs and several GLFs. This project aims to utilize existing high-resolution images of a mountain glacier located in Argyre. By creating a geomorphological map and characterizing the glacier system in more detail, interpretations can be made about the formation and evolution of non-polar ice on Mars particularly during periods of high obliquity. Another aim was to derive surface ages for different parts of the glacier using crater counting.

Methodology: For this mapping investigation, Context Camera (CTX) data from NASA's Mars Reconnaissance Orbiter (MRO) was mosaiced together for the Region of Interest (ROI). The mosaiced CTX file covers approximately 10,400km² over the region of interest. The file is georeferenced to a Digital Terrain Models (DTM) based on High-Resolution Stereo Camera Data (HRSC). The HRSC is an instrument on board the ESA's Mars Express. High Resolution Imaging Science Experiment (HiRISE) images of the glacier were laid on top of this data with a spatial resolution of 0.25–0.5cm/pixel.

Observations: The host mountain is the most significant feature in the study region with a height of ~3408m where the mountain displays a cirque-like feature. The overall shape of the mountain ~40x30km displays a rectangular mesa-like mound with a flat top ~20x5 km. The relationship between the mountain and the surrounding fretted terrain is difficult to establish because of the extensive flows from the mountain and regolith covering its margins. The lithology of the mountain is likely to be erosional remnant from the impact.

Other than the ice mountain, the lobes around the mountain are distinctive features. In total, 6 flow bodies were identified flowing in different directions. 3 lobes trending NE, NW, and SW display features which were characteristic of GLFs. The other 3 flows trending SE are quite minor in comparison. The source of the flows seems to be from 2 NE and NW-facing prominent cirques. The 3 main lobes terminate sharply without mixing with the lithology underneath around 20kms from the source mountain. Near the terminus are several boulders in the NE and NE facing lobes suggesting evidence for young glacial flow. Cross cutting relations can be seen in the NW lobes. Similarly, the NW lobe is flowing over the SW lobe suggesting possibly different phases/cycles of melting or erosion. The SE debris apron displays no ridges suggesting they may have not yet terminated, and motion is still ongoing. In the west most part of the map a minor debris flow displays Veiki moraines-like ridges, characteristic of glacial flows. The fresh surface with little to no craters could suggest a relatively young surface post-glacial recession and a recent ablation of the glacier system.

References: [1] Plaut et al.,(2009), Geophys. Res. Lett., 36, L02203.

Keywords: Geomorphology, Glacier-like forms, Ice, GIS, Martian Geology

69. Surface topographic impact of water bodies beneath Mars' south polar ice cap

N.S. Arnold, F.E.G. Butcher, S.J. Conway, C. Gallagher and M.R. Balme

Presenting author institution: Scott Polar Research Institute, University of Cambridge, Lensfield Road, Cambridge, CB2 1ER, UK

Bright radar reflections observed in Mars Advanced Radar for Subsurface and Ionosphere Sounding (MARSIS) data from at least one area of Mars’ south polar layered deposits (SPLD) have been interpreted as indicative of basal water, in the form of hypersaline perchlorate brines. Locally elevated geothermal heating is likely needed for basal melting. The interpretation of the bright radar reflections as liquid water has been contested, however, with arguments that similar radar returns could be produced by possible characteristics of solid materials at the base of the SPLD, or by showing minerals found elsewhere on Mars would be detectable beneath an ice layer equivalent to the SPLD thickness. Subglacial lakes on Earth have been detected using ice penetrating radar, but also through their influence on the ice sheet surface; reduced basal friction over the lake, and consequent ice velocity changes cause a distinct topographic signature. Here, we identify and characterise a local anomaly in the Mars Orbiter Laser Altimeter (MOLA) surface topography for the region of Mars’ SPLD overlying the inferred water. The Martian topographic anomaly we find is analogous to anomalies above similarly sized subglacial lakes on Earth. We compare the anomaly with the results from an ice flow model with reduced friction and variable enhanced geothermal heating in the region. Model results suggest comparable topographic anomalies can form within the timescales of locally elevated geothermal heating (0.5 – 1.5 Myr), or from longer-term (2 – 5 Myr) effects of low friction without enhanced geothermal heating. The shape of the topographic anomaly, linked with model results, suggest that a linear area of geothermal heating, as would be associated with an igneous dyke, may be responsible for the subglacial water. Our findings offer further support for the presence of basal water in the Ultimi Scopuli area of Mars’ SPLD, independently of the use of MARSIS data. The results also suggest that surface topographic features on Mars’ polar caps could assist in the identification of further subglacial water bodies, and help resolve different interpretations of radar returns.

Keywords: Mars, Glaciology, Modelling

70. The geological map of the ExoMars rover landing site.

Fawdon, Peter; Orgel, Csilla, Mapping team, Mapping volunteers

Presenting author institution: The Open University

Oxia Planum (OP) is the proposed landing site for the ESA-Roscosmos ExoMars Rover, with the rover mission's main goal being to search for signs of past and present life.

In preparation for the surface mission, The ExoMars mission team performed a detailed group mapping exercise of the area in which the rover was most likely to land. The goal of this effort was to develop a thorough understanding of the OP landing site's geography, stratigraphy, and geological history prior to operations, and to provide testable hypotheses to facilitate interpretation of results and further the mission's science objectives. The purpose of this map is to help formulate the rover's strategic science plan and to act as a framework to develop strategic thinking during the mission.

The reconciliation phase – in which a smaller team consolidated features digitized by a large team over a grid of 1x1 km map quads from the mapping phase – has recently been completed, and the map is now in the review phase.

Here, for the first time, we present the first draft of the completed map. This includes: (1) our working understanding of the stratigraphy, the relative timing of map units, and the most promising locations to explore how the ancient environment changed with time; (2) a summary of our interpretations of the major geological units, including their formational processes and astrobiological potential; and (3) a discussion about how the map connects to the regional geological history, how our understanding of the geological context informs our interpretations, and how observations made by the rover might affect our understanding of the region and the history of Mars more generally.

If the Rosalind Franklin rover mission flies, and searches for evidence of life in the rocks of ancient Mars, this is the map we will use to guide where those samples are collected.

This project represents the culmination of 7 years of work on landing site selection characterisation for the ExoMars rover mission. The authors wish acknowledge: Mapping, scientific and technical contribution from; Elliot Sefton-Nash, Solmaz Adeli, Matt Balme, Alex Barrett, Fred Calef III, Gabriele Cremonese, Joel Davis, Elena Favaro, Alessandro Frigeri, Peter Grindrod, Ernst Hauber, Laetitia Le Deit Damien Loizeau, Lucia Mandon, Joe McNeil, Andrea Nass, Adam Parks-Bowen, Cathy Quantin-Nataf, Amelie Roberts, Nick Thomas, Daniela Tirsch, Stuart Turner, Jorge L. Vago and Matthieu Volat; The Mapping volunteers, everyone who has contributed to this project possible and in particular the the support of the UK Space Agency.

Keywords: ExoMars, Rover Exploration, Mars, Geology, Remote sensing

71. Carbonate formation in Gale crater, Mars: a thermochemical modelling perspective

Turner, Stuart; Schwenzer, Susanne; Bridges, John; Sutter, Brad; Thorpe, Michael; Rampe, Elizabeth; McAdam, Amy.

Presenting author institution: The Open University

Identification of martian carbonate and understanding its formation are important in Mars geochemistry studies because it offers a way to track changes in atmosphere-water-crust interactions in the martian geological record [1]. The sediments of Glen Torridon (GT) in Gale crater were deposited in a predominantly lacustrine environment, and subsequently underwent multiple episodes of diagenesis [2-8]. Although traces of carbonate have been found by the SAM instrument throughout the Mars Science Laboratory mission, e.g., at Rocknest [9], Fe-carbonate has been detected using X-ray diffraction measurements from CheMin for the first time in the clay-rich GT region. Five out of seven drill samples from GT show Fe-carbonate alongside phyllosilicates [6]. Here we use thermochemical modelling to explore the possible reaction pathways of carbonate formation in GT.

We have four hypotheses for the formation of the patchy carbonate occurrences within GT:

H0: Direct formation of carbonates from CO_2-charged fluids. No/minimal phyllosilicate formation. H1: Direct formation of carbonates and phyllosilicates by interaction with CO_2-rich fluids. H2: Early diagenetic carbonate formation. Interaction of detrital igneous grains with CO_2-rich fluids followed by a second alteration event with CO_2-poor fluids. H3: Late diagenetic carbonate formation. CO_2-poor fluid alteration followed by carbonate formation with CO_2-rich fluids.

H2 tests early diagenetic carbonate formation followed by further alteration. Although geologic setting and temperature are different, this sequence of early carbonate formation followed by partial dissolution of the carbonate during clay formation has been observed in the nakhlites [10]. H3 tests a formation sequence of phyllosilicates followed by interaction of the altered rock with a CO_2-rich fluid. Fluid-fluid mixing was envisaged by [6], and percolating lake-water may have been the CO_2-rich fluid in our models.

Using CHIM-XPT, a program for computing multicomponent heterogeneous chemical equilibria in aqueous-mineral-gas systems [11], water/rock titration modelling is being carried out to investigate these hypotheses. CHIM-XPT has been used extensively in water-rock reaction studies for Gale [e.g., 12]. Here, we report on CHIM-XPT results where we react CO_2-poor and CO_2-rich versions of Gale Portage Water with APXS chemical compositions, supplemented by CheMin mineralogy, from Curiosity.

References: [1] Bridges at al., 2019. Carbonates on Mars. In 'Volatiles on Mars'. 1st edition. Elsevier. [2] Grotzinger et al., 2015. Science 350(6257). [3] Fraeman et al., 2020. JGR: Planets 125(20), e2020JE006527. [4] Rampe et al., 2020. Geochemistry 80(2), 125605. [5] Rampe et al., 2020. JGR: Planets 125(12), e2019JE006306. [6] Thorpe et al., submitted. JGR: Planets. [7] Gasda et al., submitted. JGR: Planets. [8] Rudolph et al., submitted. JGR: Planets. [9] Archer Jr et al., 2014. JGR: Planets 119(1), 237-254. [10] Bridges and Schwenzer, 2012. EPSL 359, 117-123. [11] Reed 1998. Rev. Econ Geol. 10, 109-124. [12] Turner, S. M. R. et al., 2021 MaPS, 56, 1905-1932.

Keywords: Mars, Carbonate, Gale crater, Geochemistry, Thermochemical Modelling

72. Impact-generated modification of the mineralogy at Oxia Planum

A. Dugdale; N.K. Ramkissoon, V.K. Pearson, P. Fawdon, M.R. Patel

Presenting author institution: The Open University

Phyllosilicate minerals have been detected at Oxia Planum, the ExoMars landing site, which indicates this area has been subject to aqueous activity during the Noachian [1,2,3]. This means that the site may once have been capable of supporting life, the evidence of which, such as biologically-produced organic compounds – or biomarkers, might be preserved in the sediments [1,4,5]. However, these biomarkers are likely to have experienced alteration over time, resulting from a range of processes [6,7,8], including meteorite impacts [9,10]. Orbital imaging has identified a population of impact craters at Oxia Planum[11,12].

It was initially thought that organic molecules could not survive the pressures and temperatures of impact events. However, laboratory impact simulations have shown the survival of a range of organic species [9,10,13] and, thus, impact craters on Mars may host potential organic biomarkers. However, an impact event can modify organic structures [13] *via* the elevated temperatures and pressures facilitating reactions with surrounding minerals. This can lead to the breaking or formation of chemical bonds, thermal oxidation and racemization [13]. Therefore, to determine whether biomarkers could be preserved at Oxia Planum, an understanding of the effect of impacts on the local environment at Oxia Planum is key.

Here, we performed laboratory experiments using the all-axis light gas gun (LGG) at the Open University, to understand the effects of impacts on the local mineralogy at Oxia Planum. These experiments used a simulant representative of the mineralogy at Oxia Planum [14], containing unaltered basaltic minerals, a phyllosilicate component, iron oxides and an amorphous component. The LGG exposed the simulant to the high pressures and temperatures associated with planetary impacts at a range of velocities relevant to impacts on Mars, thus encompassing the formation conditions for a range impact events evidenced at Oxia Planum [11,12]. Samples taken from the impacted simulant were analysed using Near-IR, Raman and XRD to assess mineralogical changes.

Here, we will present the preliminary results from these experiments, and will outline their application to understanding the survival of biomarkers at the Oxia Planum landing site.

References: [1] Vago *et al.*, (2017) [2] Carter *et al.*, *LPSC* (2016) [3] Quantin-Nataf *et al.*, *(*2021) [4] Parnell *et al.*, *(*2007 1998 [6] Sephton and Tan, (2020) [7] Dartnell *et al.*, *(*2012) [8] He *et al.*, *(*2021) [9] Burchell *et al.*, (2014) [10] Bowden *et al.*, (2009) [11] Roberts *et al.*, *(*2021) [12] Fawdon *et al.*, (2021) [13] Furukawa *et al.*, (2018) [14] Dugdale et al., *LPSC* (2020)

Keywords: Mars, Impacts, Mineralogy, Biomarkers, Astrobiology

73. Distribution and morphology of the dark capping unit in Oxia Planum, Mars

Harris, Emma; Davis, Joel; Peter, Grindrod

Presenting author institution: Natural History Museum, London

The stratigraphy of Oxia Planum, Mars, has been under increasing scrutiny since selection as the landing site for the ExoMars Rosalind Franklin rover mission. At the top of the strata within Oxia Planum lies a dark capping unit (DCU), thought to have offered protection to the underlying phyllosilicate-rich units, increasing the possibility of preservation of organic matter for investigation by the rover. Despite its apparent importance, the origin of the DCU remains unknown.

Theories regarding the origin of the DCU are widespread, including: lava or pyroclastic flows, ashfall, impact, fluvial or aeolian processes. Key to determining the formation mechanism is classifying the DCU in terms of distribution, morphology, mineralogy, and interaction with other units. This study aims to understand how the DCU formed, and the implications for preservation of possible organic material.

The DCU occurs as discrete outcrops across the wider Oxia Planum region, ranging from ~0.5 km^2 to ~180 km^2 totalling ~450 km^2 over a ~50,000 km^2 area of Oxia Planum. The DCU is distinct from other geological units due to its low albedo, ability to retain craters and form scarped edges, and is often found in depressions including, but not limited to, impact craters. This study has focussed on the distribution and morphology of the DCU.

This study commenced by mapping all identifiable outcrops of the DCU, before collating a database of craters into which the DCU has been emplaced. This database includes various quantitative measurements including MOLA and HRSC derived elevation, THEMIS derived thermal inertia, and degradation state. These observations will be supplemented with local stereo Digital Elevation Models (DEMs), to allow estimates of DCU thickness to be made. These observations will help refine models of the origin of the DCU in Oxia Planum, with implications for similar units elsewhere on Mars.

Keywords: Mars, ExoMars, Craters, Surface Processes

74. Tectonic shortening along the Chryse Planitia – Arabia Terra dichotomy.

Woodley, Savana; Fawdon, P.; Balme, M.; Rothery, D.

Presenting author institution: The Open University

The tectonic features along the Chryse Planitia – Arabia Terra (CP-AT) dichotomy record long wavelength crustal deformation, interspersed with phases of heterogenous erosion and deposition though the history of Mars. The tectonism modifying the Noachian landscape is expressed by a regional fabric of 'wrinkle ridges' but these have not been quantitatively studied in detail before. To provide constraints on the region's tectonic evolution, we mapped tectonic features in eastern Chryse Planitia and western Arabia Terra.

Our study site is a ~3 million km^2 area, oriented SW-NE along the CP-AT dichotomy. The widespread tectonic features in the study area are thrust-fault-related landforms, termed shortening structures. They occur across the region including in Oxia Planum (the ExoMars Rover landing site) and in the channel floors of Coogoon, Mawrth, and Ares Valles.

We digitized tectonic shortening structures at a scale of 1:50,000 using 6 m/pixel Context Camera (CTX) images, 100 m/pixel Thermal Emission Imaging System (THEMIS) daytime infrared images, and 463 m/pixel gridded Mars Orbiter Laser Altimeter (MOLA) topographic data. Our mapping approach was structural-based and we recorded fault vergence, scarp height, fault trace orientation, cross-cutting relationships, morphological complexity, and our confidence in our interpretation of each feature's tectonic relevance.

We defined five morphological zones, based on the Tanaka global geological map, the Tanaka northern plains geological map, and our own observations. These zones are: the *early Noachian highland unit*, the *middle Noachian highland unit*, the *Chryse Planitia unit*, the *Ares Vallis and Chryse outflow unit*, and the *Northern Plains unit*. We analysed the distribution, orientation, magnitude, and timing of tectonic shortening within each of these zones.

We used cross-cutting relationships between impact craters and shortening structures to explore the timing of burial/erosional processes and consider the timing of tectonic events. We checked the Robbins crater catalogue and identified all craters with diameter ≥10 km. Using CTX images, we recorded the relationship (or lack thereof) of each crater with any tectonic features and classified craters into three classes of degradation based on the most common morphologies observed in the study area (*craters with preserved impact ejecta*, *eroded craters without impact ejecta*, and *highly eroded craters and ghost craters*).

We identified numerous shortening structures in the CP-AT study area, with a combined length of ~26,000 km and a dominant N-S orientation. Shortening structures are distributed across the highland-lowland transition region and deform all units, but the highest density (structure length per unit area) and intensity (scarp height per unit area) occur in the *middle Noachian highland unit* and the *Chryse Planitia unit*. Of the three crater classes, each class deforms shortening structures and is deformed by shortening structures (except the *highly eroded craters* class which does not deform shortening structures), suggesting that at least two phases of tectonic activity occurred. More detailed analysis of the timing of tectonic activity and further implications is currently ongoing.

Keywords: Mars, Tectonics, ExoMars

75. Analysing fractured terrains at the Rosalind Franklin rover landing site Oxia Planum, and comparing these with those found at Gale Crater

Parkes Bowen, Adam; Bridges, John

Presenting author institution: University of Leicester

In order to improve the characterisation of the Rosalind Franklin rover landing site, fracture networks present across the Clay-bearing and Capping Units at Oxia Planum were mapped out and parameterised. This was done to constrain the potential mechanisms that caused fracturing within these units, and how fracturing varied between terrains within the same geological unit as well as other units at the site. These mapped areas were also compared to areas from other sites which had been characterised at ground-level, or where the prospective fracture formation mechanism was better constrained. The areas chosen for comparison were located within: Gale Crater, including the Yellowknife Bay Sheepbed member, the Stimson Unit and the Murray Unit; the Martian northern polar regions, and dry lakebeds on Earth.

These comparisons were carried out with the aim of making predictions about the material properties of the units at Oxia Planum, as well as further constraining potential formation mechanisms. For this comparison the fracture networks were mapped at each site, with several parameters being measured. These were: angle of intersection between fractures, area of polygons formed by fractures, fracture length, and orientation of the longest polygon axis to north. Data sets were compared using Kernel Density Estimation graphs and via Kolmogorov-Smirnov two-sample tests.

The results from this study [1] narrow the potential mechanisms for the fracturing seen at Oxia Planum, as well as highlighting groups within the sites mapped. From the angle of intersection distribution for each site, distinct peaks at 90° suggests that neither hydraulic fracturing, which tends to generate more varied angles of intersection, nor multiple cycles of desiccation or thermal fracturing, which generate networks with peaks at 120°, are responsible for the fracturing seen. The distinct polygon orientation seen in the Oxia Planum Capping Unit but not the Clay-bearing Unit also suggests a different formation mechanism for the fracturing within the two units, or at least that the fracturing seen occurred across separate fracturing events. The presence of a similar polygon orientation for the larger fractures seen within a unknown unit underlying the sites largest delta fan indicates that this unknown unit is an exposure of the Oxia Planum Capping Unit, suggesting the Capping Unit was emplaced before aqueous activity ceased at the site.

Similarities between a site mapped on the Murray Unit to two sites mapped on the Oxia Planum Clay-bearing Unit favours desiccation as the mechanism of fracturing at these two sites, given the presence of desiccation fractures observed by Curiosity within the Murray formation that Vera Rubin is a part of [2]. This conclusion is contested however by the dissimilarities between desiccation-derived fractures sites at the Earth-based dry lakebed sites and the Oxia Planum clay-bearing sites. This comparison could indicate that desiccation was not the cause of the fracturing seen in the Oxia Planum Clay-bearing Unit, though the differences could instead suggest the Oxia Planum Clay-bearing Unit has a lower percentage clay content in comparison.

References: [1] Parkes Bowen et al. (in prep), [2] Stein et al. (2018) Geology 46(6) 515-518

Keywords: : ExoMars rover, Oxia Planum, Gale Crater, Fracturing, HiRISE

76. Ancient Alluvial Plains at Oxia Planum, Mars

Davis, Joel; Balme, Matt; Fawdon, Peter; Grindrod, Peter; Favaro, Elena; Banham, Steven

Presenting author institution: Natural History Museum

The geologic origin of the ancient, phyllosilicate-rich bedrock at Oxia Planum, Mars, the ExoMars rover landing site, is unknown. The phyllosilicates record ancient aqueous processes, but the processes that formed the host bedrock remain elusive. Here, we use high-resolution orbital image and topographic datasets to investigate and characterize fluvial sinuous ridges (FSRs), found across the Oxia Planum region. The FSRs form segments up to 70 km long, with sub-horizontal layering commonly exposed in ridge margins. Some FSRs comprise multi-story ridge systems; many are embedded within from the phyllosilicate-rich bedrock. We interpret the FSRs as deposits of ancient, episodically active, alluvial river systems at Oxia Planum (channel-belt and overbank deposits). This suggests the phyllosilicate-rich bedrock was formed by ancient alluvial rivers, active across the wider region. Future exploration by ExoMars can verify this interpretation and provide an opportunity to investigate some of the oldest river deposits in the Solar System.

Keywords: Mars, Remote Sensing, Geomorphology, Surface Processes

Session 10:

Icy Bodies & Outer Solar System

77. The Future Exploration of Jupiter and Ganymede

Bunce Emma

Presenting author institution: University of Leicester

This We are currently enjoying the incredible new results from the NASA Juno mission at Jupiter, including a recent flyby of Ganymede – the first since the Galileo era. In this talk I will look to the future exploration of the Jupiter system by the ESA JUICE mission which has a particular focus on Ganymede. I will discuss the broad evidence for an subsurface ocean at the planet-sized moon, and will discuss details of this tantalising topic from an electromagnetic perspective

Keywords: Future missions, JUICE, Jupiter, Ganymede, Icy moons

78. Flagship Mission to Uranus: Exploring our Closest Ice Giant System

Fletcher, Leigh N.

Presenting author institution: University of Leicester

The US Decadal Strategy for Planetary Science and Astrobiology, "Origins, Worlds, and Life" (https://doi.org/10.17226/26522), has identified a Uranus Orbiter and Probe mission as the top priority for a flagship-class mission to be initiated in the forthcoming decade (2023-32). This ambitious mission would be the first dedicated orbital explorer for an Ice Giant system, unveiling the origin and evolution of a class of worlds that may be among the most common outcomes of the planet formation process. The Ice Giant explorer would study atmospheric and magnetospheric processes on a planet with the most extreme orbital configuration (and hence seasons) of any world in our Solar System. The mission would probe the (potentially) water-rich interior structure of an Ice Giant for the first time, sampling the atmospheric composition directly via a descent probe, to place constraints on the location and timing of Uranus' formation. A long-lived tour of the Uranian satellite and ring systems could reveal new ocean worlds and their subsurface oceans, sampling a geophysical wonderland in search of active processes, ancient and ongoing. A mission to Uranus provides opportunities for cross-disciplinary science: from studying a moderately-rotating, low-temperature, chemically enriched giant planet as an archetype for Ice-Giant-sized worlds across the galaxy (astrophysics); to observing how Uranus' complex and highly variable magnetic field interacts with the solar wind (heliophysics); to pushing the boundaries of potentially habitable ocean worlds out towards the edges of our Solar System (astrobiology). For all these reasons and more, an ambitious flagship-class mission to an Ice Giant is the next step in our exploration of the Solar System beyond Galileo, Juno, and Cassini.

International interest in a Uranus mission is substantial, exemplified by ESA's Voyage 2050 Survey (https://www.cosmos.esa.int/web/voyage-2050, 2021) who "strongly recommended that every effort is made to pursue this theme in order to set up a cooperation scheme on a future mission to the Ice Giants." Such an international partnership, possibly following the legacy of Cassini-Huygens, could ensure that a generation of European scientists have the opportunity to explore a destination that has thus far remained out of reach to ESA's L-class missions. This talk will provide an overview of the Uranus Orbiter & Probe study, prepared by the *Giant Planets Systems* and *Ocean Worlds/Dwarf Planets* panels of the US Decadal Survey, with the design led by the Applied Physics Laboratory (APL). The Uranus mission proved to be technically achievable and low-medium risk: an end-to-end mission concept exists with no new technology, an existing launcher (Falcon Heavy Expendable), a flexible launch date (through to 2038, but optimal in 2031-32 with a Jupiter gravity assist to shorten cruise to 12-13 years), and strong international interest. The Decadal Survey recommended a mission start in 2024, subject to funding, with international participation to be determined. The Uranus mission provides significant instrumentation opportunities for UK planetary scientists, through orbiter and probe payload provision and operations, and could help to shape planetary exploration for a generation.

Keywords: Ice Giants, Uranus, Missions, Ocean Worlds

79. Uranus and Neptune in the Infrared: Recent Observations and the Future with JWST

Roman, Michael; Fletcher, Leigh; Orton, Glenn; Harkett, Jake; Rowe-Gurney, Naomi; Moses, Julianne; Irwin, Patrick; Greathouse, Tommy; Hammel, Heidi

Presenting author institution: University of Leicester

The Solar System's ice giants--Uranus and Neptune--are among the least explored of the major planets, and recent analyses of their atmospheres have revealed new discoveries and intriguing mysteries. In this talk, we will highlight findings of recent work, including surprising variability in the atmosphere of Neptune and persistent but unexplained structure in the stratosphere of Uranus. With these questions in mind, we look at how the unprecedented infrared sensitivity of JWST will provide exciting breakthroughs in the years ahead, amid growing interest in a future Uranus mission.

Keywords: Ice Giants, Planetary Atmospheres Observations

80. External atmospheric water flux at Neptune and Uranus; constraints from Herschel/HIFI observations

Teanby, Nicholas; Irwin, P.G.J.; Sylvestre, M.; Nixon, C. A.; Cordiner, M. A.; Wright, L.

Presenting author institution: School of Earth Science, University of Bristol, UK

The ice giants Neptune and Uranus inhabit a fascinating region of the outer solar system, but have so far only been briefly visited by the Voyager 2 spacecraft during the 1980's. Water was first discovered in their stratospheres in the late 1990's when observations by the Infrared Space Observatory detected water emission features at wavelengths of 28-45 microns. These observations show that both planets must have an external source of water supplied to their stratospheres. However, the water source is unknown and could be interplanetary dust particles (IDPs), cometary impacts, or emissions from icy moons or rings. Here we use recent sub-mm observations taken in 2010 by the Herschel space telescope's Heterodyne Instrument for the Far-Infrared (HIFI) to place the most precise constraints so far on stratospheric water abundance on these planets. Observations cover the 557 GHz (~540 micron) stratospheric water emission line at very high spectral resolution (<1 MHz) and can be used to derive accurate stratospheric water column abundance and place limited constraints on water's vertical profile. By comparing our observed abundances to photochemical models, the external flux of water into each planet can also be inferred. We will discuss the implications of our new measurements in terms of potential water sources into the ice giants and compare results for the two planets to provide a better understanding of flux processes at the edge of our solar system.

Keywords: Atmospheres, Uranus, Neptune, Water, Spectroscopy

81. Observations of Titan with the James Webb Space Telescope (JWST)

Nixon, Conor; Achterberg, Richard; Bézard, Bruno; Cornet, Thomas; Hammel, Heidi; Hayes, Alexander; Lellouch, Emmanuel; Lopez-Puertas, Manuel; Milam, Stefanie; Rodriguez, Sebastien; Sotin, Christophe; Teanby, Nicholas; Turtle, Elizabeth; West, Robert

Presenting author institution: NASA Goddard Space Flight Center

On December 25th 2021 the James Webb Space Telescope (JWST) lifted off the Earth and began its voyage to the Sun-Earth Lagrange-2 point, where JWST now begins its revolutionary exploration of the infrared universe. Although designed to look at the faintest objects in the distant universe, a significant portion of JWST's observations in the first year of the mission will be directed closer to home: to the bodies of our Solar System. These include planets from Mars to Neptune, moons, asteroids and comets, which will be revealed in completely new ways by the incredibly sensitive instruments on JWST. Titan, with its dense, chemically complex, hazy atmosphere, has long been a source of fascination for planetary scientists, a truly one-of-a-kind object that may hold clues to the Earth's distant, anoxic past. JWST's investigations of Titan in Cycle 1 include observations with three of the four primary instruments: NIRCam (0.6-5 µm),

NIRSpec (0.6-5 µm) and MIRI (5-28 µm). With NIRCam imaging capabilities, JWST will be able to image Titan's lower atmosphere and surface through the haze, searching for clouds and largescale changes in the shorelines of lakes and seas since the Cassini era. With NIRSpec, JWST will make the highest spectral resolution imaging yet performed of Titan in the near infrared, exceeding the spectral resolution of Cassini's VIMS instrument by an order of magnitude, and offering the potential to investigate phenomena from high-altitude dayglow to lake and surface composition. With MIRI, JWST will obtain the most sensitive spectra yet obtained of Titan in the thermal infrared, allowing abundance measurements of complex molecules and isotopes. In this presentation, the current plans for JWST observations are discussed, along with the latest news and timelines for data acquisition, calibration, and public archiving and plans for early data analysis.

Keywords: JWST, Titan, Icy Moons

82. The Comet Interceptor Mission

Jones, Geraint H.; Snodgrass, Colin; Tubiana, Cecilia; Bowles, Neil; Galand, Marina; and the Comet Interceptor Consortium

Presenting author institution: UCL Mullard Space Science Laboratory

In 2019, Comet Interceptor was selected by the European Space Agency, ESA, as the first in its new class of F missions. At the time of this writing, formal adoption of the mission is anticipated for early June 2022. The Japanese space agency, JAXA, is making a major contribution to the project. Comet Interceptor's primary science goal is to characterise for the first time, a yet-to-be-discovered long-period comet, preferably dynamically new, or an interstellar object. An encounter with a comet approaching the Sun for the first time will provide valuable data to complement information gathered by all previous comet missions, which through necessity all visited more evolved short period comets. The spacecraft will be launched in 2029 with the Ariel mission to the Sun-Earth Lagrange Point, L2. This relatively stable location allows a rapid response to the appearance of a suitable target comet, which will need to cross the ecliptic plane through an annulus centered on the Sun that contains Earth’s orbit. A suitable new comet would be searched for from Earth, with short period comets acting as mission backup targets. Powerful facilities such as the Vera Rubin Observatory make finding a suitable comet nearing the Sun very promising, and the spacecraft could encounter an interstellar object if one is found on a suitable trajectory. The spacecraft must cope with a wide range of target activity levels, flyby speeds, and encounter geometries. This flexibility has significant impacts on the spacecraft solar power input, thermal design, and shielding that can cope with dust impacts. Comet Interceptor comprises a main spacecraft and two probes, one provided by ESA, the other by JAXA, which will be released by the main spacecraft on approach to the target. The main spacecraft, which would act as the primary communication point for the whole constellation, would be targeted to pass outside the hazardous inner coma, making remote and in situ observations on the comet’s sunward side. Planned measurements of the target include its surface composition, shape, and structure, its dust environment, and the gas coma’s composition. A unique, multi-point ‘snapshot’ of the comet- solar wind interaction region will be obtained, complementing single spacecraft observations at other comets. We shall describe the science drivers, planned observations, and the mission’s instrument complement, to be provided by consortia of institutions in Europe and Japan. UK hardware contributions include the lead roles on the MIRMIS hyper spectral and multispectral remote sensing instrument by the University of Oxford, and of the Fluxgate Magnetometer aboard the mission's probe B2 by Imperial College London.

Keywords: Comet, Mission

83. Prediction and Detection of Solar Orbiter's December 2021 encounter with Comet Leonard

Grant, Samuel R; Jones, Geraint; Owen, Christopher; Matteini, Lorenzo

Presenting author institution: MSSL, UCL

Comets eject gas from the nucleus when heated by the Sun. These gases are ionized and transported away from the Sun by the solar wind, becoming partially visible as an ion tail. Spacecraft can encounter these tails, providing a rare insight into the comets' composition and disruption of the solar wind flow. Such encounters are often difficult to identify from solely the in-situ plasma measurements, and knowledge of the flow of the solar wind is required to predict these encounters geometrically. In December 2021, comet C/2021 A1 (Leonard) travelled sunward of the spacecraft Solar Orbiter, immersing it in the cometary plasma propagating with the solar wind. Using a method that provides a relatively accurate prediction of serendipitous ion tail encounters, we present the prediction of the December 2021 Solar Orbiter-Comet Leonard encounter, and a subset of the resulting data collected. With combined images of the encounter from multiple spacecraft, and a wealth of data collected from Solar Orbiter's instruments, this encounter creates an important opportunity for collaboration to study a cometary ion tail.

Keywords: Comets, Cometary Ion Tails, Cometary Plasma, In-Situ Observations, Solar Orbiter

84. Probing Colour Transitions in the Primordial Kuiper Belt

Buchanan, Laura; Schwamb, Meg E.; Fraser, Wesley C.; Bannister, Michele T.; Marsset, Michaël; Pike, Rosemary E.; Nesvorný, David; Kavelaars, J. J.; Benecchi, Susan D.; Lehner, Matthew J.; Wang, Shiang-Yu; Peixinho, Nuno; Volk, Kathryn; Alexandersen, Mike; Chen, Ying-Tung; Gladman, Brett; Gwyn, Stephen D. J.; and Petit, Jean-Marc

Presenting author institution: Queen's University Belfast

Beyond the orbit of Neptune lies a region of small icy bodies known as the Kuiper Belt. Since its formation this population as remained largely unprocessed by the Sun, as a consequence of its distance. This means that we can study these Kuiper Belt Objects (KBOs) in order to investigate the conditions in the early Solar System. Generally, these small, dim KBOs have flat and featureless spectra. Therefore, broadband photometry can be used as a proxy for composition, as it provides enough information to characterise the optical and near-infrared spectral slopes of the KBO surfaces. It can be used to essentially take very low-resolution spectra of the surfaces of these objects.

Dynamically excited KBOs show two clusters in the distribution in their broadband surface colours, generally called the red and less red surface types. It is believed that these differing surfaces may be an indicator of where these objects formed in the early Solar System, before their emplacement due to planetary migration. Therefore, this bimodality suggests the presence of a surface change in the massive planetesimal disk from which the dynamically excited KBOs formed, possibly a surface-colour changing ice line. The Colours of the Outer Solar System Origins Survey (Col-OSSOS) probed KBO surface properties via near-simultaneous g-, r- and J-band photometry. In this work, we have combined a full dynamical model of the Kuiper with Col-OSSOS observations to investigate the relation between possible primordial variations in surface type through the early disk, and the dynamics responsible for emplacing those bodies in the Kuiper Belt. We have investigated two scenarios within the initial disk: (1) inner neutral surfaces and outer red, and (2) inner red surfaces and outer neutral, with the split between these different surfaces stepped radially out through the disk. We will present the results of these colour simulations, and what they imply about the conditions in the early outer Solar System.

Keywords: Kuiper Belt, Trans Neptunian Objects, Compositions

Session 11:

Winchcombe & Carbonaceous Chondrites

85. The Fall, Recovery, and Initial Analysis of the Winchcombe CM Chondrite

King, Ashley; Daly, Luke; Joy, Katherine; Bates, Helena; Bryson, James; Chan, Queenie; Clay, Patricia; Devillepoix, Hadrien; Greenwood, Richard; Russell, Sara; Suttle, Martin; the UK Fireball Alliance; the Winchcombe Consortium

Presenting author institution: Natural History Museum

At 21:54 (UTC) on the 28th February 2021 a bright fireball was recorded by 16 stations operated by the six meteor camera networks that collaborate as the UK Fireball Alliance (UKFAll). The main mass (~320 g) of the meteorite was discovered the next morning by the Wilcock family on their driveway in the town of Winchcombe, Gloucestershire. Upon landing, the stone shattered into a pile of dark mm- to cm-sized fragments and powder, most of which was collected only ~12 hours after the fall. In total, >500 g of material was recovered from the local area by members of the public and the UK planetary science community within seven days of the fall. The largest intact piece of the Winchcombe meteorite is a 152 g stone found on nearby farmland on the 6th March.

A consortium was quickly established to study the Winchcombe meteorite. Petrographic observations indicate that Winchcombe is a CM ("Mighei-like") carbonaceous chondrite. It consists of chondrules and calcium-aluminium-rich inclusions (CAIs) set within a matrix of phyllosilicates, tochilinite-cronstedtite intergrowths (TCIs), carbonates, magnetite, and sulphides. Many of the samples show evidence for brecciation and contain multiple distinct lithologies with sharp boundaries. Most lithologies are intermediately to highly aqueously altered (CM2.4 – 2.0), although a rare lithology containing unaltered chondrules and metal has also been identified (~CM2.6).

The classification of Winchcombe as a CM chondrite is further supported by major and minor element abundances, and oxygen, titanium, and chromium isotopic compositions. The bulk water content of Winchcombe measured within one month of the fall was ~11 wt.%. Analysis by stepped combustion yielded carbon, nitrogen, and noble gas abundances and isotopic compositions largely consistent with other highly altered CM chondrites. Low voltage SEM characterisation less than a week after the fall of fresh, unpolished fragments located several small (~10's µm) carbon- and nitrogen-bearing regions with "globule-like" morphologies. Initial analysis by both both liquid (LC-) and gas chromatography-mass spectrometry (GC-MS) revealed extraterrestrial organic components including lipids, fatty acids, and amino acids.

The Winchcombe meteorite is only the fifth carbonaceous chondrite fall with a known pre-atmospheric orbit, and due to its rapid recovery is likely the most pristine member of the CM group. The mineralogical, elemental, and organic properties of the Winchcombe meteorite provide a snapshot of conditions in the outer regions of the protoplanetary disk and new insights into the chemical and dynamic evolution of volatiles in the early solar system. The nature and timing of the Winchcombe meteorite fall also makes it complementary to samples of asteroids Ryugu and Bennu collected by the Hayabusa2 and OSIRIS-REx missions, offering an opportunity to develop and rehearse curation and analytical protocols on fresh, carbonaceous materials.

Keywords: Chondrite, Aqueous alteration, Organics, Asteroids

86. Nano-scale heterogeneity in the extent of aqueous alteration within the Winchcombe CM chondrite fall

Daly, Luke; Suttle, Martin D.; Lee, Martin R.; Bridges, John; Hicks, Leon; Martin, Pierre-Etienne; Floyd, Cameron J.; Jenkins, Laura; Salge, Tobias; King, Ashley J.; Almedia, Natasha V.; Johnson, Diane; Trimby, Patrick; Mansour, Haithem; Wadsworth, Fabian D.; Rollison, Gavyn; Genge, Matthew J.; Darling, James; Bagot, Paul; White, Lee F.; Stephens, Natasha; Mitchell, Jennifer T.; Jones, Rhian; Piazolo, Sandra; Einsle, Joshua F.; Macente, Alice; Hallis, Lydia J.; Schofield, Paul F.; Russel, Sara S.; Bates, Helena; Smith, Caroline; Franchi, Ian; Forman, Lucy V.; Bland, Phil A.; Westmoreland, David; Anderson, Iain; Taylor, Richard; Montgomery, Mark; Parsons, Mark; Vasseur, Jerome; and the UK Fireball Alliance.

Presenting author institution: University of Glasgow

Introduction: CM carbonaceous chondrites are chemically primitive, but extensively aqueously altered[1,2]. This alteration is locally heterogeneous[3] and destroys much of the primary mineralogy and texture[2]. The permeability of CM chondrites is low, permitting fluid flow only over distances <100 µm[4], however, large veins of carbonate on the B-type asteroid Bennu have been observed[5], that suggest macro-scale movement of fluids. On the 28th February 2021 a bright fireball was observed by the UK Fireball Alliance (UKFall)[6] resulting in the recovery of the Winchcombe meteorite 12 hours later[6]. It is a CM chondrite breccia with nine lithologies, with variable alteration histories ranging from CM2.0-CM2.6[6]. Thus, Winchcombe an ideal sample to explore macro-nanoscale constraints on aqueous alteration of CM chondrites.

Methods: Several rock chips and petrographic sections of the Winchcombe meteorite were analysed using a suite of techniques including XCT, EPMA, SEM, EDS, QEMSCAN, EBSD, FIB, FIB-TOF-SIMS, TEM, and APT. Permeability established via numerical simulations. **Key results:** *XCT* data indicate that a foliation fabric is present defined by relic chondrules in some Winchcombe lithologies and a fracture cleavage is present in some others. The foliations are in separate orientations in different lithologies from the same rock chip. *Numerical simulations* indicate that Winchcombe has an anisotropic permeability. *SEM* imaging of tochilinite cronstedtite intergrowths (TCIs) reveals a range from complete to incomplete replacement of carbonate and silicate phases. *EPMA* and *EDS* data show a moderate spread of compositions within the matrix, fine-grained rims (FGR), and TCIs within each lithology. *TEM* investigations reveal the presence of inclusions that resemble glass with embedded metal and sulphide (GEMS) in an FGR within a subtype 2.2 lithology. *TOF-SIMS* and *APT* data from TCIs indicate that Na is concentrated at the boundary between Mg-rich and Fe-rich intergrowths.

Discussion and conclusions: At the macro-scale, XCT results and numerical simulations show that fluids flowed more readily along a 2D plane and less-readily along the pole to that plane. Such an anisotropic permeability network would limit fluid transfer, resulting in the segregation of fluid compositions which may enhance the preservation of pockets of unaltered material. At the nanoscale, the survival of both GEMS-like phases that are readily altered by minor degrees of aqueous alteration, and the heterogeneity in the extent of carbonate alteration to TCIs over short distances, suggest that areas within otherwise severely aqueously altered lithologies of the Winchcombe meteorite experienced little fluid interaction. This may be due to local variations in permeability on the Winchcombe parent. The cause of this lower permeability could be a primary texture, a compaction texture, an impact texture, or generated by progressive alteration. Therefore, even in pervasively aqueously altered meteorites it is likely that some nano-macro scale volumes can preserve their primary mineralogy and texture.

References: [1] Brearley A.J., (2003) *Treatise in Geochemistry 1*, [2] Suttle M.D. et al., (2021) *GCA*, [3] Morlok A. et al., (2006), *GCA*, [4] Bland P.A., et al., (2009) *EPSL*, [5] Kaplan H.H., et al., (2020) *Sci.* [6] King A.J., et al., (submitted) *Sci. Adv.*

Keywords: Meteorites, Winchcombe, Carbonaceous Chondrites, Correlative Microscopy

87. Pushing the limits of SEM-based microanalysis for the characterisation of complex, heterogeneous meteorite microstructures

Haspel, Dan; Mansour, Haithem; Trimby, Pat

Presenting author institution: Oxford Instruments Nanoanalysis

The microstructures of many meteorites, such as carbonaceous chondrites, are frequently highly heterogeneous and require effective characterisation across scales ranging from the centimetre to the nanometre. This poses a particular challenge, as conventional microanalytical techniques in the electron microscope (such as energy dispersive X-ray spectrometry, EDS, and electron backscatter diffraction, EBSD) are not able to cover whole samples at the desired resolution within a reasonable timeframe. Here we present a new, smarter approach to the characterisation of complex meteorite microstructures, using analyses of the recent Winchcombe meteorite (CM2 carbonaceous chondrite) as an example. This top-down approach involves the following steps:

96. High quality sample polishing.
97. High speed, large area imaging of whole sample blocks using both backscattered electron (BSE) imaging and rapid EDS mapping, providing a fast survey scan of the microstructure.
98. The use of live chemical imaging (live, high-throughput EDS-based chemical imaging during navigation around the sample and across different magnifications) to investigate potential areas of interest for further investigation.
99. Detailed EDS mapping of key features: for ultimate resolution of small structures, this requires use of the Extreme windowless EDS detector, enabling resolution of features <100 nm using beam energies < 5 keV.
100. Further detailed combined EBSD-EDS analyses of identified areas, resolving crystallographic structures down to ~50 nm.
101. Offline advanced EBSD pattern matching processing to extract high quality information from complex phase structures, including from alteration phases such as lizardite and cronstedtite.
102. We will run through brief examples of the steps in the workflow, demonstrating how the latest combination of hardware and software can be used effectively to extract an unprecedented level of detailed information from even the most complex meteorite samples, aiding interpretation of the timing and processes of formation of the different microstructural constituents.

Keywords: Carbonaceous chondrite, Microanalysis, EDS, EBSD, Winchcombe meteorite

88. Cr, Cd, Te, Ti, Zn AND O-ISOTOPE COMPOSITION OF THE WINCHCOMBE (CM2) METEORITE

R. Greenwood; R. Findlay; R. Martins; R. C. J. Steele; M. Rehkämper; K. Shaw; P. S. Savage; E. Morton; I. A. Franchi; T. Elliot; M. D. Suttle; A. J. King; M. Anand; J. Malley; X. Zhao; D. Johnson; M-C. Liu; K. McCain; N. Stephen

Presenting author institution: The Open University

Introduction: A consortium study of the Winchcombe CM2 fall (28th February 2021) is ongoing. The results discussed here summarize the initial findings of the "Winchcombe Isotope Team" (WIT). The initial remit of WIT was to undertake high-precision isotopic analysis on a range of elements (Ca, Cd, Cr, K, Li Mg, Mo, Ni, O, Si, Ti, Te, U, W, and Zn) and to also undertake presolar grain studies. Here we discuss the initial results of our measurements of the Cd, Cr, O, Te, Ti and Zn isotopic composition of the Winchcombe meteorite.

Methods*: O-isotopes*: Analyses were undertaken by laser fluorination at the Open University on powdered 100 – 150 mg chips of Winchcombe. *Zn, Cd and Te-isotopes:* Analyses were undertaken at Imperial College on a 1.94 g sample of Winchcombe. *Cr isotopes*: Analyses were undertaken at the University of St. Andrews on 20 mg of Winchcombe material. *Ti isotopes:* Analyses were undertaken at the University of Bristol on a 101 mg sample of Winchcombe.

Results: O-isotope analyses of two Winchcombe fragments have distinct O-isotope compositions: $\delta^{17}O$ 2.75 ± 0.40‰; $\delta^{18}O$ 9.48 ± 0.50‰; $\Delta^{17}O$ -2.18 ± 0.14‰ (2SD, n=2) and $\delta^{17}O$ 0.98 ± 0.31‰; $\delta^{18}O$ 7.29 ± 0.62‰; $\Delta^{17}O$ -2.23 ± 0.00‰ (2SD, n=2); with both plotting at the isotopically heavy, more aqueously altered, end of the CM2 array close to Cold Bokkeveld and Murchison. Our analysed fragments sample the two most abundant lithologies in Winchcombe. These are both highly altered (<CM2.4) tochilinite-cronstedtite intergrowth (TCI)-rich materials. The O-isotope data and pertrography therefore appear to be providing a consistent picture concerning the extent of aqueous alteration experienced by the Winchcombe parent body. $\delta^{66}Zn$ values determined for two Winchcombe aliquots are +0.29 ± 0.05‰ (2SD) and +0.45 ± 0.05‰ (2SD). The small difference between these analyses likely reflects minor sample heterogeneity. Zn isotope compositions for Winchcombe show excellent agreement with published CM2 data. $\delta^{114}Cd$ for a single Winchcombe aliquot was +0.29 ± 0.04‰ (2SD), which is close to a previous result for Murchison. $\delta^{130}Te$ values for three aliquots gave indistinguishable results, with a mean value of +0.62 ± 0.01‰, and are essentially identical to published values for CM2s. $\varepsilon^{53}Cr$ and $\varepsilon^{54}Cr$ for Winchcombe were 0.319 ± 0.029 (2SE) and 0.775 ± 0.067 (2SE) respectively. Based on its Cr isotopic composition, Winchcombe plots close to other CM2 chondrites. $\varepsilon^{50}Ti$ values for Winchcombe are in line with recently published data for CM2s.

Discussion and conclusions: Zn, Cd, Te, Ti and Cr isotope data are consistent with a CM2 classification for Winchcombe. O-isotope analysis indicates that it experienced extensive parent body aqueous alteration. However, like other CM2s, Winchcombe displays significant lithological variation. Further O-isotope analysis will be undertaken on the less altered material from Winchcombe to better constrain the extent of hydration on its parent body. In addition, we will be undertaking Si isotope measurements, presolar grain studies and leaching experiments (Ni, Cr and Zn).

References: See companion abstract: Greenwood R. C. et al. (2022) 85th Meteoritical Society Meeting, Glasgow.

Keywords: Winchcombe, CM2, carbonaceous chondrite, isotopes, Fall

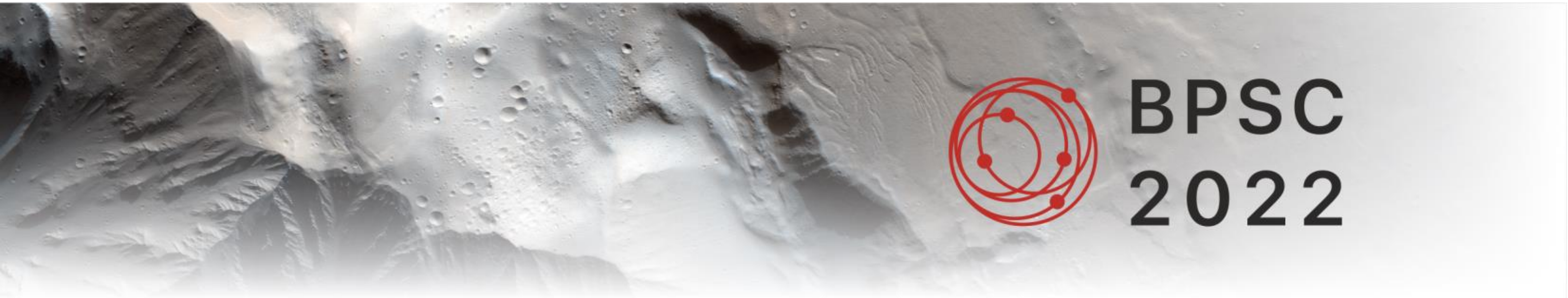

89. Surface Melting Processes on C-class Asteroid Ryugu

Bridges, John; Hicks, Leon; Noguchi T. and the Hayabusa2 Fine Grained Mineralogy Team

Presenting author institution: University of Leicester

Samples from Chamber A of the Hayabusa2 mission to C-type asteroid Ryugu are demonstrating the diversity of surface processes ('space weathering') that act to alter the near surface mineralogy and spectral characteristics of airless bodies. Here we report on the origin of a phyllosilicate-rich assemblage and melted zones in Ryugu Chamber A grains as part of the Hayabusa2 Fine Grained Mineralogy team [1,2]. In previous work on space weathered sw samples from the Itokawa S class asteroid we used Fe K XANES, STEM, TEM to demonstrate changing $Fe^{3+}/\Sigma Fe$, vesicular blistering, and $npFe^0$ growth associated with that style of sw [3]. Here, and in [2], we use the same techniques to provide accurate $Fe^{3+}/\Sigma Fe$ and mineral-textural identifications on Ryugu grains to help characterise a different set of sw processes, likely associated with micrometeorite bombardment [2].

We have analysed FIB-TEM wafer samples A0058-C2001-08, A0104-00200502, and A0104-01700602 prepared from Hayabusa2 near surface samples (Chamber A) by Noguchi at Kyushu University [4]. As part of a Hayabusa2 consortium of complementary analytical work, we conducted Fe-Kα XAS measurements using the I-14 X-ray Nanoprobe Beamline at Diamond Light Source. To achieve XAS mapping, a series of maps were obtained over regions of interest, each map measured from 7050 to 7350 eV with a higher energy resolution over the XANES features (~7100-7150 eV). Similar to Itokawa asteroid samples [3], mineralogical identity can be constrained, including oxidation states in Fe-oxides and Fe-silicates, by observing increased energy shifts in the 1s→3d pre-edge peak centroid positions, and comparing to reference minerals of known $Fe^{3+}/\Sigma Fe$. EELS was performed using the JEOL ARM200CF instrument at ePSIC in the Diamond facility, using an accelerating voltage of 200 keV, current 15 µA, and measuring 0.25 eV/ch. Additional TEM imaging, calibrated STEM-EDX have been performed using JEOL 2100 FEG and LaB_6 TEM's at the University of Nottingham, UK.

The interior of these samples are a fibrous phyllosilicate and magnetite rich (Fig. 1) with lesser amounts of phosphate and sulphides. The phyllosilicate has two layered lattice spacings of 0.75-0.78 nm and $100*(Si+Al)/(Mg+Fe_{tot})$ atomic of 48-60. Its $Fe^{3+}/\Sigma Fe$ varies considerably on the 3 wafers we have analysed from 20-50%. However, the melt zone, as shown by vesicularity and less crystalline nature, has $Fe^{3+}/\Sigma Fe$ of 15%.

The reduction of the phyllosilicate-rich Ryugu grains associated with micron scale surface melt zones is in contrast to the $>Fe^{3+}/\Sigma Fe$ associated with sw nm-thick zones in Itokawa samples returned by Hayabusa [3,4]. The latter is thought to be a result of the implanted solar wind H^+ ions reacting with the segregated ferrous Fe in the surface material [3]. Surface melting and associated changes in Fe-rich mineralogy present a different type of primitive asteroidal process [5].

References: [1] Yokoyama T. et al. *Science* (subm.). [2] Noguchi T. et al. (2022) *Nature Astronomy* (subm.). [3] Hicks, L. et al. (2020) *Meteorit. Planet. Sci. 55*, 2599–2618. [4] Noguchi T. et al. (2014) *Meteorit. Planet. Sci. 49*, 188–214. [5] Bridges J. et al. 2022 Meteoritical Society.

Keywords: Ryugu, Hayabusa2, Mineralogy

90. Thermal History of Dehydrated CM Chondrites Reconstructed from their Fe-sulphide Grains

Harrison, Catherine S.; King, Ashley J.; Jones, Rhian H.; Suttle, Martin D.; Bartoschewitz, Rainer

Presenting author institution: The Natural History Museum

A number of CM carbonaceous chondrites experienced post-hydration heating (>300 °C) on their parent body [1]. However, the timing, duration and mechanism of the dehydration event(s) remain poorly defined. Fe-sulphides are widespread in carbonaceous chondrites and are highly sensitive to aqueous alteration and thermal metamorphism. The dominant Fe-sulfides are pyrrhotite ($[Fe,Ni]_{1-x}S$) and pentlandite ($[Fe,Ni]_9S_8$). Kimura et al. [2] used Fe-sulphide textures and compositions to classify CM chondrites into three categories: A) unheated meteorites; B) mildly heated (~Stage II-III, ~300 – 750°C), characterized by blebs or lamellae of pentlandite in all pyrrhotite grains; C) severely heated (~Stage III-IV, ~500 - >750°C), with abundant Ni-rich metal inclusions and an absence of pentlandite exsolution textures. The evolving sulphide assemblages with increasing peak metamorphic temperature reflect exsolution of pentlandite from a monosulphide solid solution at temperatures <610 °C, and thermal decomposition of pentlandite into Ni-rich metal at temperatures >610 °C [2]. To further constrain the thermal history of the CM parent body, we have characterized coarse (>10 µm) Fe-sulphide grains within polished sections of Jbilet Winselwan (CM2, Stage II), Dhofar (Dho) 1434 (CM_{an}, Stage III) and Pecora Escarpment (PCA) 02012 (CM2, Stage IV) using a ZEISS EVO 15LS scanning electron microscope (SEM) equipped with an energy dispersive X-ray spectrometer (EDS), operated at 20 kV and 1.5 nA.

In Jbilet Winselwan, ~80% of the analysed grains are pyrrhotite with inclusions of pentlandite (PoPn), which form either ~5 µm sized oriented laths or patches 10-50 µm in size. We also observed individual pyrrhotite (Po) and pentlandite (Pn) grains. The PoPn grains are consistent with Category B Fe-sulphides. However, the pentlandite patches themselves occasionally contain pyrrhotite inclusions similar to the "snowflake texture" in CM and CR chondrites described by Singerling and Brearley [3], who interpreted them as primary Fe-sulphides that condensed from the solar nebula prior to accretion. We therefore suggest that Jbilet Winselwan contains distinct lithologies that experienced varying degrees of metamorphism, including at least one lithology that was never heated to temperatures >300°C and still retains primary Fe-sulphide grains from the nebula.

In Dho 1434, the grains are either PoPn, pentlandite with inclusions of metal (PnM), or pyrrhotite with inclusions of both pentlandite and metal (PoPnM). The majority of Fe-sulphide grains within PCA 02012 are PoPn and PoPnM grains, although we also found one individual Po grain, and one pyrrhotite grain with metal inclusions (PoM). In Dho 1434 and PCA 02012, the Fe-sulphide grains are consistent with both Category B and Category C Fe-sulphides, perhaps indicating localized variations (on the order of 1000's of µm) in peak metamorphic temperature. Additionally, the presence of PnM and PoPnM grains, where pentlandite has only partially broken down into metal, suggests the heating event was too rapid to allow for equilibrium to be maintained. Rapid and potentially heterogeneous heating is more consistent with impact heating rather than heating via solar radiation or radiogenic decay.

References: [1] King A.J. et al. (2021) *GCA*. 298:167. [2] Kimura M. et al. (2011) *M&PS.* 46:431. [3] Singerling S.A. and Brearley A.J. (2018) *M&PS.* 53:2078.

Keywords: Carbonaceous Chondrites

91. Planetary Science in the UK: An update on LARES and CAFES

Grady, Monica; Russell, Sara; Gilmour, Jamie

Presenting author institution: The Open University

A few years ago, we established a network called LARES – Laboratory Analysis for Research into Extraterrestrial Specimens. The purpose of the network was to facilitate dialogue between practitioners, to act as a lobbying agent to research funders and to take a forward look at how the shape of the planetary sciences community might develop and its instrument needs evolve. The network has no funding and exists mainly as a mailing list and a website (https://ukcosmochemanalysisnetwork.wordpress.com/), the latter of which is inherited from the predecessor UK CAN. It has no committee structure – the authors of this abstract are the founders and custodians of LARES. We have explored opportunities to attract funds to develop LARES, with limited success. Why have we failed to take this initiative forwards? Because as a community, we do not have a clear vision of what LARES is, or would like to be, so we do not speak with a single voice when it comes to funding applications.

So much for LARES. Now on to CAFES. One of the most important events that will occur in the next decade (or so) is the return of samples from Mars – and much of the imperative behind LARES was to ensure that we are adequately prepared for the samples, such that the UK can play a leading role in their analysis. In parallel with the requirement for state-of-the-art instrumentation has been an aspiration that the UK should play a leading role in curation of any European allocation of Mars samples. Two years ago, the UK Space Agency handed responsibility for leading the effort to develop a facility over to the STFC.

The most recent effort to acquire funding for a facility was CAFES (Curation and Analysis Facility for Extraterrestrial Samples). A business case was prepared by a committee (initially established by UKSA; MMG and SARR were members) in 2021 for consideration by STFC. Each Research Council can submit one case to the UKRI Infrastructure Fund (IF) for a BIG THING (to give you an idea of how big a BIG THING is, NERC won out a few years ago with funding for SS David Attenborough, aka Boaty McBoatface). Unfortunately, CAFES was not selected by STFC, but we were encouraged to undertake an architectural review of a potential facility, which would strengthen the case for CAFES if there is a further IF call.

Where are we going with this? There has been a blurring of boundaries between LARES and CAFES – mainly because the same people are involved in the two projects. One of the major criticisms of the CAFES project was that it (again) did not have a clear vison of what it was for. We would like to take this opportunity to clarify the distinctions between LARES and CAFES and request input from the community, such that we can better articulate our goals if and when funding opportunities arise.

Keywords: Planetary Science, LARES, CAFES, Curation Facility, Sample Return

Session 12:

Habitability and Life

92. Reassessing Earth's oldest records of carbon and nitrogen cycling

Stueeken, Eva

Presenting author institution: University of St Andrews

Back to 3.5 billion years ago (Ga) evidence for life on Earth is now widely accepted. However, biosignatures from even older rocks are subject of intense debate. Putatively biogenic features that have been reported by various studies include carbon isotope ratios in graphite and carbonates, microfossils and stromatolites, dating back to 3.7 and possible 4.1 Ga. However, many of these reports have been questioned, largely because the host rocks of this age have undergone severe metamorphic alteration and deformation. This talk will revisit this debate with new carbon and nitrogen isotopic data of graphitic shales from turbidite deposits in the Isua Supracrustal Belt (3.7 Ga). After subtracting potential metamorphic and detrital perturbations, the data reveal new insights into the Paleoarchean nitrogen cycle. Specifically, the nitrogen concentrations of the shales are inconsistent with abiotic sources of ammonium that would form in equilibrium with non-biogenic graphite. This conclusion is further supported by thermodynamic modelling and comparison to truly hydrothermal graphite veins of younger age. Calculated pre-metamorphic nitrogen isotopic ratios (15N/14N) appear to be several permil lower than most of the Archean sedimentary rock record, which may indicate a distinct mode of biological N-acquisition. It is tentatively proposed that these values may reflect atmospheric nitrogen input from high-energy sources such as lightning, as supported by experimental data. If so, then these Paleoarchean rocks offer an important window into processes that contributed towards establishing habitability.

Keywords: Biogeochemistry, isotopes, biosignatures, Archean

93. The cosmic desert: exogenous sediments on Early Earth

Walton, Craig; Shorttle, Oliver; Lipp, Alex; Suttle, Martin

Presenting author institution: University of Cambridge

Earth's surface is deficient in available forms of many elements considered limiting for prebiotic chemistry, e.g., phosphorus (P), and many of the transition metals (Schwartz et al., 2006). In contrast, many extraterrestrial rocky objects are rich in these same elements (Pasek and Lauretta, 2006). Limiting prebiotic ingredients may therefore have been delivered by exogenous material. Today, the flux of extraterrestrial matter to Earth is dominated by fine-grained cosmic dust (Pasek and Lauretta, 2006). However, this material is rarely discussed in a prebiotic context due to its delivery over a large surface area (Pasek and Lauretta, 2006). Here, we argue that cosmic dust may have accumulated in prebiotic arid areas to form sedimentary deposits. We justify our proposal by considering the sedimentary accumulation rate of cosmic dust today and predicted for early Earth, comparing these to the accumulation rates observed in modern sedimentary systems, and developing a simple model of dust transport and chemical evolution during subaerial sedimentary cycling. Our models suggest that, within the range of estimated cosmic dust fluxes for early Earth (> 4 Ga) and the range of surface denudation rates in the catchment zones of internally drained closed basins (Pasek and Lauretta, 2006; Willenbring et al., 2013), dust would have accumulated substantially in-situ under semi-arid to arid climatic conditions. Next, considering sediment transport rates within the catchment zones of closed basins, cosmic dust could have either been supplied to basins en masse with a low precipitation recurrence interval (10s to 100s of years), or continuously given an interval of days to months. Either way, sedimentary processes allow the concentration of cosmic dust relative to endogenous sediment sources within closed basins. Modelling the dissolution of cosmic dust within closed basins, we find that P could have been sustained at > 1 mM concentrations even given many conservative assumptions about dust flux, dissolution rate, settling rate, and P sinks. We are presently pursuing more detailed calculations to understand whether cosmic dust could also have supplied useful quantities of C, N, and various transition metals and potentially highly siderophile elements of catalytic interest. Overall, the relevance of cosmic dust has likely been underestimated as a source of limiting elements for prebiotic chemistry. However, specific combinations of extraterrestrial and endogenous processes are needed to supply and concentrate this prebiotically interesting material. Our results speak to the probable utility of regional-to-local scale Earth surface processes in both concentrating starting ingredients for prebiotic chemistry, and constructing unique end-member environments in which such chemistry may take place.

References: Schwartz et al., 2006, Phil. Trans. R. Soc. B. 361. 10.1098/rstb.2006.1901. Pasek et al., 2008, OOLEB. 38. 10.1007/s11084-007-9110-5. Willenbring et al., 2013, Geology. 41.3 10.1130/G33918.1. Trail et al., 2011, PNAS. 480. 10.1038/nature10655.

Keywords: Prebiotic chemistry, Planetary science, Cosmic dust, Meteorites, Early solar system

94. Carbon and Nitrogen Cycling within a Geothermal Mars Analogue

Galloway, Toni; Cousins, Claire; Stüeken, Eva; Nixon, Sophie; Moreras-Marti, Arola; Fox-Powell, Mark

Presenting author institution: University of St Andrews

Since the discovery of ancient Noachian-age (4.1-3.7Ga) terrestrial hot spring deposits on Mars, many recent studies have focused on their analogues on Earth due to their potential to host Mars-relevant microbial communities. Following on from the discovery of nitrogen compounds on Mars, our aim is to examine the biological nitrogen and carbon cycling within Mars analogue geothermal systems in Iceland, how they link to other metabolic cycles and geochemical environments which are relevant to Mars, and how we can use this knowledge to establish geochemical biosignatures that can be recognised in future missions.

Fieldwork for this study was carried out at Ölkelduháls which lies within the active Hengill volcanic system. Physiochemical measurements taken in situ were combined with major ion water chemistry, and $d^{15}N$ and $d^{13}C$ measurements of sediment and biomass from both sites. These data are being compared to genomic data, which includes identifications of microbial taxa and metabolic pathways present in these springs.

The system sampled at Ölkelduháls hosted a diverse range of environments including a small, low temperature stream with red sediment and suspended materials which was intersected by the outflow of an acidic, iron-sulfate pool. This spring's geochemistry was affected by the influence of the acidic pool; dissolved iron levels increased after the input of the acidic pool, while the pH dropped from 7.5 to 3.3. The $d^{13}C$ values of total organic carbon (TOC) around the acidic pool were around -22‰ while the red spring's biomass samples were closer to -30‰, indicating the presence of multiple different carbon fixation pathways. $d^{15}N$ of the biomass sampled within the red spring was -6‰ before the inflow of the acidic pool, which may be consistent with nitrogen fixation via alternative nitrogenases. Genetic data have so far indicated that species capable of nitrogen fixation are present in this section of the spring. The presence of ferrous iron in the acidic pool and downstream site correlates with the detection of iron-oxidising prokaryotes. This could include nitrate-dependent iron oxidation, which has been suggested as a possible metabolism plausible for early Mars. When examining the C:N:P ratios with respect to the Redfield Ratio, it was discovered that this system is extremely nitrogen-limited. The alternative nitrogenases have been shown to require more energy than the conventional Mo-based enzyme, and this may be one explanation as to what is limiting the influx of nitrogen into this system.

The geochemical and biological parameters which regulate nitrogen fixation are extremely important to these environments and the isotopic biosignatures produced. The energy produced by these metabolisms helps to govern their viability in extreme environments and is the subject of future work to gauge the suitability of Martian geothermal environments for nitrogen cyclers.

Keywords: Mars analogues, Biogeochemistry, Hot springs, Biosignatures, Nitrogen

95. Reactive iron species and organic carbon interactions in planetary materials

Bonsall, Emily; Tisdall, Eileen. Schröder, Christian

Presenting author institution: University of Stirling

It is estimated round a fifth of all organic carbon in sediments is preserved by reactive iron [1]. Reactive iron is defined by nanoparticulate iron oxides (npOx) or iron-rich x-ray amorphous material [2]. The preservation is mutually beneficial between the reactive iron and organic carbon, where the reactive iron is protected from mineral transformation and the organic carbon is protected from oxidation by microbial metabolisms [1]. Reactive iron has been detected in some carbonaceous chondrite falls like Orgueil [4-7] and Tagish Lake [8]. The Paris meteorite shows evidence of organic molecules being associated with iron [9]. Further analyses of different carbonaceous chondrites like the Winchcombe meteorite with Mössbauer spectroscopy do not reveal reactive iron species but clay minerals such as the serpentine group mineral cronstedtite [10]. Instead of preservation, the contribution of iron to organic molecule evolution needs to be investigated here. Reactive iron species have also been detected on Mars by the Mars Exploration Rovers, Spirit and Opportunity, as npOx [11-14] and by the Mars Science Laboratory Rover, Curiosity, as iron-rich x-ray amorphous material [15,16]. Whilst reactive iron can preserve organic carbon, it can also have a deleterious effect. When energy is inputted into the system, this can cause transformation of the iron minerals and oxidation of organic carbon [2, 17-19]. As the current Mars 2020 rover, Perseverance, and the suspended ExoMars rover, Rosalind Franklin, both have Raman spectrometers on board [20-22], suitable parameters for the detection of reactive iron are needed to prevent mineral transformation due to the laser energy.

References: [1] Lalonde et al (2012) *Nature Letters* 483, 198-200 [2] Bonsall et al (2022) *53rd LPSC* 2148 [3] Fisher and Burns (1991) *LPSC XXII* 389-390 [4] Madsen et al (1986) *Nature* 321, 501-503 [5] Knudsen (1989) *Hyperfine Interactions* 47, 3-31 [6] Madsen et al (1989) *Hyperfine Interactions* 50, 659-666 [7] Bland et al (2004) *M&PS* 39, 3-16 [8] Bland et al (2002) *LPSC XXXIII* 1754 [9] Noun et al (2019) *Life* 9:44 [10] Bonsall et al (submitted) *MetSoc 2022*, abstract ID 6379 [11] Morris et al (2006) *JGR*, 111, E02S13 [12] Morris et al (2006) *JGR*, 111, E12S15 [13] Morris et al (2008) *JGR*, 113, E12S42 [14] Morris et al (2019) in *Remote Compositional Analysis: Techniques for Understanding Spectroscopy, Mineralogy, and Geochemistry of Planetary Surfaces*, pp. 538-554, Cambridge University Press [15] Rampe et al (2017) *Earth Planet. Sci. Lett.*, 471, 172-185 [16] Rampe et al (2020) *Geochemistry* 80, 125605 [17] Hanesch (2009) *Geophys. J. Int.*, 177, 941-948 [18] Tan et al (2021) *Astrobiology*, 21, 199- 218 [19] Royle et al (2021) *Astrobiology*, 21, 673-691 [20] Bhartia et al (2021) *Space Sci. Rev.*, 217:58 [21] Wiens et al (2021) *Space Sci. Rev.*, 217:4 [22] Rull et al (2017) *Astrobiology*, 17, 627-654

Keywords: Biogeochemistry, Mars, Meteorites, Reactive Iron

96. Cryophilic microorganism utilisation and analogues for space biology

Davey, Matthew P., Pardasani, Yash

Presenting author institution: Scottish Association for Marine Science / University of Highlands and Islands

Cryophilic microorganisms, such as snow algae, can survive and bloom in the liquid phase of snow and ice. These species are often found in polar and high alpine regions but can in theory bloom anywhere there is suitable snow and correct summer conditions (Davey et al. 2019, Gray et al. 2020). Outside their active growth phase the cryophilic algae can remain dormant, often during the long, dark and freezing temperatures of a polar winter.

These species, given their resilience to extremes of abiotic conditions have the potential to provide a large number of human life support functions during space flights and on lunar or Martian bases. They could provide health benefits in terms of vitamin, antioxidant and other micronutrient supply as well as crucial functions such as waste regeneration through carbon sequestration, oxygen evolution and food production. In addition, they could provide organic material for artificial soils should the lunar and Martian substrate be used as a mineral basis for growing plants. They also provide astrobiological Earth Analogue information on possible microbial activity on extra-terrestrial habitats.

This talk will provide an overview to my groups current and future UKRI research on the detection and physiology of Antarctic polar algae, the effects of space radiation on algal cells and our upcoming Europlanet TA1 Planetary Field Analogue fieldwork in Iceland to study the cryopreserved algae in glacial systemshttps://www.europlanet-society.org/europlanet-2024-ri/ta1-pfa/ . I will also introduce our upcoming PhD research on the limits of microbial life, this project will investigate the complete limit of life in this specialised group of organisms by subjecting the cells to a range of low and high atmospheric pressures and gravity, temperatures and light at the Scottish Association for Marine Science (SAMS) and the UK Centre for Astrobiology at the University of Edinburgh. The growth and reproductive, photosynthetic and metabolic composition phenotypes will be measured. The findings will expand our understanding of physiological traits and their plasticity in algae exposed to extreme conditions. In particular, the metabolomic analysis will reveal which metabolic pathways and compounds are vital to sustain life at these extremes. The research will also contribute to wider applications in astrobiology and space biotechnology as the conditions these organisms will be tested under are analogous to some Martian and lunar environments and space flight conditions.

Keywords: Microbes, Astrobiology, Earth Analogue, Extremophiles, Life support

97. Theoretical limits to land coverage on rocky planets

Guimond, Claire; Rudge, John and Shorttle, Oliver

Presenting author institution: University of Cambridge, Department of Earth Sciences

Do we expect many rocky planets to have both oceans and dry land? Directly detecting exoplanet surfaces will be at the least extremely difficult, yet this information is key to interpreting climate models and biosignatures. Whilst Earth's marbled appearance seems to have emerged from complex, entwined systems, one imagines multiple ways to create the same effect on planets in different geodynamic regimes. We take first steps towards estimating the frequency of extrasolar blue marbles by modelling the simplest processes that set planetary land/ocean fractions. On one hand, topography increases land propensity by hollowing out ocean basins, storing surface water. To this end we quantify how dynamic topography---surface undulations caused by upwelling mantle---scales with constrainable bulk planet properties. Such scalings can tell us the minimum (pessimistic) ocean mass that would flood a planet. On the other hand, a higher total water budget will push a planet towards a fully water-covered regime. We expect planetary mantles to be a large reservoir for water (i.e., hydrogen stored in minerals), which over time supplies the surface via outgassThus we also preliminarily estimate maximum mantle water capacities as a function of stellar-derived mineralogy. Together, limits on topography and on water budgets present two uses of deterministic geophysical modelling towards understanding aspects of rocky worlds not accessible to observation.

Keywords: terrestrial exoplanets, planetary interiors, planetary surfaces, topography, water worlds

98. (Some) Land and Ice Albedo Feedbacks and the Climate and Habitability of Terrestrial Planets Orbiting M-dwarf Stars

Andrew Rushby

Presenting author institution: Birkbeck, University of London

The climate of terrestrial planets can be affected by the reflective properties of their land, ocean, and frozen surfaces in predictable, but also occasionally non-linear and complex, ways. In this keynote talk, I will provide a short introduction to land and ice albedo feedback processes operating on planets in the orbit of M-Dwarf stars, and present results from my recent work, as well as that of collaborators and colleagues, pertaining to these novel destabilising or stabilising feedbacks in the planet system. Using climate modelling approaches, from zero-D and 1-D energy balance models, to basic photochemical/climate models, up to complex 3-D GCMs, the effect of varying fractional and latitudinal coverage of land and ocean surfaces on the overall planetary albedo, climate, and ice-albedo feedback response of small, rocky planets is slowly being revealed to be a complex and sometimes 'non-Earth-like' in operation. I will highlight, in particular, some results from a recent paper leveraging the Community Earth Systems Model (CESM), a 3-D global circulation model, with ExoCAM, a climate module for CESM developed specifically for exoplanet studies, in which the effect of the composition of the land surface on the climate state of land-covered, tidally-locked planets in the TRAPPIST-1 system was investigated. Using empirical spectra for a range of terrestrial materials we demonstrated the considerable effect of the radiative properties on the land surface on the overall heat transport, atmospheric dynamics, and climate of the approximately Earth-sized, nearby exoplanets TRAPPIST-1d, e, and f, with implications for habitability studies and future observations. I will also, time allowing, describe and discuss the NASA 'Research Coordination Network' (RCN) model (of which NExSS was the first) and the means by which the astrobiology research and funding landscape within NASA (and beyond) is evolving to meet the needs of the diverse, interdisciplinary scientists working in the field and leverage upcoming NASA, ESA, JAXA missions and observational platforms.

Keywords: Modelling, CGM, Climate models

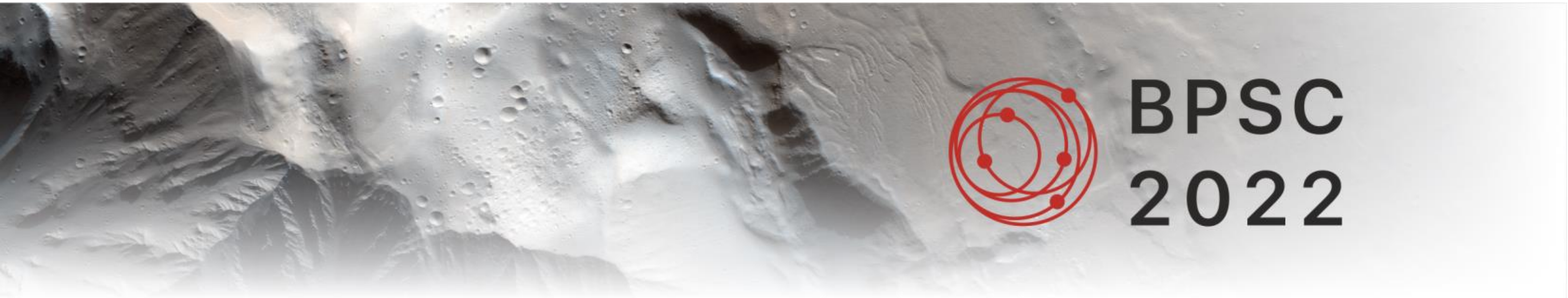

Session 13:

Exploring Mars

99. A primordial Scottish delta: a roadmap for assessing habitable environments on the ancient Martian surface?

Banham, Steven; Favaro, Elena

Presenting author institution: Imperial College London

Ancient deltas represent favourable locations for the exploration of habitability during Mars' early history. Delta deposits currently feature in two selected landing sites – Jezero & Oxia Planum – and are frequent contenders on landing site selection short-lists. Recorded within their stratigraphy, are the preserved expression of many potentially habitable environments, which can additionally serve as a location favourable for preservation of the resulting biosignatures. Martian deltas can be large: Jezero, Oxia planum and Eberswalde cover areas of ~30 km^2 ~70 km^2, 120 km^2 respectively. Rovers, once on the surface of Mars, typically make a linear traverse ~30 km long, covering a swath of ground ~30-40 m wide. Traversed and observed area represents an area of ~1 km^2, or much less than 5% of a delta's total area. In addition, the targets indicating life (e.g. algal mats or adhesion structures) or preserving life (concretions or clay minerals) may be small or invisible to optical instruments used during the preliminary search. This presents a major exploration problem: where on the delta do we search and what do we look for, given a rover's finite resources and time?

To aid with exploration of Martian deltas, we can examine delta stratigraphy on Earth – at leisure –for locations most suited for habitation, and subsequent preservation of biosignatures. These investigations can generate useful exploration tools to help scientists and engineers understand the geologic features they encounter, and how the rocks formed over space and time. Tools include: facies descriptions & annotated photographs; architectural panels explaining distribution of facies and geometric relations; depositional models depicting the ancient environment; and diagrams explaining how processes formed the environment. Understanding spatial and temporal relations across the delta deposits can be used to develop exploration strategies, and to understand the link between the preserved rock facies and the ancient environment that deposited them.

To understand the stratigraphic and sedimentary architecture of ancient deltas in the rock record, we chose to investigate the Cailleach Head Formation of NW Scotland. This formation represents the preserved expression of a primordial delta, which accumulated during the late Proterozoic: before complexed life sullied Earth's surface, and could exert an influence on depositional processes.

Here we present: examples of key sedimentary facies, and explain their depositional processes; their geometric relations within larger architectural elements, and how autogenic processes regulate their distribution; then discuss the stratigraphic architecture of the delta, and evidence of temporal changes within the environment. Finally, we provide a reconstruction of the ancient environment to describe the distribution of potentially habitable sub environments. From this, we link back to the original depositional facies to highlight primary habitable environments, and secondary locations for preservation of biosignatures. Visual recognition of these features during mission operations will enable engineers and scientists to locate themselves within the Martian stratigraphy, and efficiently home in on locations favourable for biosignature preservation.

Keywords: Mars, Earth Analogue, Delta, Stratigraphy

100. The effect of salinity to propagation and morphology of small-scale mudflows in low pressure environment: Insights from laboratory simulations

Kryza, Ondrej; Broz, Petr; Fox-Powell, Mark; Conway, Susan; Mazzini, Adriano; Hauber, Ernst; Sylvest, Matthew; Patel, Manish

Presenting author institution: Institute of Geophysics of the Czech Academy of Sciences

The behaviour and the rheology of mud during the emplacement of terrestrial sedimentary volcanism has been previously investigated (e.g., [1,2]). In contrast, this is not the case for Mars nor for other planetary bodies within the Solar System for which sedimentary volcanism has been proposed [e.g., 3]. The propagation behavior of low viscosity mud in a low-pressure chamber that partly simulated the environment of Mars was firstly experimentally studied by [4,5]. Their work revealed that low viscosity mud could flow over cold (<273 K) surface at martian atmospheric pressure, however, the mechanism of such propagation would be very different from that observed on Earth. On Mars, mud flowing over cold surfaces would rapidly freeze due to evaporative cooling [6] forming an icy-crust leading to the behavior of some of the mud flows in a similar manner to pahoehoe lava on Earth [4]. These experiments were performed by a mud mixture that contains only 0.5% of salt ($MgSO_4$). However, we lack the knowledge how variations of salt types and their content would affect the flow style and finite pattern of such mudflows as a presence of various salts can be natural on Mars as well (e.g., [7,8]).

In a set of experiments performed in the Mars Simulation Chamber (Open University, UK), we tested several selected salts relevant for the Mars environment (namely NaCl, $MgSO_4$, Na_2SO_4 and $CaSO_4$) and various salinities of these salts (0.5-15 wt%). The experiments were performed in metallic trays infilled with dry and precooled sand to -25 °C (to simulate the martian surface) and which were inclined to 5°. A container filled with 500 ml mud was positioned above the tray. Then we decreased the pressure to 4.5-6 mbar and released mud. Experiments were documented by a system of video cameras situated around the model box.

Results revealed contrasting scenarios of mud propagation which result in a wide range of shapes. We also found several transitional regimes in behavior between current concentrations and various salts. This is because the high content of salt in a mud or mud composed by different salts can undergo slightly to significantly different cooling according to thermodynamic equilibria which shifts both freezing and boiling point. Thus, the resultant style of flow process and finite morphology of such mudflows can be highly variable. For example, high content of $MgSO_4$ (typically >5 wt%) leads to development of long and narrow streams and with increasing content also develops a “ropy pattern” structure, whereas the same behavior occurs for 2.5 wt% of the NaCl.

References: [1] O'Brien and Julien (1988), Journal of Hydraulic Engineering 114 [2] Laigle and Coussot (1997), J. Hydraul. Eng., 123 [3] Ruesch et al. (2019) Nature Geoscience 12 [4] Brož et al. (2020), Nature Geoscience [5] Brož et al. (2020), EPSL 545 [6] Bargery et al. (2010), Icarus 210(1*), Chevrier et al. (2020), The planetary science journal, 1(3) [8] Nuding, et al. (2014), *Icarus*, *243*.

Keywords: Sedimentary Volcanism, Mudflow, Salinity, Mars Simulation Chamber

101. An Updated Global Catalogue of Rayed Craters on Mars: Potential Source Locations for Martian Meteorites

Grindrod, Peter; Harris, Jennifer; McKeown, Lauren; Parenti, Carlotta; Tornabene, Livio

Presenting author institution: Natural History Museum

Martian meteorites represent the only samples of Mars available for study in terrestrial laboratories. In addition to their crystallization and surface ejection ages, these samples provide a detailed understanding of the geochemistry of the martian crust. One of the major outstanding problems regarding martian meteorites is locating the exact source regions on Mars. Although the composition and texture of these meteorites limits the source locations to mostly igneous provinces on Mars, the inherent uncertainties in age-dating methods means that source craters remain speculative. To help the search for source craters, we have created an updated global catalogue of impact craters greater than 3 km diameter with thermally-distinct radial patterns, many of which represent large well-preserved and potentially young impact events. We defined search criteria for identifying rayed craters, assigning a confidence level to each crater, and noted the presence or absence of secondary craters. Using daytime and nighttime thermal infrared image data we identified 118 rayed craters between ±60° latitude, of which 89 had not appeared in previous catalogues of rayed craters. We discuss some potential uses of this catalogue in terms of understanding the morphology, location, and composition of each rayed crater. In addition, we used crater counting to derive model surface ages for the ejecta, effectively the age of the impact event, at 77 of the rayed craters, and derived model ages for the target surface at 59 of the rayed craters. Our preliminary analysis demonstrates the potential future use of this catalogue in finding the source location of martian meteorites.

Keywords: Mars, meteorites, craters

102. Mechanochemical generation of perchlorates on Mars.

John Edgar; Jamie Gould; Kamal Badreshany; Jon Telling

Presenting author institution: School of Natural and Environmental Sciences, Newcastle University, Newcastle upon Tyne, NE34QN

Perchlorates (ClO_4^-) are widespread in the solar system having been detected on Earth, on Mars, in chondrite meteorites and in lunar samples. On Mars, perchlorates expand the potential for habitable conditions by lowering the freezing point of liquid water in the formation of brines. In future manned space exploration their presence poses a hazard to human health, however, it also represents opportunities as a source of oxygen and fuel. Despite their prevalence, the mechanism(s) of perchlorate formation in different environments are poorly understood. Here, we demonstrate that perchlorates can be generated through the mechanical activation of silicates in the presence of chloride; a process that is widespread in environments on Mars through aeolian abrasion, and likely other solar system bodies, including Earth. The results of laboratory experiments are reported where a suite of single-phase rock forming minerals, common to the Martian crust, were crushed with halite and the formation of perchlorate measured with ion chromatography.

All of the silicate minerals tested generated detectable perchlorate (maximum of 7.0 ± 0.4 nmol), whereas the non-silicate controls were non-productive (< 0.6 nmol). A relationship between the crystal structure of the minerals and the amount of perchlorate generated was observed, consistent with the hypothesis that the breaking of silicate bonds was required to generate perchlorate in this study. We further use a generic dust generation equation to estimate the perchlorate production potential of Nili Patera, a Martian dune field where sand fluxes have been constrained from orbit. Results indicate that perchlorate generation may have been occurring on Mars much more rapidly than previous models have predicted. This provides a possible mechanism for geologically young perchlorate on Mars and the potential for more widespread habitable aqueous niches for life to have existed over the Amazonian on an otherwise largely dry Mars.

Keywords: Mars, Perchlorate, Mechanochemistry, Silicate, Fracture

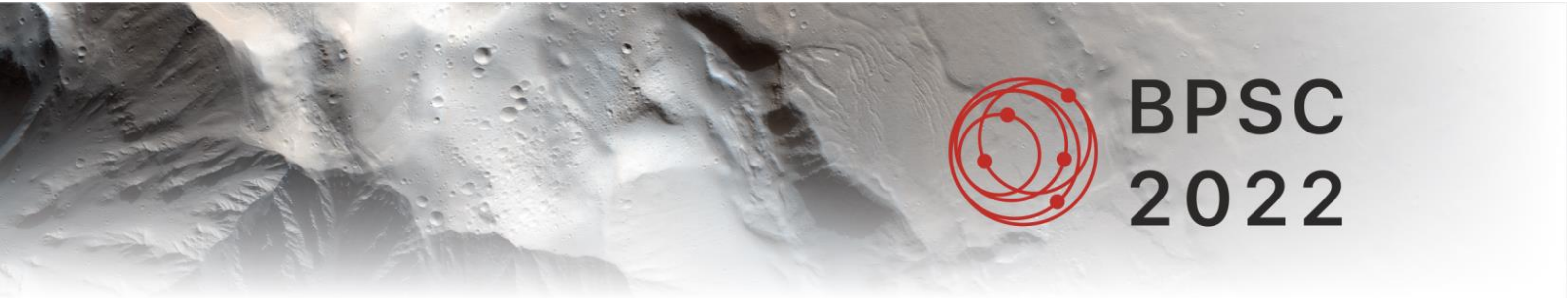

103. The Aeolian Environment of Oxia Planum

Favaro, Elena; Balme, M.R., Davis, J., Grindrod, P.M., Fawdon, P., McNeil, J.D., Barrett, A.M., Lewis, S.R.

Presenting author institution: The Open University

The surface of Mars is replete with evidence of aeolian processes. Landforms and bedforms encode in them signals of paleo- and contemporary atmospheric conditions. Decoding these signals allows researchers to piece together the complex landscape evolutionary history of the Martian surface.

Here, we outline how we have used bedrock landforms and granular bedforms to characterize the aeolian environment at Oxia Planum – the landing site of the ExoMars *Rosalind Franklin* rover.

We used multiple methods of data acquisition and analysis to characterize the landscape in and around the proposed rover landing site: (i) machine learning, (ii) manual mapping, and (iii) change detection techniques were used to identify, map, and determine the migration, morphometrics, distribution, and orientations of transverse aeolian ridges (TARs) and periodic bedrock ridges (PBRs), as well as dust devils, dust devil tracks, and windstreaks in HiRISE, CTX, CaSSIS, and HRSC images. Then, we used (iv) Global Circulation Models (GCM) and obtain the best possible understanding of the current wind regime at Oxia Planum.

We measured 10,753 TARs and, based on established grainsize-albedo relationship of stoss and lee slopes observed in terrestrial megaripples, interpreted the formative wind direction as originating from the NW-NNW and blowing towards the SE-SSE. PBRs were interpreted to have been formed when winds blew from the north to the south, or from the south to the north. We also recognized a relationship between PBRs and Fe/Mg-rich phyllosilicate terrain (hydrous clay-bearing units). This relationship was later found to be widespread throughout the Circum-Chryse region. HRSC and CaSSIS images were used to identify and track 6 active dust devils in OP, while change between consecutive CTX images (captured 50 Earth days apart) identified 649 dust devil tracks or windstreaks. These features exhibited two orientations: a dominant WNW-ESE (180° ambiguity) direction, and a secondary NNE-SSW (180° ambiguity) direction. Based on these landscape-level observations, we identified three separate and distinct aeolian regimes that have affected the surficial expression of Oxia Planum. We then compared these data with modelled GCM winds and found that no modelled winds can account for the orientation of TARs or PBRs.

This work was the first study to comprehensively evaluate the aeolian environment at OP using granular bedform, bedrock landforms, inferred near-surface winds, and GCMs.

Keywords: Mars, Aeolian Geomorphology, Transverse Aeolian Riddges, Periodic Bedrock Ridges, ExoMars 2020

104. Reconstructing the palaeoenvironment of the sediment fan at Oxia Planum, Mars

Roberts, Amelie; Gupta, Sanjeev; Fawdon, Peter; Davis, Joel; Banham, Steve

Presenting author institution: Imperial College London

Introduction: Sediment fans preserve a record of the palaeoenvironment of their formation. Fans form due to a fluvial system's reduced sediment transport capacity, typically from flow deceleration: where rivers intersect a body of standing water (delta), a change in accommodation space (fluvial fan), or a change in gradient (alluvial fan). On Mars, evidence for bodies of standing water are of particular scientific interest and are proposed as habitable environments capable of preserving evidence of ancient biosignatures. Oxia Planum contains phyllosilicate-bearing strata interpreted to represent aqueous activity. Subsequently, it was selected as the landing site for the ESA's ExoMars Rosalind Franklin rover mission. A prominent fan body is located close to the landing ellipse. Previous broad-scale investigations of this fan indicate either a fluvial or deltaic origin. To develop a more robust depositional model for the origin of the sediment fan, we conducted a photogeological investigation of strata associated with this fan using orbital images and derived digital terrain models at a 1:1250 digital map scale. This investigation used newly created HiRISE and HiRISE DTM mosaics covering the fan at a resolution of 25 cm/pixel and 1 m/pixel respectively.

Observations: Here we present the geomorphology of the Oxia Planum sediment fan and associated units. The sediment fan comprises two distinct units identified by different photointerpreted textures and elevations. The lower fan unit (~17km long, ~8 km wide, and 3-10m thick) has a smooth, cratered surface and forms three finger-like protrusions at the western side of the fan. This unit's scarps exhibit three prominent dark-toned and two lighter-toned layers and, at one location, inclined surfaces that dip to the north-west. A crater is embedded between two layers and one finger-like protrusion cross-cuts another. Within the lower fan unit is an infilled crater partially covered by the upper, triangular-shaped unit (~5km long, ~4km wide, and ~5m thick) that expands in width westward from Coogoon Vallis. Its western termination forms an irregular scarp with linear ridges orientated approximately north-east to south-west. This unit has a surface texture that is predominantly smooth but displays metre-scale blocks or boulders either on top or embedded within. The concentration of blocks/boulders decreases from 30% to 5% from the proximal (east) to distal (west) part of this unit. Four other rock units stratigraphically below the fan are identified: a dark-toned, pitted unit transitioning to a sub-polygonally fractured unit, a raised linear feature bearing unit, and a light-toned, orthogonally fractured unit. The sub-polygonally fractured unit contains craters which are partially covered by the sediment fan.

Discussion: Our results indicate evidence for at least four different episodes of sediment deposition with two significant hiatuses from the presence of embedded craters between three sediment fan layers. We hypothesise that the sloping depositional surfaces within the lowermost sediment fan episode are clinoforms indicative of deposition into a shallow standing body of water. The upper fan unit may have formed in a terrestrial setting due to the preserved ridges and potential boulders and could represent superposition of a fluvial fan or an upper-deltaic plain.

Keywords: Mars, Deltas, Sedimentology, Rovers, Habitability

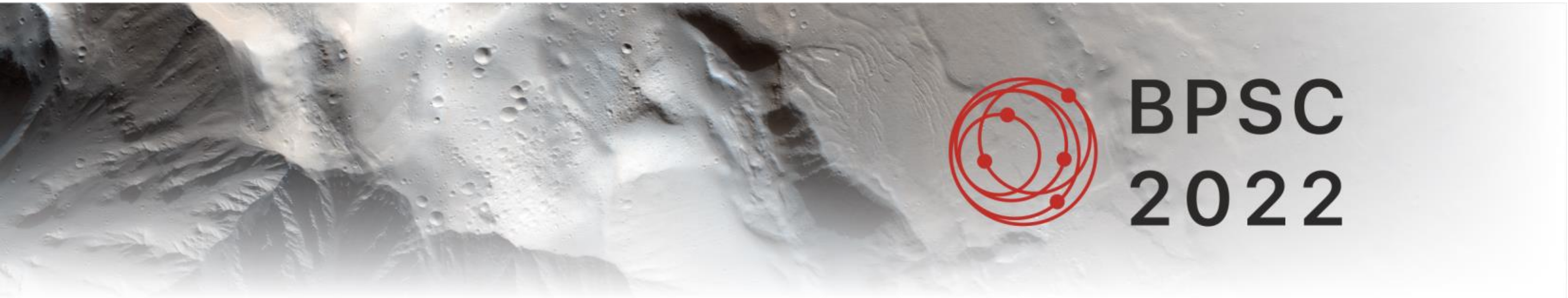

105. The Former Extent of the Mawrth Vallis Phyllosilicates

Joseph D. McNeil; Peter Fawdon, Matthew R. Balme, Angela L. Coe

Presenting author institution: The Open University

The highland plateaus surrounding Mawrth Vallis (MV) contain the largest exposures of Noachian-aged, stratified phyllosilicate-rich rocks on Mars. The nature of this ancient deposit is well-documented in the highlands surrounding the main channel (e.g. Noe Dobrea et al., 2010), however, its possible basinward extent in the lowland of Chryse Planitia and its origins are not well defined. In this study, we document morphological, compositional, and morphometric observations of bright-toned, stratified, clay-bearing outcrops within a population of kilometre-scale mounds in the lowland regions surrounding the MV plateau, in order to ascertain the relationship between the mounds and the plateau.

The bright-toned mound outcrops are morphologically similar at the HiRISE and CTX scale (bright-toned, stratified at the metre-scale, densely fractured and banded) to the clay-rich deposits of the MV plateau. Transects across the dichotomy from the MV plateau to the lowland mounds reveal that there is parity in elevation between the MV phyllosilicates and these mound outcrops. Additionally, CRISM spectra acquired from mound outcrops ubiquitously exhibit absorptions around 1.4, 1.9, 2.3 and 2.4 µm, indicating that, like the lower clay-bearing strata of the MV plateau (e.g. Poulet et al., 2005, Loizeau et al., 2007), they are primarily composed of Fe/Mg-rich phyllosilicates. These similarities in morphology, composition and elevation show that clay-rich highland material – and by extension, large amounts of water – once extended hundreds of kilometres further into the northern lowlands, supporting the previous hypothesis (McNeil et al., 2021) that the mounds were formed through differential erosion and backwasting of a clay-rich deposit. Al-rich clays – formed through leaching or pedogenesis – dominate the upper section of the MV phyllosilicate stratigraphy but are absent in all but one plateau-adjacent mound. This suggests one of two scenarios: (1) this Al-rich clay layer has been completely removed through erosion, or (2) the mounds were distinct landforms inaccessible to any surface water which altered the plateau.

Our study implies that the MV clay-bearing deposit was at least 100,000 km^2 more extensive than previously thought (although given that we observe Mawrth-like material in mounds up to 700 km away from MV, the additional area may be several hundred thousand kilometres). By extension, this work also shows that in the Noachian, the dichotomy boundary was approximately 200 km north of its present configuration in the MV area. The intervening clay-rich material was removed prior to the deposition of the pervasive dark capping unit in the Early Hesperian, indicating a substantial amount of erosion took place after deposition/alteration of Fe/Mg-rich phyllosilicates, and prior to the pedogenesis/alteration which formed the Al-rich clays.

The extent of such a large deposit – along with its homogenous clay compositions – could indicate that widespread and geochemically consistent palaeoenvironmental conditions existed throughout the circum-Chryse region in the early-mid Noachian, possibly facilitated by an early northern ocean. This study has shown that the Noachian-aged phyllosilicate-bearing units in the MV region occur over a much larger swathe of the dichotomy than previously thought. They may, therefore, be far more representative of the global conditions on early Mars than previously realised.

Keywords: Mars, Geomorphology, Stratigraphy, Landscape Evolution, Early Mars

Session 14:

The Earth and the Moon

106. What have we learnt so far from the samples returned from the Moon by the Chang'e-5 mission?

Tartese, Romain; Snape, Joshua; Joy, Katherine

Presenting author institution: The University of Manchester

The Chang'e-5 (CE-5) mission landed on 1st December 2020 in Northern Oceanus Procellarum, in the Northwest part of the Moon's nearside. It collected ~1.73 kg of samples (~1.5 kg of soil scooped from the surface, and a ~250 g drill core) that were returned to Earth on 17th December 2020. The CE-5 landing site was in part selected because crater counting studies suggested that the basalts there could be some of the youngest on the Moon, with model formation ages between ~0.8 and 2.5 billion years (Ga) old [1]. Therefore, the analysis of CE5 samples aimed to provide invaluable information on the evolution of lunar volcanic activity with time, and allow better constraining the lunar impact cratering flux then [2].

Scientific teams in China were invited to request CE5 samples in April 2021, and the first samples were allocated in July 2021. In less than a year, studies of the CE5 samples have already yielded key results.

Constraining the crystallisation age(s) of basalt fragments picked out from CE5 soils was the top scientific priority. Two teams carried out Pb/Pb dating in situ using secondary ion mass spectrometry and obtained similar dates, indicating a crystallisation age of 2030 ± 4 Ma [3,4]. This crystallisation age, which is right in the middle of the crater counting model age range, has already been used to refine models of the lunar cratering flux through time [5].

Geochemical studies of CE5 basalt fragments showed that they are some of the most ferroan mare basalts (bulk rock Mg# ~ 30), have intermediate TiO_2 abundances (~5-10 wt.% TiO_2), and are enriched in incompatible trace elements (ITE) such as Th and the rare earth elements (REE) [3,6]. The Sr and Nd isotope systematics of CE5 basalts are akin those of Apollo 12 basalts though [6], and imply very limited involvement of KREEP in their petrogenesis, which is consistent with their initial $^{238}U/^{204}Pb$ values of ~670-680 [3,4]. Altogether, this indicates that elevated ITE abundances in CE5 basalts resulted from low-degree partial melting followed by extensive fractional crystallisation, rather than involvement of KREEP in their petrogenesis. In addition, the water abundance of CE5 basalt melt inclusions suggests that their mantle source was relatively water-depleted compared to Apollo mare basalts [7]. At present, it remains unclear what mechanism(s) drove partial melting of a KREEP- and water-poor mantle source 2.5 Ga after the formation of the Moon.

On-going studies targeted at other CE5 soil components, such as impact melt breccias, agglutinates, and impact glass beads, should soon provide crucial information on impact processes and surface-exosphere interactions at the CE5 landing site.

References: [1] Le Qiao et al. (2021) Geophysical Research Letters 48, e2021GL095132. [2] Tartèse et al. (2019) Space Science Reviews 215, 54. [3] Che et al. (2021) Science 374, 887. [4] Li et al. (2021) Nature 600, 54. [5] Yue et al. (2022) Nature Astronomy, doi:10.1038/s41550-022-01604-3. [6] Tian et al. (2021) Nature 600, 59. [7] Hu et al. (2021) Nature 600, 49.

Keywords: Moon, Sample Return, Chang'e-5, Lunar Volcanism, Crater Counting

107. Identification of potential exogenously-derived components in Apollo 17 73002 continuous core thin sections using QEMSCAN mapping techniques

Bell, S. K.; Joy, K. H.; Nottingham, M.; Tartèse, R.; Jones, R. H.; Kent, J. J.; Shearer, C.K.; the ANGSA science team

Presenting author institution: University of Manchester

During the Apollo 17 mission, a double drive tube was used to collect a core sample (73001/2) of the lunar regolith [1]. The core was taken at Station 3 from the surface of the light mantle deposit, found at the base of the South Massif in the Taurus-Littrow Valley [1]. This study is part of the Apollo Next Generation Sample Analysis (ANGSA) initiative, analysing the continuous thin sections from the upper portion of the double drive tube (73002), opened in 2019 [2].

Quantitative Evaluation of Minerals by SCANing electron microscopy (QEMSCAN) is a non-destructive system of automated quantitative petrology. QEMSCAN can be used to produce mineral phase maps and is, therefore, a valuable method for investigating the mineralogy of clasts in the Apollo 17 continuous core sections. Here we build on the preliminary petrographic analysis of thin sections 73002,6011, 73002,6012, 73002,6013 and 73002,6014 [3], by using QEMSCAN processing techniques to identify potential exogenously-derived components within the regolith which are important for understanding the bombardment history of the Earth-Moon system [4]. Thin sections were analysed using an FEI QUANTA 650 field emission gun (FEG) scanning electron microscope at the University of Manchester, equipped with a single Bruker XFlash energy dispersive X-ray (EDS) spectrometer. The FEI QEMSCAN was operated in field image mode with a step size (i.e. pixel size) of 5 µm. QEMSCAN uses a Species Identification Protocol (SIP) list to assign a mineral to a pixel based on the EDS spectra and BSE brightness at each individual point. All QEMSCAN mineral phase maps were initially classified in the iExplorer software using our lunar specific SIP list [4]. Additional secondary SIP lists were used to view the data in a number of useful ways including to highlight minerals commonly found in meteorites (e.g. Fe-Ni alloys, Fe-sulphides, high-Mg olivine, high-Mg pyroxene, and Na-rich plagioclase).

Several hundreds of occurrences of selected minerals of interest were highlighted in clasts across the four thin sections. Further manual examination of the data, to exclude endogenous occurrences of highlighted minerals of interest (i.e. a Fe-sulphide grain in a mare basalt clast), was used to narrow down the number of regions of interest which are now being examined by quantitative electron-beam techniques to help classification and to identify their sources. QEMSCAN has proven to be a valuable tool for rapidly identifying regions of interest within petrologically complex samples, which could be applied to other existing Apollo core samples and drill cores retuned on future lunar sample-return missions.

Acknowledgments: We thank the NASA JSC curatorial teams for preparing the continuous core sections. UoM research was supported by grants URFR201009 and STFC ST/M001253/1. CKS activities were supported by NASA ANGSA 80NSSC19K0958, University of New Mexico, and Lunar and Planetary Institute.

References: [1] Wolfe E.W. et al. (1981) USGS Prof. Paper, 1080, 280 [2] Shearer et al. (2022) 53rd LPSC, #2546), [3] Bell S.K. et al (2022) 53rd LPSC, #1974, [4] Bell S.K. et al (2020), J.Pet., 61(4), [4] Joy K.H. et al (2016) Earth, Moon, and Planets, 118(2).

Keywords: Apollo 17 , Petrology, QEMSCAN, Regolith, Moon

108. Evidence of recent slope deformation and the lasting effect of local tectonic stress in Taurus-Littrow Valley, the Moon

Magnarini, Giulia; Grindrod, Peter; Mitchell, Thomas

Presenting author institution: Natural History Museum, London

The South Massif and Taurus-Littrow Valley, location of the Apollo 17 landing site, host recent, late-Copernican geomorphological landforms and tectonic structures. This is a unique area on the Moon for the presence of two recent, overlapping landslide deposits, and boulder falls, suggesting that a repetitive instability has affected the north-east facing slope of the South Massif. The presence of the young Lee-Lincoln lobate scarp associated with a thrust fault suggests that seismic shaking may have been an important factor in triggering surface changes and mass-wasting events in the area. Moreover, it has been suggested that the thrust fault could be still active.

In the first part of this work, we use the younger landslide deposit as a geomorphological marker. The age of the deposit, 70-110 My, was obtained thanks to the returned sample of the Apollo 17 mission, therefore allowing to set a time constraint to surface changes that have occurred since its emplacement. Using LROC NAC imagery and Apollo 17 astronauts' ground photos, we present evidence of slope deformation of the north-east slope of the South Massif post-dating the emplacement of the young landslide deposit. We map boulders tracks, zones of disturbed regolith, summit and slope structures, and extensional structures linked to the thrust fault. We described the mutual relationships of such structures, and their relationships with the topography and local tectonic structures. We identify features directly related to the local stress field, as well as features derived from gravitational adjustment following basal slope support removal due to extensional stresses. Our interpretation favours a scenario in which recent tectonism, coupled with long-lasting influence of the subsurface geometry, has caused continuous slope deformation of the South Massif.

In the second part of this work, we use LROC NAC multitemporal imagery dataset to generate DTMs and orthoimages of the South Massif and Taurus-Littrow Valley (48 repeated images as of January 2020; temporal baseline 2009-2020) and apply co-registration techniques. We present our initial results of the search for active surface processes in Taurus-Littrow Valley.

Keywords: Moon, Surface changes, Apollo 17

109. Probability of accessing stable water-ice in the lunar south polar region

Orgel, Csilla; Sefton-Nash, Elliot; Warren, Tristram; Boazman, Sarah J.; King, O.; Bowles, Neil

Presenting author institution: ESA-ESTEC

The South Pole of the Moon and its potential for cold-trapped volatiles to persist became the focus for future landed missions. Landing site selection for any surface mission typically involves optimizing a balance between quantities or criteria that indicate the extent to which the mission's objectives can be met or exceeded. Often, a first step is to filter out unviable landing sites by applying operational or engineering requirements to environmental or terrain characteristics. A second step involves optimization or trade-offs to maximise satisfaction of mission objectives, including potential science return. Leading thermophysical model results indicate zones of thermal stability are preferentially distributed in the top few 10s of cm. We also consider factors related to mission operations, namely: Earth visibility for direct-to-Earth communication and solar illumination for power. In this study we show results quantifying (1) the distribution of 'compliant terrain', and (2) the probability of being able to target areas where thermal conditions permit the long-term stability of cold-trapped volatiles in the shallow sub-surface. Additionally engineering constraints are satisfied for almost any given missions.

We combine datasets sampled at a spatial resolution of 120 m/pix, spatial coverage extending from the pole to 80°S at the cardinal meridians and include metrics of two volatile stability models (Paige et al., 2010, Warren et al., 2020) as indicators of science potential, as well as LOLA derived slope, average solar illumination, and Earth visibility maps (Mazarico et al., 2011). We define a least and a most constrained scenario, to explore the distribution of 'compliant terrain', both spatially and in selected parameter spaces of the constraining criteria. We prepare boolean rasters that are true where terrain is compliant with slope, solar illumination, and Earth visibility constraints. For the least constrained scenario, we set (1) slope values ≤ 15°, (2) solar illumination ≥ 0.15, and (3) Earth visibility ≥ 0.25. To create the most constrained scenario, we combine (1) slope values ≤ 7°, (2) solar illumination ≥ 35%, and (3) Earth visibility ≥ 50%.

We found that the maximum connected area size (where compliant pixels are connected) is ~430 km^2 for the least constrained scenario and ~5.6 km^2 for the most constrained scenario. We conclude that sub-km landing precision (<1km radius) is required to confidently target places with potentially stable sub-surface water ice that on average receives enough sunlight to power a spacecraft and communicate directly to Earth.

Keywords: Moon, South Polar Region, Landing Sites, Volatiles, Landing Precision

110. Legal Perspectives on In-Situ Resource Utilisation in Outer Space

Bhatt, Mukesh Chiman

Presenting author institution: Birkbeck, University of London

In situ resource utilisation is the preferred option for the exploration and use of outer space and is presumed to be covered by the Outer Space Treaty. However despite further provision in the moon treaty which has already entered into force, major players in the space resources field have not ratified or supported this treaty. The use of such resources for in situ utilisation is clearly under the supervision authority of the sovereign national government of those agencies in current space law. However when contracted out by these space agencies to other companies, the Outer Space Treaty and space law in general extends the jurisdiction of the national sovereign government to these subcontractors on the basis of the legal definitions of the launching state and of space objects. Removal of said resources such as the regolith which needs processing appears clear enough in the space law. However the equipment and processing of this material is then likely subject to the laws of the launching state: equipment will be classified as space objects. The use of the local resource is justified in law under these jurisdictions through the distinction of movable as opposed to immovable property. This notion of movable and immovable property is also the basis of the many and varied mining laws in the different countries on Earth, and which would apply if any of these countries became a launching state. Therefore on the one hand equipment used for processing is subject to patent and other laws of the launching state. On the other hand, the removed material is subject to concepts and laws of proper extant within the launching state. Further legal complications arise at the completion of the processing of the removed material which is then becomes a product. As this product may not be freely available through the right of economic activity allowed within the outer space treaty this product needs to be treated as a commodity. This then makes the final product subject to the laws of commerce and finance under the jurisdiction of the launching state. Whereas the immediate utilisation of in-situ resources appear straightforward, any further use and utilisation needs to examine the legal consequences and perspectives applicable to the situation.

Keywords: space resources, space law, mining law, property, patents

111. Dynamic Strength and Fragmentation during High-Rate Brittle Failure

Rae, Auriol; Kenkmann, T.; Collins, G.; Poelchau, M. H.; Padmanabha, V.; Schäfer, F.

Presenting author institution: University of Cambridge

During impact cratering, target materials are subjected to extreme deformation conditions. Brittle deformation under these conditions, where strain rates can exceed 10^1 to 10^2 s^{-1}, is rate-sensitive. Typically, rocks are stronger when deformed at high strain-rate conditions. This occurs because fracture propagation has a limited velocity; at high loading rates, the weakest flaws in a material are not able to cause failure before other, increasingly strong flaws are activated. This results in significant changes to mechanical properties and causes fragmentation of the target material. Dynamic compressive strength and fragmentation in brittle materials is not currently implemented in numerical impact simulations.

In this study, we present results of high strain rate mechanical tests to determine the characteristic strain rate for rate-dependent brittle failure and dynamic strength increase, and the fragment size and shape distributions that result from failure at these conditions. We investigated a variety of rock types and considered whether the fragment characteristics can be used as diagnostic indicators of loading conditions during brittle failure. In addition, we use numerical impact simulations to assess the significance of dynamic strength increase and compressive fragmentation during impact cratering at a variety of scales.

We find that the characteristic strain rates of rocks, where the dynamic strength is twice the quasi-static strength, ranges between ~150 and ~350 s^{-1} depending on lithology.

Fragment size analysis demonstrates an inverse power-law relationship between fragment size and strain rate for dynamic failure under uniaxial compression. The constant of this relationship varies as a function of porosity (or a related property) while the exponent has a value of 1.93 +/- 0.14 for all rocks. Unlike fragment size, we find that fragment shape is independent of strain rate under dynamic uniaxial loading.

Numerical impact simulations demonstrate that strain rates are sufficiently high to produce rate-dependent effects in all planetary impacts (impact velocities from ~5-20 km/s) where impactor diameters are ~100 m or smaller. Rate-dependent strength and fragmentation therefore plays an important role in small planetary impacts and laboratory impact experiments. Based on the results of this study, we are developing a semi-empirical approach to account for rate-dependent shear strength in numerical impact simulations. An important development due to the need to accurately ground-truth numerical impact models against laboratory scale experiments.

An additional implication of this study is that fragment size may be used as a diagnostic indicator of the strain rate at failure during impact loading while fragment shape cannot be used. However, our experiments only used uniaxial compressive loads, it is uncertain how truly triaxial stress states may affect fragmentation behaviour.

Keywords: Impact Cratering, Planetary Geophysics

112. Shock deformation in feldspar in the Chicxulub impact structure

Riches, Liza; Pickersgill, Annemarie; Daly, Luke

Presenting author institution: School of Geographical & Earth Sciences, University of Glasgow, Gregory Building, Lilybank Gardens, Glasgow, G12 8QQ, UK

Shock deformation is caused by a hypervelocity impact of two planetary bodies [1,2]. Shock barometry is the process of determining pressure to which material was exposed during impact. Feldspar group minerals are valuable tools in shock barometry due to their high abundance in Earth's crust [3]. Both Na-rich and K-rich feldspars from the Chicxulub impact structure have been analysed in this study. Shock deformation features have been characterised within these samples using a range of methods, primarily electron backscatter diffraction (EBSD).

Three samples were analysed in this study from the Chicxulub impact structure The samples were collected in 2016 during the IODP-ICDP Expedition 364 [4]. The three samples were collected from between 1160.7 and 1216.5 mbsf (metres below the seafloor) and were analysed using a range of methods. These methods were scanning electron microscopy (SEM), including backscatter electron (BSE) imaging and EDS mapping and optical microscopy (all at the University of Glasgow) and electron probe microanalysis (EPMA) which was carried out at the university of Edinburgh). One of the samples in this study was analysed further using EBSD to further investigate the shock microstructures found.

The Na-rich feldspar was found to contain more evidence of deformation than the K-rich feldspar in the same samples. One key feature found in Na-rich feldspar was the presence of partially amorphised alternating twins. Several EBSD maps showed alternating indexed and unindexed twins. The crystalline set of twins contain a low level of Ca (no more than ~2.5 at. %) however, the partially amorphous twins that alternate with these crystalline twins contain even less Ca (~1 at. %).

Deformation in alternating twins has been found in previous research [5,6]. The variation of Ca content across this alternate twin deformation in Na-rich feldspars has however not been as discussed before. Based on the evidence in this study it has been deemed more likely that this change in Ca content is due to partial amorphisation influencing Ca levels post shock.

References: [1] Melosh, H. (1989) *Impact cratering: a geologic process.* [2] French, B & Koeberl, C. (2010) *Earth Science Reviews* 98:1-2. [3] MacKenzie, W. S. and Adams, A. E. (1994) *A colour atlas of rocks and minerals in thin section.* [4] Gulick, S. et al. (2017) *Proceedings of the International Ocean Discovery Program 364. [5]* Stöffler, D. (1966) *Contributions to mineralogy and petrology* 12:15–24. [6] Pickersgill, A, E. et al. (2015) *Meteoritics & Planetary Science 50:*1546–1561.

Keywords: Impacts, Shock deformation

113. Raman mapping of shocked basalts from Lonar Crater, India: Evidence for diamond as a biosignature resulting from shocked organic carbon

Tanbakouei, Safoura; Michalski Joseph R., Wright, Shawn P.

Presenting author institution: University of Hong Kong. Department of Earth Science

Introduction: All planetary surfaces have been subjected to meteoritic bombardments throughout their histories. Studying the effects of these collisions on the target materials has significance applications for in situ investigations and planetary remote sensing. Lonar impact crater in India with an average diameter of 1830 m and a depth of about 150 m, is the only well-preserved terrestrial impact crater and a suitable analog for understanding the effects of impact on the Martian basaltic crust. The target rock geology in which the Lonar impact occurred c.a. 570 Ka is Deccan flood basalt [1] in the east ejecta suevite, but soils had formed within these volcanic deposits [2]. The impact resulted in physical and mineralogical modification of the targets, forming some new rock types (Wright), as well as breccias, glasses and shocked bedrock [3]. Previous works have described shock effects in feldspars, and the formation of glass [4,5]. Here, we provide the EDX mapping of major elements and microRaman mapping of the thin section of an unusual breccia. The sample contains graphitic carbon and presence of diamond which is indicative of the effects of shock.

Methods: Thin section sample named LCO9-EES-3B from Lonar Crater collected by S. P. Wright has been analyzed [6]. Sample was examined using an inVia Raman imaging spectrometer (Renishaw Company) in the Planetary Spectroscopy and Mineralogy Laboratory (PSML) at The University of Hong Kong. The green excitation laser (λ= 532 nm) has been used with high spectral (1 cm^{-1}) and spatial resolution. The objective lens of Raman microscope is X50. The 2D maps were taken in an area of 635,040 $(\mu m)^2$ as grids with 6 µm spacing, each point consisting of 1 acquisition recorded over 7s and laser power of 2.29 mW cm^{-2}. BSE images were taken with Hitachi S-3400N Scanning electron microscopy (EMU, Hong Kong University). The EDX detector for elemental information mapping has been used to determine the abundances of the major elements (Si, Fe, C, Al, Ca, Mg).

Results: The sample contains abundant graphitic carbon, based on the occurrence of two Raman peaks at 1344 and 1586 cm^{-1} corresponding to D and G-bands [7] as well as EDX mapping of carbon in the sample. Within the amorphous carbon are coherent zones of diamond, which we suggest representing shocked organic materials. Existence of diamond has been confirmed at Ries crater [8] and in impact melt rocks from the Popigai crater [9] because of direct shock conversion of graphite to diamond [10]. High enough pressure - beyond 35 GPa [11]- and low enough temperature form impact diamonds, as high temperature might melt the rock and caused graphitization [9]. Diamond also contains minor inclusions with CO_2 at high pressure, which must have been inserted during the high-pressure shock transformation of graphite to diamond [12]. Moreover, the heterogeneity of diamond content in the crater depends on the distribution of graphite in the impact. Formation of diamond from carbon-bearing rocks at any impact site could be used as an evidential tool for hypervelocity impact on early Earth [10].

Keywords: Impact crater, Biosignature, Shocked basalt, Raman spectroscopy

Session 15:

Venus and Mercury

114. What Venus reveals about the nature of Earth-sized planets

Ghail, Richard

Presenting author institution: Royal Holloway, University of London

Venus has enjoyed a renaissance in recent years, with four missions scheduled in the next decade, and a paradigm shift in our understanding. New discoveries and fresh insights are shedding light not so much on why Venus is so different to Earth, but what their similarities tell us about Earth-sized (tellurian) planets generally, and how they differ from smaller terrestrial planets like Mars and the Moon. Our understanding of Venus was hampered by the peculiar distribution of its impact craters, which appears to require the surface to be everywhere young (<1 Ga) and uniform in age despite the contradictory geomorphological evidence for a variety of terrains of different ages. The resolution to this paradox is that the high surface temperature inhibits extrusion, generating a locally mobile plutonic squishy lid that results in both the globally random distribution of impact craters and the wide variety of geomorphic terrain types. Evidence for this behaviour is now recognised everywhere on Venus in the form of coronae and campus blocks in the plains, and their accreted orogenic remains in the highlands. A network of rift systems on the scale of oceanic spreading ridges, is indicative of globally organised convection, but regional concentrations of volcanism resemble terrestrial supercontinent breakup suggestive of mantle overturns. We are this approaching a more realistic understanding of Venus: in a real sense, we're starting to appreciate what we don't know and what questions the four planned missions might address. While these features may appear rather different to their terrestrial counterparts, there are strong reasons to infer genetic links between them. Venus appears to be in a state equivalent to the Proterozoic Earth; indeed, in a geological sense, Earth may well be in that state even now, with the Cretaceous 'superplume' an example of an overturn event. The key message is that tellurian planets are complex, with the outcome of fundamental processes (like convection) more strongly dependent on happenstance, both initial conditions and external forcing. The Moon-forming impact is a good example: the result for Earth was a larger core and relative orbital stability; Venus either had no such impact, or its effects were different, perhaps causing its slow retrograde rotation. Earth narrowly avoided a runaway icehouse through volcanogenic gases; those same gases may have triggered a runaway greenhouse on Venus, or it never had oceans to begin with. The implications for exoplanet studies are profound. While we can now be confident about the intrinsic behaviour of tellurian planets, we cannot know the host of contingencies upon which the actual outcome depends without detailed – and probably in situ – observations and hence, whether those planets are as rich in life as Earth or as hostile as Venus.

Keywords: Venus, exoplanets, tectonics, geology, astrobiology

115. Composition-Induced Density Variations in the Venusian Crust and their Implications for Tesserae Formation

Baker, Aedan; Semprich, Julia; Schwenzer, Susanne; Greenwood, Richard; Filiberto, Justin

Presenting author institution: The Open University

Venus is one of Earth's closest neighbours in the Solar System and is the only terrestrial body of a similar size. However, the planet has harsh conditions on the surface, making long-lasting lander or rover missions difficult, and a thick atmosphere blocking visual imaging of the surface, meaning radar mapping must be used. Consequently, relatively little is known for certain about the main surface features on Venus. Among these poorly understood features are tesserae, which are areas of elevated terrain characterised by being very bright in radar imagery and have at least two sets of intersecting fractures. Tesserae may be the oldest material on Venus and make up around 8% of the planet's surface, with the rest being predominantly basaltic plains.

Tesserae are of interest as measurements taken by mapping missions have revealed that they generally have a lower emissivity and higher reflectivity compared to the surrounding plains material. Several possible explanations have been proposed for this reduced emissivity including felsic compositions and the formation of minerals with high dielectric constants due to weathering and alteration. The possibility of felsic surfaces feature on Venus, a planet with no significant crustal recycling due to its current "stagnant lid" tectonic regime and little to no liquid water at present, has implications for the early development of the planet. Understanding the composition of tesserae is of importance as different compositions would affect the stability of the crustal root supporting the elevated terrain.

Here we present the results of thermodynamic modelling of four possible tesserae compositions varying from basaltic to felsic under Venus pressure/temperature conditions using the Gibbs free energy minimisation software Perple_X. Density diagrams for each composition, with possible geotherms for the Venusian subsurface, are used to analyse the stability and behaviour of the crustal roots. The implications of these results will be discussed with respect to melting and densification behaviour of the different compositions. These results will then be used to constrain the composition of tesserae, while considering varying geothermal gradients.

Keywords: Venus, Modelling, Tesserae

116. Is Lada Terra the Site of a Venus Overturn Upwelling ZOne (OUZO)?

Hoad, Connor; Ghail, Richard

Presenting author institution: Royal Holloway, University of London

Introduction: Venus is sometimes considered to be the closest planetary analogue in our Solar System to the Archean Earth [1], wherein juvenile lithospheric plates were too warm and buoyant to allow for subduction and the initiation of plate tectonics. A recent pre-plate tectonic model [2] proposes that mantle Overturn Upwelling ZOnes (OUZO's) could have provided an efficient planetary cooling mechanism. A morphological study of Lada Terra, a highland area of proposed mantle upwelling [3], aims to test whether its volcanotectonic character is consistent with the hypothesis that Lada Terra is undergoing cratonisation and resurfacing via an OUZO-like mantle overturn event.

The OUZO hypothesis: The OUZO model states that in the absence of cooling via plate tectonics, the mantle is cooled inefficiently through conduction, forming short-wavelength convection cells which cannot penetrate the lower mantle. This produces an increasingly unstably stratified mantle system, in which heat builds up in the lower mantle and is episodically released via OUZO events. In these overturn events a voluminous upwelling of hot, primitive lower mantle material with a mass equivalent to multiple large Phanerozoic plumes ascends and resurfaces 10-20% of the Earth’s surface over a few 100 Ma.

Lada Terra – a possible OUZO? Lada Terra, located on Venus at 70°S, 005°E, is one of three highland regions that might be analogous to terrestrial Archean continents. Lada is a region with likely ongoing volcanic activity [4], and is characterised by a diverse array of volcanic terrains, multiple large coronae on the scale of Large Igneous Provinces, including the third largest on Venus [5], ridges, rifts, a distinctive 3 km high volcanic rise, and ancient tesserae disrupted by the more recent upwelling event.

Tessera: Lada’s two tesserae show distinct histories throughout the upwelling event: Cocomama has undergone fragmentation, flexure and flooding by the formation of the Lada Rise and Quetzalpetlatl Corona; while the smaller Lhamo has undergone extensive rifting as a result of the opening of Derceto-Quetzalpetlatl rift system and Sarpanitum corona.

Careful mapping of these fragmented tesserae have revealed a process of destruction by tectonic slicing and flooding by sheet lavas. Ironically, if highland tesserae represent ancient Venusian continental cratons, this slicing and embayment is consistent with ongoing cratonisation and resurfacing via mantle upwelling, unless Lada is somehow a frozen snapshot in time.

Conclusions: The number and range of volcanic and tectonic features across Lada Terra are consistent with a mantle overturn upwelling zone, similar in scale to the Cretaceous superplume. Mapping demonstrates that tessera can be destroyed by slicing and embayment, but these processes may ultimately stabilise the region into a craton.

References: [1] Harris L. B.and Bédard J. H. GSLSp.Pub.,(2015) 401, 327–56. [2] Bédard J. H. Geoscience Frontiers, (2018) 9 (1), 19–49[3] Ivanov M. A. and Head J. W. PSS, (2010) 58 (14–15), 1880–94. [4] Gülcher et al. Nature Geoscience (2020) 13(8), 547-554. [5] Kratter K. M. et al. JGR-P, (2007) 112 (E4).

Keywords: Venus, Tectonics, Mantle Overturn , Tessera, Lada Terra

117. Retrieval of main cloud structure using Venera 13 and 14 descent probe data

Kulkarni, Shubham; Wilson, Colin; Irwin, Patrick

Presenting author institution: University of Oxford

The spectrophotometers onboard Venera 13 and 14 probes recorded internal radiation field from an altitude of 62 km down to the surface, covering a field of view of 20° and a wavelength range of 0.48 to 1.14 µ. The original data from the magnetic tapes was lost, however, a secondary dataset was created using the graphic material published earlier. This dataset contains radiation only from two directions (one close to zenith and one close to nadir) instead of six original directions. While analysing the secondary dataset, [1] found an indication of a near-surface cloud layer. In light of upcoming Venus missions, we are currently re-analysing this dataset to learn more about a possible near-surface cloud layer.

In order to constrain the properties of the near-surface cloud layer, it is important to first constrain the abundances of all four particle modes in the main cloud deck in the atmosphere of Venus. In this work, the model of the internal radiation field in the NEMESIS radiative transfer and retrieval tool [2] is modified for simultaneous fitting of upward and downward radiation at all altitudes. The effectiveness of this method in contrast to fitting either upward or downward radiation is described. The cloud abundances are then retrieved using the secondary dataset. The retrievals from Venera 13 and 14 are compared with each other and compared with the previous estimates of cloud abundances. In the end, the suitability of the secondary datasets for an accurate estimation of the near-surface cloud layer is briefly discussed.

References: [1] Grieger, B., Ignatiev, N. I., Hoekzema, N. M., and Keller, H. U. in European Space Agency, (Special Publication) ESA SP, number 544, 63–70 (ESA Publications Division, Noordwijk, Netherlands, 2004). [2] Irwin, P. G., Teanby, N. A., de Kok, R., Fletcher, L. N., Howett, C. J., Tsang, C. C., Wilson, C. F., Calcutt, S. B., Nixon, C. A., and Parrish, P. D. Journal of Quantitative Spectroscopy and Radiative Transfer 109(6), 1136–1150 (2008).

Keywords: Radiative Transfer, Venus, Planetary Atmosphere, Clouds

118. Searching for Phosphine in the Atmosphere of Venus using SOFIA GREAT

M. A. Cordiner, G. L. Villanueva, H. Wiesemeyer, S. N. Milam, A. Moullet, R. Aladro, I. de Pater, R. Cosentino, V. Kofman, G. Liuzzi, S. Faggi, C. A. Nixon, A. E. Thelen, S. B. Charnley, B. A. McGuire, J.Stutzki

Presenting author institution: NASA GSFC;

The presence of phosphine (PH3) in the atmosphere of Venus was reported by Greaves et al. (2020), based on spectroscopy of the J=1-0 transition using the Atacama Large Millimeter/submillimeter Array (ALMA) and the James Clerk Maxwell Telescope (JCMT). This unexpected discovery presents a challenge for our understanding of Venus's atmosphere, and has led to a reappraisal of the possible sources and sinks of PH3, for example, from photochemical, geochemical, meteorological and even biological processes (e.g. Bains et al. 2021; Truong et al. 2021). The claimed detection of PH3, however, was contested by several subsequent, independent analyses of the ALMA and JCMT data (Snellen et al. 2020; Thompson et al. 2020; Villanueva et al. 2021; Lincowski et al. 2021), and searches for infrared signatures of PH3 using other ground and space-based instruments have resulted in non-detections (Encrenaz et al. 2020; Trompet et al. 2021). Phosphine on Venus remains a serious topic for discussion in the planetary science community due to its potentially profound implications, and the fact that PH3 was also found in a recent reanalysis of Pioneer Venus mass spectrometry data (Mogul et al. 2021). Here we present results from a new search for PH3 on Venus based on observations made using the GREAT instrument onboard the SOFIA aircraft, over three flights conducted in November 2021. Multiple PH3 transitions were targeted in the far-infrared/sub-mm wavelength range, enabling the derivation of a sensitive upper limit on the atmospheric PH3 abundance.

Keywords: Venus, Atmosphere, Spectroscopy, far-Infrared, Molecules

119. Newly discovered widespread extensional grabens on Mercury's compressional structures

Man, Benjamin; Rothery, David; Balme, Matthew; Conway, Susan; Wright, Jack

Presenting author institution: The Open University

Mercury is a shrinking planet with a surface dominated by compressional tectonic landforms as first identified by Mariner 10 and then confirmed by MESSENGER. Extensional structures are present but are much rarer, with almost all reported examples found exclusively in smooth plains material within craters [1]. The only two reported examples of extensional structures outside of the aforementioned setting are extensional grabens associated with lobate scarps; pristine back-scarp grabens associated with small lobate scarps (10s of kms in length and 10s of metres in relief) [2], and crestal grabens found on Calypso Rupes (381km in length and ~1km in relief) [3,4]. These grabens form when thrusting produces a hanging wall anticline resulting in local tensional stresses along the anticlinal axis parallel or sub-parallel to the hinge zone. Here, tensional stresses cause antithetic faults to form, which results in a narrow down-dropped fault block.

We find that extensional grabens on compressional structures are much more common than previously recognized. These small-scale landforms (often less than 1km in width, 10s of km in length and likely 10s to 100s meters in depth) are not expected to survive 100s of millions of years due to continual regolith formation and impact gardening masking their signature [1,2]. Our discovery and documentation of potentially young extensional grabens may indicate that many of Mercury's compressional structures have continued to move until geologically recent times. This work therefore may call into question the old absolute age estimates of tectonic features' last movements calculated using crater counting [5–9].

[1] P.K. Byrne, C. Klimczak, A.M.C. Şengör, in: S.C. Solomon, L.R. Nittler, B.J. Anderson (Eds.), Mercury: The View After MESSENGER, 1st ed., Cambridge University Press, 2018, pp. 249–286.

[2] T.R. Watters, K. Daud, M.E. Banks, M.M. Selvans, C.R. Chapman, C.M. Ernst, Nat. Geosci. 9 (2016) 743–747.

[3] C. Klimczak, P.K. Byrne, A.M.C. Şengör, S.C. Solomon, Can. J. Earth Sci. 56 (2019) 1437–1457.

[4] M.E. Banks, Z. Xiao, T.R. Watters, R.G. Strom, S.E. Braden, C.R. Chapman, S.C. Solomon, C. Klimczak, P.K. Byrne, J. Geophys. Res. Planets 120 (2015) 693–706.

[5] E.R. Fegan, D.A. Rothery, S. Marchi, M. Massironi, S.J. Conway, M. Anand, Icarus 288 (2017) 226–234.

[6] V. Galluzzi, L. Ferranti, M. Massironi, L. Giacomini, L. Guzzetta, P. Palumbo, J. Geophys. Res. Planets 124 (2019) 2543–2562.

[7] L. Giacomini, M. Massironi, S. Marchi, C.I. Fassett, G. Di Achille, G. Cremonese, Geol. Soc. Spec. Publ. 401 (2015) 291–311.

[8] L. Giacomini, M. Massironi, V. Galluzzi, S. Ferrari, P. Palumbo, Geosci. Front. 11 (2020) 855–870.

Keywords: Mercury, Terrestrial planet, Tectonics, Geology, Geomorphology

120. The Distribution of Peak-ring Basins on Mercury and their Correlation with the High-Mg/Si Terrane

Hall, Graeme P.; Martindale, A.; Bridges, J.C.; Nittler, L.R.; ou, E.J.

Presenting author institution: University of Leicester

A catalogue of mercurian craters that retain their central peak or peak-ring structure was created to aid target prioritisation for the Mercury Imaging X-ray Spectrometer (MIXS), now on its way to Mercury aboard BepiColombo. Preliminary analysis of the MIXS crater catalogue suggested a potential spatial correlation between an abnormally high spatial density of peak-ring basins and a region of Mercury with elevated Mg/Si values (High-Magnesium Terrane, HMT). Robust statistical analysis of previously published crater catalogues confirmed that the spatial correlation exists, with an overall confidence level of 97.7 %, specifically between peak-ring basins and the HMT, where the HMT is delineated by a contour of Mg/Si = mean+2σ = 0.648. Applying empirical impact cratering scaling laws to the fifteen basins intersecting the HMT (Boethius, Polygnotus, Baker 18, Scarlatti, Baker 27, Jobim, Wang Meng, Al-Hamadhani, Aksakov, Praxiteles, Larrocha, Sholem Aleichem, Vivaldi, Baker 91, and Vyasa) suggested that all have excavated material from ~13–20 km depth. None of the basins excavated mantle material, predicting instead that deep crustal material contains elevated Mg/Si material. However, five of the basins (Al-Hamadhani, Larrocha, Sholem Aleichem, Vivaldi, and Vyasa) are predicted to have melted underlying mantle material, which might be a contributing factor in the elevated Mg/Si signature. In the absence of resolvable volcanic features associated with the rise of basaltic melts from the mantle, we favour excavation of deep crustal, high Mg/Si material. MIXS-T is capable of spatially resolving individual features associated with peak-ring basins and it is proposed that the fifteen basins within the HMT are prioritised targets for MIXS, in order to test the hypothesis of exposed deep-crustal material.

Keywords: Mercury, Basins, Geochemistry, BepiColombo, MIXS

121. Ejecta flows on Mercury: Prevalence, significance, and timing of emplacement

Lennox, Annie; Blance, Alistair; Rothery, David; Balme, Matt; Conway, Susan; Wright, Jack; Galluzzi, Valentina

Presenting author institution: Open University

Impact ejecta flows have a layered morphology with a steep, lobate margin, and maintain thickness across the direction of flow. They contrast with ballistically emplaced ejecta, which thins exponentially from crater rims, and has a smoother texture. Ejecta flows are found on many planetary bodies, whilst on Mercury they are considered relatively rare with seven ejecta flow deposits previously reported by Xiao and Komatsu (2013). Here we present the combined efforts of Blance et al. (2022) and Lennox et al. (2022) in adding to that database.

Blance et al. (2022) conducted a global survey of lobate ejecta deposits on Mercury, identifying 36 craters with ejecta flows and a further 27 probable examples. The majority occur around craters ~30–80 km in diameter and are widespread across the planet. In the examples found by Xiao and Komatsu (2013) and Blance et al. (2022), the flow deposits could have been emplaced during the impact process, or afterwards by mass-wasting. Lennox et al. (2022) focused on lobate ejecta deposits they discovered at H15. At Nairne crater, from which two distinct lobes propagate into the floor of a pre-existing crater, Lennox et al. (2022) identified perched impact melt occupying topographic lows on top of the larger of the two lobes. These impact melt deposits are evidence that flow emplacement was contemporaneous with impact, rather than post-impact mass movements.

Here we discuss the key factors affecting the formation of ejecta flows on Mercury. On Mars, Earth, and some icy moons, volatiles are proposed to drive the fluidisation of the flow. As Mercury has volatile-bearing materials at the surface, these could be a factor in ejecta fluidisation. However, we find no evidence for volatile involvement, and features indicative of local volatile concentration (e.g., hollows) don’t occur preferentially near to ejecta flows.

The slope of the underlying terrain seems to be a key factor affecting the formation of ejecta flows on Mercury. Most ejecta flows extend downslope into adjacent, older craters. At least two exceptions to this rule were identified: at Hokusai crater and an unnamed crater in the northern plains, the apparent ejecta flows occur on relatively flat ground (<2° slope) without extending into adjacent craters. These examples look distinct from most lobate ejecta flows on Mercury, resembling single-layer ejecta craters on Mars, with distal ramparts and a ropey texture. Hokusai crater exhibits evidence of excess impact melt: proposed as a possible fluidising agent (Barnouin et al., 2015). However, the unnamed crater has no identifiable impact melt outside the crater rim. This crater is also considerably smaller than Hokusai (~37 km vs 95 km diameter), and smaller craters tend to have proportionally less impact melt. Understanding how this crater’s ejecta flow formed would give insight into the factors influencing ejecta fluidisation on Mercury, as for this crater the slope of local terrain, volatile presence, and impact melt excess do not appear to be obvious factors.

Keywords: Mercury, Impact Cratering, Geological Mapping, Ejecta Flows, Volatiles

122. New Images from Bepi-Colombo

Rothery, Dave

Presenting author institution: Open University

We will present a preview of Images from Bepi-Colombo’s 2nd swing-by on Mercury will be received and processed late on Thursday 23 June, ready for public release on Friday 24 June

Keywords: Bepi Columbo, New data, Mercury, remote sensing

Session 16:

Community session

14:00 RAS update

Robert Massey

Royal Astronomical Society

14:15 STFC roadmap update

John Bridges

14:25 ESA funding opportunities

Jack Wright

European Space Agency

14:35 SPAN update

James Endicott

The Open University

14:45 UKSA space science and exploration update

Caroline Harper & Sue Horne

UK Space Agency

15:15 UKPF update

John Pernet-Fisher

15:25 Future of BPSC

Lee White & BPSC local organising committee

Closing notes

Author index